

Tunnelling In The Quantum Hall Regime

Electron Vs. Fractional Charge

Thesis submitted in partial fulfillment
of the requirements for the degree of
"DOCTOR OF PHILOSOPHY"

by

Elad Shopen

Submitted to the Senate of Ben-Gurion University
of the Negev.

December 4 2003

Kislev 9 5764

BEER-SHEVA

Tunnelling In The Quantum Hall Regime Electron Vs. Fractional Charge

Thesis submitted in partial fulfillment
of the requirements for the degree of
"DOCTOR OF PHILOSOPHY"

by

Elad Shopen

Submitted to the Senate of Ben-Gurion University
of the Negev.

Approved by Prof. Yigal Meir, adviser:

Approved by Dean of Kreitman School of Advanced Graduate Studies:

December 4 2003

Kislev 9 5764

BEER-SHEVA

This work was carried out under the supervision of

Prof. Yigal Meir
Department of Physics
Faculty of Natural Sciences
Ben-Gurion University.

Many thanks to Prof. Yigal Meir and Prof. Yuval Gefen, my formal and informal supervisors . I have learned a lot from your wisdom and experience.

Thanks to all my friends who have suffered my moods and complaints along the way. Your direct and indirect support (naturally depending on how involved you are in physics...) is invaluable.

Special thanks to my family. To my parents who have gave me love and care from my infancy up to these days and showed me a way to become educated and smart as well as kind and loving. To Elinor, my daughter, for feeling my world with inestimable happiness during the last months of this thesis writing. To Ofira, my wife, for everything.

Dedicated to Ilana and Yoske, my parents.

Contents

Abstract	3
1 Introduction and Survey	6
1.1 The Quantum Hall Effect	6
1.2 Tunnelling In The Quantum Hall Regime	20
1.3 This Work : A Pictorial Description	25
2 Tunnelling Through A Barrier	30
2.1 Electrons on a Torus	31
2.2 Slater Determinant Decomposition Of Laughlin's Wave Functions	40
2.3 Valley States	49
2.4 Tunnelling Through A Barrier : An Electron Versus A Quasi Particle	54
2.5 Summary	60
3 Tunnelling Through The Quantum Hall Liquid	62
3.1 The Cylinder Tunnelling Problem	63
3.2 Fixed Number Of Impurities	69
3.3 Constant Density Of Impurities	77
3.4 Summary	80
4 Conclusions and Plans	82
4.1 Tunnelling Through A Mountain	82
4.2 Tunnelling Through The Sea	83
4.3 Plans	85
4.4 Closing Notes	87

APPENDICES	89
A Periodicity, Vanishing and Equalization	89
B A Useful Identity For The Single Particle Torus Wave Function	91
C A Summary Of Torus Wave Functions and Translation Operations	94
D Localized Hole Wave Function's Coefficients	97
E Effective Hamiltonian Approach	99
F Notations and Abbreviations	102
BIBLIOGRAPHY	104

Abstract

Many physical systems dealing with interacting particles share the idea of a quasi-particle - a fictitious effective particle that for many aspects can be treated as a fundamental particle in the problem, despite the possibly non trivial relation between it and the "real" particle. When considering superconductors as an example, one finds that the phenomenon involves pairs of electrons. These have some particle properties, and might even 'boson condensate' although the "real" particles in the problem are fermions. In the description of the fractional quantum Hall effect, the electron combines with vortices of magnetic flux, and together they form the effective particle. The idea of a quasi-particle reappears. Furthermore, this quasi-particle carries a charge which is not an integer multiple of electron charge but rather a fraction of it. The existence of such a fractional charge was first raised by R.B. Laughlin in a fractional quantum Hall effect explanation he proposed. The main question we shall ask is the following: "Can tunnelling of a fractional charge (i.e. a quasi-particle) occur through a potential barrier?"

The question has been investigated by a number of researchers. The most quoted work is probably the one by Kane&Fisher. They have studied the backscattering between two Luttinger liquid channels in the limit of weak and strong scattering limits. The backscattering corresponds to tunnelling between edge states in the quantum Hall regime. Under the influence of the weak scatterer it was found that the dominant tunnelling is that of a Laughlin's quasi-particle. This tunnelling occurs through the "electron sea". The noise accompanied with the backscattering current has been measured and the results confirmed that fractional charge does exist, as it was the measured noisy charge. On the other hand, when taking the strong scattering limit the possibility of a quasi-particle tunnelling (occurring through a "mountain" dried of electrons) was not considered. The reason is physical - a strong scatterer divides the system into two disconnected areas (electron "lakes"), each containing an integer number of electrons, the real particles. Hence the only possible tunnelling in this limit is that of an electron. If one artificially keeps the possibility of a quasi-particle tunnelling, one finds that it is a relevant quantity. But, as noted already, this studied two-lakes geometry physically forbids this possibility.

Nevertheless one can consider a connected geometry, i.e. a torus, with a potential barrier present on its surface. Fractional charge tunnelling is

now allowed because charge going through the barrier does not change the number of real particles present on the torus.

In this work we shall study the probability of fractional charge tunnelling and compare it to electron tunnelling. The logic is as follows- we shall find an expression for a state with an electron/quasi-particle present on one side of the barrier, and another state with the tunnelling object being on the other side. The probability to start at one state and end on the other is calculated. There are two essentially different possibilities for such a transition. The tunnelling can indeed occur through the barrier. But there also exists the possibility to tunnel roundabout through the electron sea. One can distinguish the two possibilities by finding out how the transition probability depends on the size of the system. If the probability strongly decreases when the system size is increased, we conclude that the tunnelling occurs through the liquid, and in case the dependence will be weak the tunnelling occurs through the barrier.

In the first chapter we describe the quantum Hall effect, and give the essential ideas we need for the description of the tunnelling problem and its solution. This includes the Laughlin's wave function, Kane&Fisher above mentioned work and also other tunnelling related works. The chapter ends with a relatively non formal description of this thesis.

The second chapter is the heart of the thesis. It presents our results regarding the tunnelling system-size dependence, for an electron and for a quasi-particle. The studied geometry is that of a torus. We therefore start with presenting Haldane&Rezayi's work regarding Laughlin's wave functions (with and without localized holes) on a torus. We investigate the expansion of these wave functions into Slater determinants and build the states of electron and quasi-particle (actually hole and quasi-hole) living on the two sides of the barrier. By studying the transition probability between these states we conclude that the electron can tunnel through the mountain while the fractional charge tunnels only through the sea.

In the third chapter we compare the transition of a fractional charge and an electron through the quantum Hall liquid. The geometry is cylindrical geometry, as we would like to disable the possibility of tunnelling through the barrier, present when considering the torus. We shall study the tunnelling from one side of the cylinder to the other. We also examine how disorder affects the tunnelling. It will be shown that addition of impurities enhances the tunnelling probability. Regarding electron versus fractional charge we

will show that the latter tunnelling decays slower than the electron tunnelling when the system size is increased. This result was previously obtained by Auerbach and is generalized here to the case of a number of impurities. We also find that in the limit of a fixed impurity density, the system size dependence changes from a gaussian decrease to an exponential one, a result previously obtained in the integer quantum Hall regime and which remains valid in the fractional regime as well.

Chapter four summarizes the results and concludes, together with further possible planned studies. These include investigating the crossover between the limits of weak and strong scattering, corresponding to tunnelling through a mountain or through the sea respectively.

Chapter 1

Introduction and Survey

In this introductory chapter we describe and crudely explain the quantum Hall effect. We shall introduce Laughlin's wave function which is of major importance in understanding the effect in general (including the prediction of fractionally charged quasi-particles) and this work in particular. Other relevant works are also reviewed. This includes the Shklovskii-Li-Thouless results regarding Green function's exponential tail, Auerbach who investigated the tunnelling of fractional charges and electrons across a quantum Hall strip and Kane&Fisher arguments about "transmission through barriers and resonant tunnelling in an interacting one-dimensional electron gas". We summarize the chapter with a presentation of the main idea in this work and also give some informal description of the results to be shown in the next chapters.

1.1 The Quantum Hall Effect

The Observations

Many reviews exist which cover the Quantum Hall Effect (QHE) [1]-[6]. Still we would like to give the basics, emphasizing issues that are relevant to this work, in particular Laughlin's "almost exact" wave function (WF) and the idea of fractional charge which appears pretty naturally in the description of the effect.

The Quantum Hall Effect appears in a two dimensional (2D) system of

electrons present in a uniform magnetic field B . The field is perpendicular to the 2D surface (we shall choose the magnetic field direction to be the z -axis). An example of such 2D surface is the interface between two semiconductors (or a semiconductor and an insulator). Electrons are trapped very close to this interface, therefore creating an effectively 2D system. These electrons are also influenced by a longitudinal electric field (let us choose the x -axis in this direction) and due to the uniform magnetic field they experience a Lorentz force along the y (actually $-y$) direction. The electrons drift aside and create a transverse electric field responsible for a transverse voltage difference called "Hall voltage", named after Edwin H. Hall, who discovered the classical Hall effect. Figure 1.1 summarizes this description.

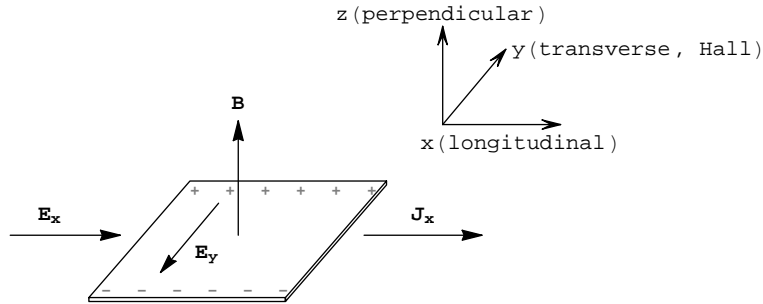


Figure 1.1: The quantum Hall bar. we shall follow the same choice of coordinates along the way, also when discussing other geometries, such as a cylinder.

The main experimental measurement involves the current, the longitudinal voltage and the Hall voltage. These quantities define the longitudinal and Hall conductivities (σ_{xx} and σ_{xy} respectively) by

$$J_a = \sigma_{ab} E_b$$

where \mathbf{J} is the current density, \mathbf{E} the electric field, σ the conductivity matrix, and a (and b) is an index that stands for either x or y .

In the classical Hall effect one finds that the Hall conductivity depends linearly on $1/B$. The effect is easily explained by the Drude model [7]. The balance between the Lorentz force and the transverse electric field leads to

$$\sigma_{xy} = \frac{ne}{B}$$

where $(-e)$ is the electron charge and n the carrier density, so indeed the dependence is linear in $1/B$. The longitudinal conductivity is expected to be magnetic field independent. This behavior is observed at a variety of temperatures, magnetic field strengths and in different samples.

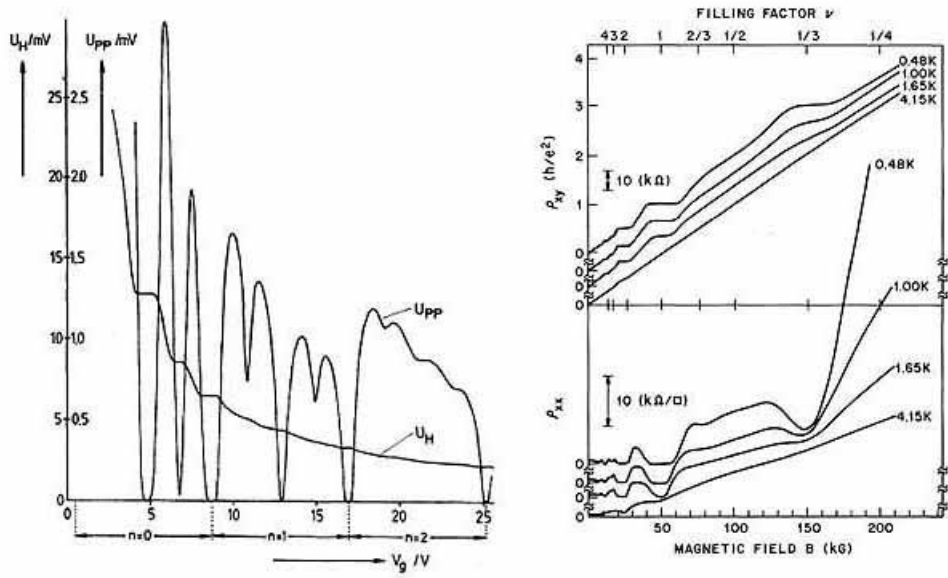


Figure 1.2: The quantum Hall effect observations: integer (left) and fractional. We present the original graphs. In Klitzing et.al. (left) the Hall and longitudinal voltages (U_H and U_{pp} respectively) are plotted as a function of gate voltage. Temperature is 1.5 Kelvin and the magnetic field is 18 T; In Tsui et.al. (right) the longitudinal and Hall resistivities are given as a function of magnetic field. The different lines correspond to different temperatures.

However when performing the measurements at very low temperatures and high magnetic field, the experimentalists [8] have observed a totally different behavior (see Figure 1.2, right).

The Hall conductivity exhibits a step-like dependence in $1/B$, with steps of equal height, independent of the sample's characters such as size or shape:

$$\sigma_{xy} = j \frac{e^2}{h}, \quad (1.1)$$

with j equals an integer. This (quantum mechanical) behavior is called the Integer Quantum Hall Effect (IQHE). Later on the experimentalists [9] have observed that for cleaner samples (usually at higher magnetic fields and lower temperatures), j can take fractional values of the form

$$j = q/p \quad (1.2)$$

with integer q and odd integer p (Figure 1.2, right). This is referred to as the Fractional Quantum Hall Effect (FQHE). We hereinafter give a simple illustrative explanation for these observations. As we shall see the explanation involves some features of electrons present in (strong) magnetic field together with sample's disorder (this basically explains the IQHE) and the interactions between the electron (that will be essential to the explanation of the FQHE). The spin degrees of freedom are supposed to be frozen by the magnetic field. Let us begin by describing the much simpler problem of one electron in a magnetic field.

An Electron In A Magnetic Field

The starting point is the Hamiltonian of a particle having mass m_e and charge $(-e)$ moving in a uniform magnetic field B :

$$H = \frac{1}{2m_e} \left(\mathbf{p} + \frac{e}{c} \mathbf{A} \right)^2, \quad (1.3)$$

where \mathbf{p} is the momentum operator and \mathbf{A} the vector potential satisfying $\nabla \times \mathbf{A} = B\hat{z}$. The obtained energy eigenvalues are the so called Landau levels given by

$$\varepsilon_n = \hbar\omega_c \left(n + \frac{1}{2} \right), \quad (1.4)$$

where $\omega_c \equiv \frac{eB}{m_e c}$ is the cyclotron frequency, the classical circular motion's frequency.

As long as one deals with an infinite sample the problem has infinite degeneracy¹. But when a finite sample is treated, the degeneracy becomes finite and turns out to be equal to the magnetic flux ϕ perpendicular to the sample's area S , in units of $\phi_0 = hc/e$ (one "flux quanta"). Marking the degeneracy by N_ϕ we have

$$N_\phi = \frac{\phi}{\phi_0} = \frac{S}{2\pi l_H^2}, \quad (1.5)$$

where we have defined $l_H \equiv \sqrt{\hbar c/eB}$, the magnetic length.

Let us demonstrate how one might obtain this relation. The eigenfunctions of the Hamiltonian given in eq.(1.3) and written in the symmetric gauge

$$\mathbf{A} = -\frac{1}{2}\mathbf{r} \times \mathbf{B}. \quad (1.6)$$

are [3]

$$\varphi_{m,n} = (2^{m+n+1}\pi m!n!)^{-1/2} e^{+|z|^2/4l_H^2} \left(\frac{\partial}{\partial x} + i\frac{\partial}{\partial y}\right)^m \left(\frac{\partial}{\partial x} - i\frac{\partial}{\partial y}\right)^n e^{-|z|^2/2l_H^2} \quad (1.7)$$

with $z \equiv x + iy$. These energy eigenfunctions are also eigenstates of angular momentum operator with eigenvalues $(m - n)$.

For the lowest Landau level (LLL) the eigenfunctions are

$$\varphi_m = (\pi l_H^2 2^{m+1} m!)^{-1/2} \left(\frac{z}{l_H}\right)^m e^{-|z|^2/4l_H^2}. \quad (1.8)$$

The distribution of these states in the radial direction has a l_H -width gaussian-like shape and is uniform in the azimuthal direction. This shape is that of a ring with radius $\sqrt{2m} l_H$. The m -th ring encloses m flux quanta of magnetic flux. Therefore assuming these wave functions are still valid for a finite sample² we conclude that the degeneracy for this particular example is indeed as given in (1.5).

¹Classically the kinetic energy does not depend on the cyclotron orbit's center, so this degeneracy is expected. The degeneracy is revealed by building quantum orbit center operators. This is explained clearly in [3].

²This assumption is valid for disk geometry far from the sample's edge. If the magnetic field is high, which is the QHE case, we have a large number of such wave functions, so this assumption is pretty good. Still we should keep in mind the (important) edge physics is being left out of the game.

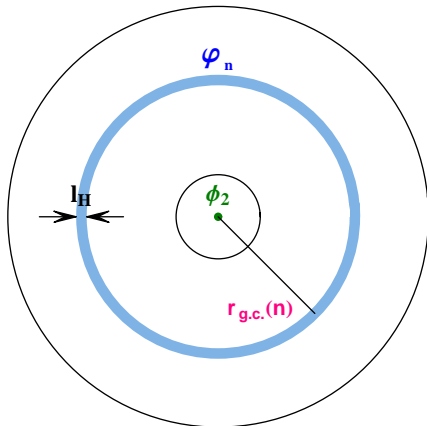


Figure 1.3: A schematic presentation of single particle eigenfunctions (of the Hamiltonian and the angular momentum operators) for the annulus geometry. The wave function distribution depends on the radial coordinate like a gaussian with width of the order of l_H and which is centered around the $r_{g.c.}(n) = \sqrt{2nl_H}$, called the guiding center. By adiabatically changing ϕ_2 (the magnetic flux through the annulus center) the wave functions' guiding center is smoothly increased, keeping the total flux enclosed by the each guiding center an integer multiple of ϕ_0 .

This symmetric-gauged LLL example also points at another idea which is of major importance to our work. The idea we will refer to as "solenoid flux". Figure 1.3 presents an annulus geometry sample (so called "corbino disk"). Far from the edges one can still take (1.8) as good energy eigenfunctions. But what happens if the magnetic flux through the central hole is adiabatically increased (e.g. by adding a thin solenoid at the origin)? It turns out that the WF's ring radius (called guiding center) adiabatically increases in order to keep the enclosed total flux an integer multiple of ϕ_0 . When this solenoid flux is changed exactly by one flux quanta the problem becomes physically identical to the starting problem as now the solenoid can be "gauged out", so each guiding center just evolved to an adjacent one. Formally this procedure can be done by defining a generalized gauge potential \mathbf{A} , still satisfying $\mathbf{B} = \nabla \times \mathbf{A}$, but whose line integral around a closed loop gives the desired solenoid flux³.

³More explicitly one can use $\mathbf{A} = -\frac{1}{2}\mathbf{r} \times \mathbf{B} + \frac{\phi_2}{2\pi r}\hat{\varphi}$. $\hat{\varphi}$ is an azimuthal oriented unit

Quantum Hall Effect Explanation

When dealing with a system with many electrons a general typical Hamiltonian will contain a kinetic term H_0 , a background potential V_{back} (possibly including a random potential presenting the system's disorder) and an electron-electron interaction V_{int} . More explicitly

$$H = H_0 + V_{back} + V_{int} , \quad (1.9)$$

where

$$H_0 = \frac{1}{2m_e} \sum_{j=1}^N (\mathbf{p}_j + \frac{e}{c} \mathbf{A}(\mathbf{r}_j))^2 ,$$

$$V_{back} = \sum_{j=1}^N V_b(\mathbf{r}_j) ,$$

$V_b(\mathbf{r})$ being the one particle background potential, and

$$V_{int} = \sum_{i < j} V(\mathbf{r}_i - \mathbf{r}_j)$$

with $V(\mathbf{r})$ being the two-body interaction energy.

Neglecting everything but the kinetic energy the many body ground state is obtained by filling the Landau levels one after another. A useful characterization is the so called filling factor ν defined by

$$\nu \equiv N/N_s , \quad (1.10)$$

where N is the number of particles.

In a system without randomness and interactions whenever a Landau level is full and therefore ν is an integer, there is a discontinuity in the chemical potential, because the next added electron is being added to a higher Landau level. Keeping that in mind we would like to introduce randomness into the picture. Figure 1.4(a) qualitatively gives the density of states as a

vector and ϕ_2 is the solenoid flux.

function of energy. The (previously infinitely thin) Landau levels are broadened by the random potential. The energy spectrum in between each Landau level is being filled with localized states which are unable to carry current. Randomness divides the possible states into two categories - extended ones at the middle of each Landau level and "frozen" localized states. A very constructive related work was done by Prange [10] who treated electrons in a perpendicular magnetic and transverse electric fields, and also influenced by one delta function impurity. As a result of the delta impurity there exists a non-carrying current localized state. This work was later extended by Prange and Joynt [11, 12] to more general random potentials. It is interesting to note that even though the random potential localizes some states, the remaining extended states carry current as if the whole relevant Landau level is filled, so the vigorous electrons are going faster and compensate the laziness of the localized ones.

The existence of localized and extended states can sketchily explain the IQHE. Figure 1.4(b) shows schematically the experimental observation of the IQHE. When the density of electrons is increased⁴, the Fermi energy increases. As long as the extended states are favorable energetically (the Fermi energy lies in an extended state zone) the conductance increases as more current-carrying electrons are being added. But as the Fermi energy exceeds the localized states energy, increasing the density does not increase the conductivity, as the added electrons are stuck. That is the plateau.

So far so good for the IQHE. What about the fractional one? Recall that for non-interacting electrons and zero disorder the chemical potential is discontinuous whenever ν is integer. And the conductance quantized value was as if ν is an integer. So if we find some mechanism giving such discontinuity at fractional valued ν , we can keep the above IQHE explanation. The mechanism is given by introduction of interactions. That was investigated extensively by R.B. Laughlin [13, 14, 1].

The Many Body Laughlin's Wave function

Laughlin has studied interacting electrons in the presence of a magnetic field for low particles number ($N = 2$ and 3) [13]. This study encouraged him to guess a variational ground state WF for the case of a general N [14]. The first

⁴this is equivalent to changing $1/B$.

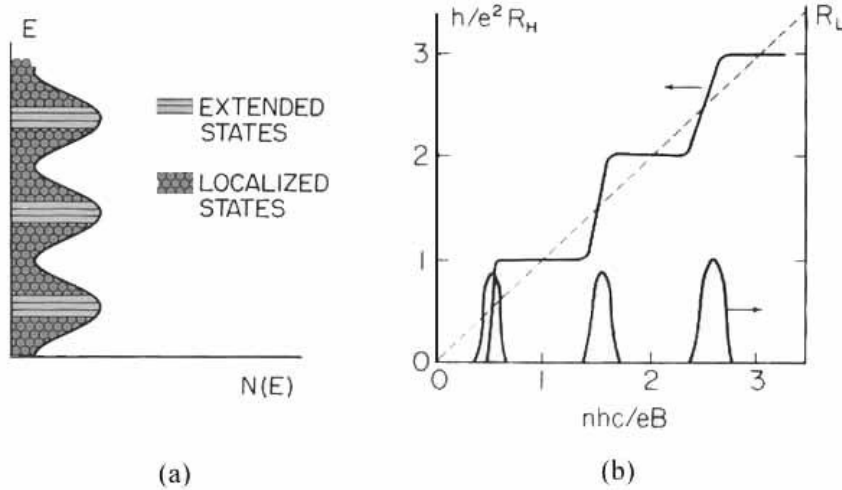


Figure 1.4: (a) The density of states for a system present in a magnetic field. Disorder broadens the Landau levels into two possible states: extended and localized. (b) A schematic graph based on the experimental measurements of the QHE. R_L and R_H are the longitudinal and Hall resistivities respectively.

studies were done for the already mentioned disk geometry. Laughlin first guessed the state's general form, based on the study of plasma physics. The suggested form has the so called Jastrow form, $\prod_{i<j} f(z_i - z_j)$, multiplied by $e^{-\sum_j |z_j|^2/4l^2}$, $z_j = x_j + i y_j$ (j being the particle index). Then by few assumptions and remarkably without really doing any variation (besides the above mentioned general form) he concluded that $f(z) = z^m$, with odd m . This WF was numerically compared to the exact ground state WF for few selected interactions⁵ and small particle number, and the overlap between the compared WFs was very closed to unity, regardless the specific interaction form! This is why people call the LWF "almost exact".

In deducing the given form one should restrict the search to the LLL (therefore $f(z)$ should be a polynomial) and keep in mind that the total angular momentum (TAM) is a good quantum number (because the interaction energy does not mix states with different TAM⁶). The power m must be

⁵In Laughlin's original work the compared interactions are coulomb, gaussian and logarithmic.

⁶The Hamiltonian naturally conserves angular momentum.

odd in order to keep the WF's antisymmetry for particle's exchange. So the Laughlin WF (LWF) Ψ_L is finally given by

$$\Psi_L = C_L \prod_{i < j} (z_i - z_j)^m e^{-\sum_j |z_j|^2 / 4l_H^2}, \quad (1.11)$$

C_L is a normalizing constant. The TAM of this LWF is $mN(N-1)/2$.

Many properties of LWF were deduced by the "plasma analogy" [1]. One such property is the density of LWF which turns out to be $1/m$, in units of $(2\pi l_H^2)^{-1}$. Following the degeneracy relation, eq. (1.5), this leads to a filling factor of $1/m$:

$$N_\phi = mN \text{ for LWF} . \quad (1.12)$$

The LWF density can be hand-wavily obtained also by noting that the maximal occupied angular momentum in Ψ_L is $m(N-1) \approx mN$, therefore⁷ the particle's density is

$$\frac{N}{S} = \frac{N}{\pi(\sqrt{2mN}l_H)^2} = \frac{1}{2\pi l_H^2} \frac{1}{m} .$$

Giving a unique ground state for $1/m$ filling factor, the LWF can therefore basically explain the observed $1/m$ conductivities. The state Laughlin proposed is a state of incompressible liquid. In a slight modification of the overall density (e.g. by compression), the system prefers to keep the density $1/m$, creating localized quasi holes (or particles) to overcome the modification. A suggestion for a quasi hole WF was also made by Laughlin [14]. The LWF was later generalized to filling fractions other than the Laughlin's $1/m$ states [15].

We should note a useful property of Laughlin's WF - the fact that for $m = 1$, it is built only out of all the first N LLL single particle states. As now $\nu = 1$, an integer, the WF is just the non-interacting one - a (Vandermonda) Slater determinant (SD)

$$\text{For } m = 1 : \Psi_L = |0, 1, \dots, N - 1 \rangle \quad (1.13)$$

where

⁷assuming uniform density which is a good approximation far from the boundaries.

$$|j_1, j_2, \dots, j_N \rangle \equiv \frac{1}{\sqrt{N!}} \begin{vmatrix} \varphi_{j_1}(z_1) & \varphi_{j_2}(z_1) & \dots & \varphi_{j_N}(z_1) \\ \vdots & \vdots & & \vdots \\ \varphi_{j_1}(z_N) & \varphi_{j_2}(z_N) & \dots & \varphi_{j_N}(z_N) \end{vmatrix} . \quad (1.14)$$

Haldane [16, 1] and later on Trugman and Kivelson [17] (TK) have shown that LWF is an exact groundstate of a Hamiltonian consisting of a kinetic term together with the so called "hardcore" interaction between the particles. This interaction is just

$$V(\vec{r}) = \nabla^2 \delta(\vec{r}) , \quad (1.15)$$

one of a truly short range, which presumably captures many characteristics shared by a wide range of possible (real or purely theoretical) interactions. Trugman and Kivelson first discuss some general properties of short range interactions⁸ and only then prove the exactness of LWF regarding the short hardcore interaction, mainly by showing that the interaction energy for LWF is zero, obviously the minimal possible energy for repulsive interaction. This exactness is very useful in numerically getting the decomposition of Ψ_L into SDs $|j_1, \dots, j_N \rangle$ for a general m . We return to this point in Chapter two.

Localized Holes States

Together with proposing the trial ground state WF, Laughlin also suggested the form for an excited (un-normalized) WF

$$\Psi_{(z_0)} = \prod_{j=1}^N (z_j - z_0) \Psi_L . \quad (1.16)$$

The state is physically interpreted as a quasi hole (having a fractional charge) localized at z_0 . The function's variational form is motivated by a gedanken experiment in which one inserts an infinitely thin solenoid into the origin and slowly changes the solenoid flux from zero to ϕ_0 . By this procedure the Hamiltonian is changed to a gauged equivalent version of the original Hamiltonian (the one of no flux), and adiabatically following the

⁸interactions shorter than $1/r^2$.

LWF, will lead to a new eigenfunction of the (original) Hamiltonian. If this state is not degenerate we have an excited state. This procedure takes each of the single particle states composing Ψ_L (the eigenstate of no flux), to the "next" adjacent single particle state : $\varphi_n \propto z^n e^{-|z|^2/4l_H^2} \rightarrow z^{n+1} e^{-|z|^2/4l_H^2}$, so the overall function Ψ_L is transformed into $\prod_{j=1}^N z_j \Psi_L$ ⁹. Generalizing the above to a case of a flux tube located at arbitrary z_0 , leads to (1.16).

The charge fractionality can be shown (at least for a localized hole at the origin) to indeed be fractional, specifically e/m , in the following manner. By increasing the solenoid flux from zero to ϕ_0 , each single particle state, holding a charge of e/m ¹⁰ evolves to the adjacent state, therefore the overall effect of inserting the solenoid is a charge of e/m that has been pushed from the origin to the boundaries. One can prove that the quasi particles carry fractional charge by more general methods (see for example [1, 5]) using only (1.1). Laughlin himself has predicted the existence of fractional charges also by the plasma analogy [14].

The above procedure can be repeated in order to create a LWF with N_h localized (quasi) holes,

$$\Psi_{\{z_{0k}\}} = \prod_{j=1}^N \prod_{k=1}^{N_h} (z_j - z_{0k}) \Psi_L \quad (1.17)$$

where z_{0k} is the location of the k -th localized hole and the subscript $\{z_{0k}\}$ is a short for $\{z_{01}, z_{02}, \dots, z_{0N_h}\}$. Note that the wave function depends explicitly on x_j and y_j . Still we use this shortcut notation. We shall call this state LWF with N_h localized holes. It is sometimes helpful to notice that the creation of m quasi holes at the same location z_0 , is equivalent to the creation of one "real" hole (with charge e) at the same place, so that the function one gets in that manner looks like a function of $(N+1)$ particles with $z_{N+1} = z_0$. Girvin has shown [18] that for $\nu = 1$, the LWF with one localized hole is exact. Starting from a ($\nu = 1$) LWF of $(N+1)$ particles $\Psi_L(z_1, \dots, z_N, z_0)$, one can build a state ψ_n which is composed out of all single particle WFs within the LLL $\{\varphi_0, \dots, \varphi_N\}$, except the n th single particle WF φ_n . This is

⁹This statement is exact for $m = 1$. For different m single particle normalization factors enter into the picture. We, following Laughlin, will ignore this difference.

¹⁰The total charge is eN and there are N_ϕ single particle WFs participate in the expansion on Ψ_L , therefore using the degeneracy condition (1.5) and assuming each single particle WF holds the same charge, this charge is indeed e/m .

done by

$$\psi_n \propto \int_{\text{all space}} dz'_0 \varphi_n^*(z'_0) \Psi_L(z_1, \dots, z_N, z'_0) . \quad (1.18)$$

It was then shown that if instead φ_n one takes a function with the most localized distribution possible¹¹ around z_0 , the above integral exactly gives the hole state, localized at z_0 , proposed by Laughlin. Equation (1.18) will be further investigated in the next chapter.

As LWF with N_h localized holes vanishes whenever any particle coordinate coincides with the localized hole coordinate, it can be interpreted as a ground state of a Hamiltonian (1.9) with interaction being hardcore and a background potential of the form

$$V_b = \sum_{j=1}^{N_h} v_j \delta(\mathbf{r} - \mathbf{r}_{0j}) \quad (1.19)$$

where \mathbf{r}_{0j} is the location of the j -th hole, and v_j is a positive constant. Physically the j -th term in this sum can represent a very localized impurity at \mathbf{r}_{0j} , having v_j strength. Using this fact we shall study the effect of (positive) impurities in a tunnelling problem. This is done in chapter three.

Other Geometries - A Cylinder And A Torus

We would like to close this section introducing the corresponding expressions of the single particle states and LWF (with and without localized holes) for the two main geometries we shall study in the following chapters, the cylinder and the torus.

The LLL single particle Hamiltonian eigenfunctions for the case of cylindrical boundary conditions- periodicity in $2\pi R$ regarding one axis only, chosen to be the x axis ($\varphi(x + 2\pi R, y) = \varphi(x, y)$), are

$$\varphi_n = C e^{-(y-nl_H^2/R)^2/2l_H^2} e^{-inx/R} \quad (1.20)$$

$$= C e^{-n^2 l_H^2 / 2R^2} e^{-y^2/2l_H^2} e^{-inz/R} \quad (1.21)$$

with $C = (2\pi R l_H \sqrt{\pi})^{-1/2}$. Landau gauge $\mathbf{A} = -By\hat{x}$ was chosen. These are eigenstates of momentum operator. The distribution of these states is

¹¹The most localized distribution one can built is a gaussian [18].

gaussian in the y -direction, the main cylinder axis (see Figure 1.5) and it is uniform in the x direction. Different states corresponds to different locations of the gaussian's (guiding) centers and the distance between adjacent WFs is l_H^2/R . As for a disk or an annulus, one can define a solenoid flux penetrating the cylinder. By adiabatically changing this flux the gaussians slide in the y direction. Again, due to gauge symmetry, changing the flux by ϕ_0 does not effect the whole WFs set, so each WF has been shifted in l_H^2/R .

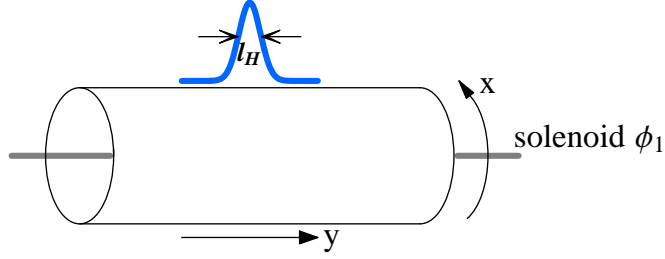


Figure 1.5: The cylinder Hamiltonian eigenfunction form gaussians of width l_H in the y direction, the symmetry axis of the cylinder. Varying ϕ_1 , the magnetic flux through the cylinder's hole results in the "sliding" of the gaussians along the symmetry axis.

The LWF for the cylinder can be immediately guessed by noting the similarity between the single particle WFs (1.20) to those living on a disk (1.8). One just has to replace z by $e^{-iz/R}$. The result (given by Thouless [19]) is

$$\Psi_L = e^{-\sum_j y_j^2/2l_H^2} \prod_{i<j} (e^{-iz_i/R} - e^{-iz_j/R})^m . \quad (1.22)$$

In a same manner one can write the cylindrical LWF with N_h localized holes

$$\Psi_{\{z_0\}} = \prod_{j=1}^N \prod_{k=1}^{N_h} (e^{-iz_j/R} - e^{-iz_{0k}/R}) \Psi_L . \quad (1.23)$$

Both LWFs are not normalized.

The Laughlin's WF (*without* any localized holes) is composed only out of SDs with the same total momentum in the x direction. Because of the

similarity with the disk format, we will continue to use the term TAM, to represent the total momentum in the x direction, whenever the cylinder will be treated. For the torus, the TAM will stand for "total quasi momentum" (also in the x direction), this quasi-momentum now being the good quantum number (see eq. 2.17).

The torus geometry is the folded version of either the cylinder or the annulus. In the next chapter we review the work of Haldane and Rezayi [20] regarding the LLL single particle WF and LWF written for electrons living on a surface of a torus. As we shall see, one cannot achieve total periodicity in boundary conditions. Instead "quasi-periodic" boundary conditions are required. The resulting single particle WFs obtained are described in detail in the next chapter and summarized in the appendix. They form gaussian-like distributions along the y axis, and are almost uniform along the x direction (see Figure 2.1 on next chapter). For the torus case, two independent solenoid fluxes are possible - one (ϕ_1) inside the torus and the other (ϕ_2) passing through the torus' center (see Figure 1.9). Mathematically they naturally enter via the generalized boundary conditions. The effect of increasing ϕ_1 and ϕ_2 is sliding the WFs in the y or x directions respectively. This is true for any many-body WF as well, as it can be expressed in terms of single particle states. Haldane and Rezayi also discussed the localized hole Laughlin's state, which is generalized in the next chapter to N_h localized holes.

1.2 Tunnelling In The Quantum Hall Regime

In this section we shall describe few works dealing with the problem of charge tunnelling in the quantum Hall regime. First the tunnelling of fractional and integer charges as described in a series of articles by Kane and Fisher [21, 23]. These actually motivated this thesis. We also review a result obtained by Li and Thouless [26] (previously obtained by Shklovskii [27]), regarding the influence of weak random potential on the IQHE Green function, namely the function's "exponential tail". In chapter three we shall prove this result by a different mechanism, and generalize it to the case of the FQH regime. Another result to be repeated and generalized is the work of Auerbach [28] who compared fractional charge versus electron tunnelling through the quantum Hall liquid. This section is meant to be very sketchy and illustrative.

Tunnelling A-la Kane And Fisher

The Kane and Fisher (KF) arguments deal with the QHE edge states. The importance of edge states in the QHE regime was studied by many. Halperin [29], for example, has shown, by elaborating a previous argument made by Laughlin [30], that the edge states remain extended even in the presence of a random potential. One can get an intuitive understanding of the edge states thinking about it semi classically. The classical trajectory of an electron in a magnetic field is circular. But when these circulating electrons become very close (distance of the order of the magnetic length) to the system's edge, the motion is disturbed by the edge. For a sharp edge the electrons are totally reflected by the walls therefore creating a chiral motion around the edge (Figure 1.6). When the system is also influenced by an external electric field in the longitudinal (x) direction, this motion splits into (a one dimensional (1D)) left and right movers, as the symmetry in the x direction breaks.

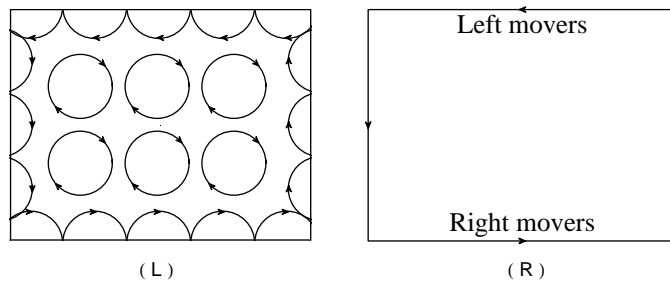


Figure 1.6: (L) Electrons semi-classical circular motion. The electrons near the edge are being bounced of the walls creating an effectively 1D motion around the sample's edge. (R) Influenced by the longitudinal electric field, the 1D electron motion splits into left and right movers, depicted here schematically. This motion was mapped to the Luttinger liquid model.

The 1D edge motion was mapped by Wen [31] to a theoretical model known as the Luttinger-Tomonaga liquid, describing right and left moving particles in 1D¹². One can study this system for non-interacting or interacting particles, and get a comparison between the I and F QHE respectively,

¹²The Luttinger liquid is a model of (generally) interacting electrons with energy spectrum which is linearized around the Fermi energy. This model has been studied extensively since its first formulation. Amongst the techniques used to study the model is the idea of

including the existence of integer versus fractionally charged particles¹³. By introducing a scattering mechanism, one can also study the tunnelling of particles (or quasi-particles) in between the right and left channels. This was lengthily done by KF. Amongst other topics they have looked at two major limits which are illustrated in Figure 1.7.

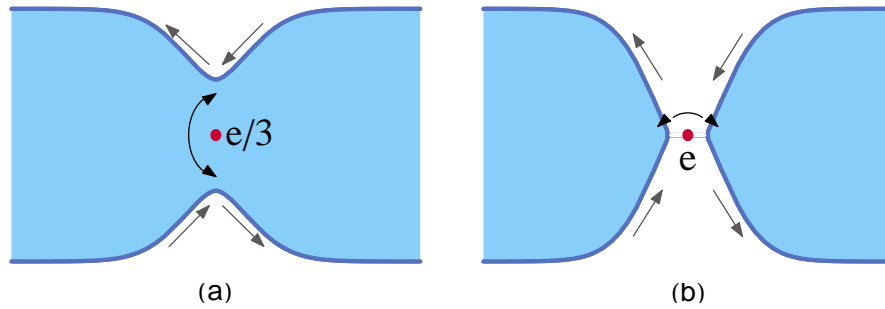


Figure 1.7: Kane and Fisher have investigated the Luttinger liquid 1D motion of integer and fractional charge, with applications to measurements in the quantum Hall regime. Two limits were treated: (a) weak scatterer, the edge states are slightly pushed one towards the other. Integer or fractional charge tunnelling are possible in principle, the latter was found to be the dominant tunnelling object; (b) strong scatterer, cutting the sample into two islands, and therefore physically allowing only electron's tunnelling.

First comes the limit of "weak backwards scattering" (in Luttinger liquid language) depicted in Figure 1.7(a). The two channels are being slightly pushed one towards the other. Experimentally this might be done by imposing a gate voltage in the y direction. Tunnelling of particles (electrons or fractionally charged quasi-particles) in such a system can occur through the quantum Hall liquid. KF have showed that in this weak scattering limit the dominant backwards tunnelling is that of a fractional charged quasi-particle. It was found that in this limit, if the tunnelling is slow enough, the noise fluctuations will have a form of classical shot noise with a fractional charge carrier. This work is related to experiments in which the existence of frac-

bosonization. This idea together with the KF work are reviewed by Glasman and Fisher in [23].

¹³The mapping includes identification of the filling factor ν with the Luttinger liquid interaction parameter. The existence of fractionally charged quasi-particles in the Luttinger liquid was predicted by their finding in the QHE Laughlin explanation.

tionally charged particles was observed by measuring the current shot noise [24, 25].

The second studied limit is the "strong scattering" limit (Figure 1.7(b)), being achieved by increasing the gate voltage so much that the system is being split into two very weakly connected islands. In this limit KF did not take into account the tunnelling of fractionally charged particles, based on physical considerations- the fractional charges exist in a system with integer number of electrons, therefore a quasi particle cannot tunnel in between two disconnected electron islands. So in the limit of strong backscattering the only physical relevant tunnelling is that of electrons . This limit, as explained in the next section, is the main motivation for our work. One can think of a system which lacks the restriction. For example, one can connect the two islands from around. We shall refer to the strong and weak limits as tunnelling through a barrier (this is the subject of chapter two) and tunnelling through the QHE liquid (chapter three) respectively.

Tunnelling A-la Auerbach

Auerbach [28] has compared electron and fractionally charged particle passing through the QH liquid with the aid of a localized (delta function) impurity. The system Auerbach has looked at is described in Figure 1.8. The geometry is cylindrical. The calculated property is the probability for the system to start in the Laughlin's state Ψ_L and to end in a state with all the single particle states shifted by one. As described in the first section, such a transition is that of one quasi-particle (an electron for integer filling) tunnelling from one cylinder's edge to the other. The shifted state is marked by $\tilde{\Psi}_L \equiv T_y \Psi_L$, T_y being an operator increasing each single particle state quantum number by one.

For a clean system the possibility for such an event to occur is zero as the two states are orthogonal (their TAM is different). So one should introduce an additional potential that would couple the two states. Auerbach chose two such potentials (v is a constant) :

1. $V(x) = v \delta(x)$.
2. $V = v \delta(x) \delta(y - L/2)$ is a localized impurity at $x = 0$ and $y = L/2$, where L is the cylinder's center.

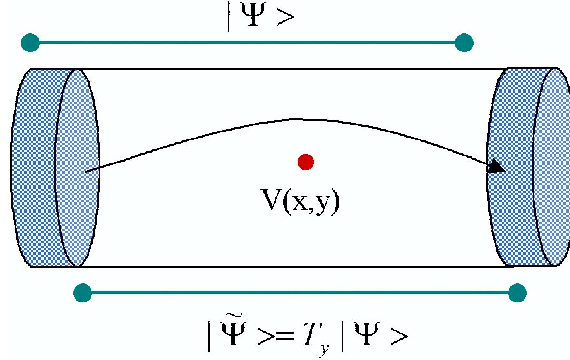


Figure 1.8: Auerbach has studied the tunnelling of e/m charges from one cylinder's side to the other by introducing a perturbing impurity potential, and calculating $\langle \Psi | V_{imp} | \tilde{\Psi} \rangle$, $|\Psi\rangle$ and $|\tilde{\Psi}\rangle$ being two displaced Laughlin states with filling factor $1/m$.

The calculated tunnelling probability is

$$\mathcal{T} \equiv \langle \tilde{\Psi}_L | V | \Psi_L \rangle, \quad (1.24)$$

so speaking in terms of Hamiltonian (1.9) this is a first order calculation. The unperturbed Hamiltonian is $H_0 + V_{int} + V_{conf}$, where V_{conf} is a confining potential selecting Ψ_L and $\tilde{\Psi}_L$ as lowest energy states out of all possible Laughlin's states (this confining potential therefore defines the cylinder). The perturbing potential is one out of the two above mentioned potentials. So indeed (1.24) gives the required tunnelling rate. Auerbach has shown that for these two possibilities

$$\mathcal{T} \approx \exp[-L^2/4m l_H^2], \quad (1.25)$$

where m is either 1 (electron tunnelling) or 3 (fractional $e/3$ charge tunnelling). As the exponent decreases slower for the fractional charge Auerbach concludes that a fractional charge tunnelling through the QH liquid is faster than the electron's tunnelling. Note that this is true if the tunnelling is compared at the same value of l_H^2 , i.e. same magnetic field. Nevertheless the particle's density is higher for the integer case. For the same density¹⁴, rather

¹⁴This means that the magnetic field one should take for any m is m times the magnetic field for $m = 1$.

than magnetic field, the result for both an electron or a fractional charge is identical in the thermodynamic limit, supporting a belief that the tunnelling in the OH regime, integer or fractional, is basically equivalent.

Tunnelling A-la Shklovskii-Li-Thouless

Schklovski and then Li and Thouless dealt with the influence of a random potential on a system of non-interacting electrons present in a magnetic field. We shall concentrate on Li&Thouless. Starting from the Green function for the system without disorder [12]:

$$G_0(\mathbf{r}, \mathbf{r}'; E + i\varepsilon) = \sum_{n=0}^{\infty} \int dk \frac{\phi_{nk}(\mathbf{r}) \phi_{nk}^*(\mathbf{r}')}{E - E_n + i\varepsilon}$$

they introduced a random (white-noise) potential perturbatively into the picture. After some simplifications and assumptions¹⁵, using variational method applied to Dyson's equation, it was shown that the Green function for the white-noise-perturbed system has an exponential tail

$$\langle |G(\mathbf{r} - \mathbf{r}'; E)|^2 \rangle \approx e^{-2\alpha|\mathbf{r}-\mathbf{r}'|} . \quad (1.26)$$

$\langle \rangle$ denotes averaging over disorder and α is a constant which is determined by the strength of the random potential¹⁶. This calculation is relevant for the (hopping) tunnelling of electrons in the presence of randomness. We emphasize the fact that the non-disordered system has a gaussian tail becoming exponential as the randomness is introduced.

1.3 This Work : A Pictorial Description

The KF work dealt with electron versus quasi-particle tunnelling in the limits of very weak or strong scatterer, which corresponds to tunnelling between the sample's edges through the Quantum Hall Liquid, or through a barrier

¹⁵As explained in [26] the assumptions are valid far from the center of the energy band and for weak enough disorder.

¹⁶For large value of α it was found that $\alpha \approx (-\frac{1}{2} \ln W)^{1/2}$, W parameterizes the strength of the disorder.

respectively. In the latter case, taking into account the tunnelling of quasi-particle in KF's studied configuration is physically not reasonable, so this process was ignored. Motivated by this we thought of looking at the barrier tunnelling problem, in a geometry that lacks KF's restriction. This can be achieved by connecting the two previously disconnected liquids "round about". One possible such geometry is that of a torus¹⁷ which basically allows tunnelling of fractionally charged quasi-particles through the barrier, still keeping the total charge an integer multiple of electron's charge. The sample model is sketched in Figure 1.9: a torus with a (positive) barrier the particles want to avoid, but finite enough to allow them to tunnel through it.

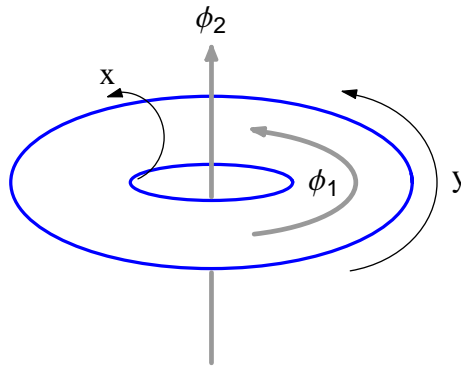


Figure 1.9: The Torus. The double line stands for the potential barrier through which an electron (or a quasi-particle) can tunnel. The solenoid fluxes ϕ_1 and ϕ_2 are also shown.

The system will be described by many-body WFs having the following properties : they all lie in the LLL, they minimize the (hard core) interaction between the electrons, and their (single particle) density has a valley landscape: an area dried of electrons which minimizes the energy when the valley is chosen near the barrier. The valley WFs can be thought of as a full Laughlin's state of $N + 1$ electrons with one single particle WF removed,

¹⁷A torus with uniform magnetic field perpendicular to its surface is unreasonable experimentally. Theoretically it provides a rather convenient geometry for answering the questions we will address. Still, one can think of other geometries with the same physics which are experimentally possible - a annulus with a barrier located along the radial axis is one such possible example.

therefore creating an extended hole, a valley¹⁸. For $m = 1$ it is basically an exact solution. Generalizing this to other values of m is done in chapter two. In any case the distribution of these WFs is uniform in the x direction, while in the y direction it has a minima (the valley location) located at a certain y_0 (see Figure 2.3 for the real obtained density). The distance between adjacent valleys is L_2/N_ϕ . We will introduce N_ϕ such valley-WFs, equal to the number of flux quanta perpendicular to the torus surface. The tunnelling problem will be described in terms of these N_ϕ valley-states. Finally we need the solenoid flux passing through the torus holes (see Figure 1.9), denoted by ϕ_1 . By changing ϕ_1 adiabatically, the valley WFs continuously slide in the y direction.

Now we are ready for the description of the (naive) tunnelling, described in figure 1.10. We start with one valley-state sitting on the barrier. Let us call this state Ψ . For the case of no barrier, the set of N_ϕ valley WFs is degenerate, but as the barrier enters the problem it removes this degeneracy, picking Ψ as the lowest energy state. The magnetic flux through the torus, ϕ_1 , is now adiabatically increased. All the valley states, including Ψ start sliding in the y direction. The starting state Ψ remains a lowest energy state as long as its valley is closest to the barrier. But as the flux increases, an adjacent state's valley, marked by $\tilde{\Psi}$, gets closer and closer to the barrier, until it becomes energetically favorable. The density of two states is different by a charge of e/m sitting on a different side of the barrier. A transition from Ψ to $\tilde{\Psi}$ therefore fits a jump of e/m charge from one side of the barrier to the other. So if the system indeed follows the line of minimum energy, we have a fractional charge tunnelling event. Figure 1.10 shows the energy levels as a function of ϕ_1 for few selected valley states.

Still the tunnelling event is not clear, as the energy levels cross (the two states become degenerate at a certain value of the magnetic flux). These two levels cross unless the symmetry in the x -direction is broken¹⁹. Therefore, in order to be able to investigate the tunnelling event (and get a more reasonable physical situation), we introduce an additional potential, marked by V_{imp} , which breaks the symmetry in the x -direction (e.g. we can add an impurity potential). By doing that a gap opens and the levels separate (see Figure 4.1).

¹⁸In principle one can start with a many-body WF of $N + N_{ext}$ electrons, throwing away N_{ext} chosen single particle states, thus creating a WF having N_{ext} extended hole, a wider valley. We will be satisfied with one such extended hole.

¹⁹This is, of course, proven in Chapter two.

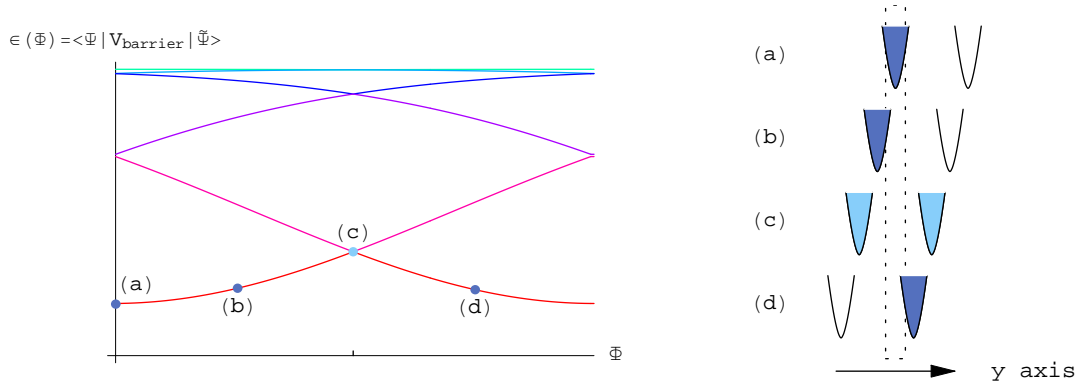


Figure 1.10: Increasing the flux adiabatically results in sliding of the valley-WFs to the left. This changes the energy as a function of ψ_1 (Right figure). The valley-states which are closest to the barrier mountain as depicted on the right figure. Naively following the minimal energy line, results in a tunnelling of e/m charge from one side of the mountain to the other. The tunnelling is shown in four frames, (a)-(d). In (a) and (b) the state having minimal barrier energy is the right valley WF, in (c) the two states are degenerate. Increasing the flux further makes the left valley energetically favorable. A real tunnelling must involve a perturbing potential, which is necessarily non-symmetric regarding the y axis, otherwise the energy levels cross. Such potential will open a gap. The larger the gap the larger the tunnelling probability is.

We shall study the gap's dependence on the size of the system (the gap being, at least qualitatively, a measure of the tunnelling probability). This will be done for a quasi-hole and for an electron.

We would like to describe our main results regarding this comparison. The calculated quantity is the off diagonal matrix element $\langle \Psi | V_{\text{imp}} | \tilde{\Psi} \rangle$, referred to as "the gap". As the valleys' shape is a gaussian this gap is proportional to the overlap between two gaussians. But the important quantity entering this calculation is not the real distance between gaussians (which is always L_2/N_ϕ) but the "distance" in quasi-momentum (TAM) space²⁰, which is N . Keep in mind that the electrons live on the surface of a torus therefore the quasi-momentum is defined modulo N_ϕ . So for $m = 1$ (where $N_\phi = N + 1$) a quasi momentum difference of N is equivalent to quasi-momentum difference of 1

²⁰In order to get more details, refer to Chapter two. This is very qualitative.

which obviously does not depend of the size of the system. This is in contrast to the case of $m \neq 1$. For this case $N_\phi = mN + 1$ therefore the difference in quasi-momentum remains N , and the periodicity in quasi-momentum is not very helpful. The particle number N grows with the size of the system, therefore the tunnelling will be system size dependent. Following this we can show that the gap decreases exponentially with the system's size for the case of $m = 3, 5, \dots$ but not for $m = 1$. This leads to the conclusion that while the electron ($m = 1$) indeed tunnels through the barrier, the quasi-particle tunnels through the quantum Hall liquid, therefore exhibiting a strong dependence on the size of the system.

Next we will compare fractional to integer charge tunnelling through the quantum Hall liquid. This has been done for one impurity by Auerbach. As previously explained, the dependence is exponentially small for both the electron and the fractional charge, with slower decrease for the fractional charge. We were interested to find out how this dependence is modified as one increases the number of impurities in the sample. It turns out that for fixed density of impurities, spread all over the sample, the dependence changes from a gaussian $e^{-\text{constant} \times L^2}$ to an exponent $e^{-\text{constant}' \times L}$. The dependence is restrained but is still strong. The passage from gaussian to exponent behavior resembles Li& Thouless' result and is obtained here also at the FQH regime. The Auerbach' result regarding the fractional charge going faster than the electron remains valid also in this limit. This QH liquid tunnelling is explained in detail in chapter three.

Chapter 2

Tunnelling Through A Barrier

The main problem we are presenting in this thesis is the problem of tunnelling through a barrier- electron versus fractional charge. In the previous chapter we have given the motivation for treating a torus- this geometry basically allows any amount of charge to tunnel through a barrier. In this chapter we will start by reviewing the work of Haldane and Rezayi ([20]) who introduced the single particle LLL wave functions as well as Laughlin's trial function both satisfying periodic boundary condition, i.e. living on the surface of a torus. Then we will decompose the suggested many body wave functions into Slater determinants. This decomposition is helpful for calculations and moreover will motivate the definition of the valley wave functions, a set of wave functions we will use in the tunnelling description. These valley wave functions have Laughlin's characteristics as well as a valley-like distribution, which minimizes the barrier energy. Using this valley set, we study the tunnelling, and in particular how it scales with the system's size. We show that while the electron indeed tunnels through the barrier, the fractional charge actually tunnels roundabout, through the quantum Hall liquid. The chapter is closed with a summary of the main obtained results.

2.1 Electrons on a Torus

Single Particle Wave Functions

An electron living on the surface of a torus is described by the same Hamiltonian given in equation (1.3). Naively the wave function is expected to be invariant under translations in L_1 and L_2 along the x and y axes respectively. The square $L_1 \times L_2$ is referred to as the torus' unit cell (called principal region in Haldane-Rezayi's paper). One possible starting point in tackling the problem might be to look for a vector potential \mathbf{A} (and therefore a Hamiltonian) which is invariant under such translations. But it turns out that such a vector potential does not exist¹. Nevertheless, the vector potential inside a given unit cell is a gauged version of the vector potential in any other translated cell. The possible boundary conditions can be read from this gauge connection. Let us show this explicitly for a Landau gauged vector potential

$$\mathbf{A} = -By\hat{x} . \quad (2.1)$$

Written in this gauge the Hamiltonian is invariant under any translation in the x direction but not under a translation along the y direction : $H(x, y + L_2) \neq H(x, y)$. Still

$$\mathbf{A}(x, y + L_2) = \mathbf{A}(x, y) + \nabla\Lambda ,$$

with $\Lambda = -BL_2x$. Therefore one finds that the WF $\varphi(x, y + L_2)$ is related to $\varphi(x, y)$ by a phase:

$$\varphi(x, y + L_2) = e^{-ie\Lambda/\hbar c}\varphi(x, y) = e^{iL_2x/l_H^2}\varphi(x, y) .$$

As the Hamiltonian is independent of x it is possible to require the WF to be invariant under L_1 translation along the x axis.

We can summarize the generalized possible boundary conditions imposed on the WFs:

¹This can be proven as follows : The integral $\oint \mathbf{A} \cdot d\mathbf{l}$ around the unit cell equals (by Stokes theorem) to BL_1L_2 . On the other hand if the vector potential is invariant under L_1 and L_2 translations, this integral must vanish.

$$\varphi(x + L_1, y) = e^{i\phi_1} \varphi(x, y) \quad (2.2)$$

$$\varphi(x, y + L_2) = e^{i\phi_2} e^{-iL_2x/l^2} \varphi(x, y) \quad (2.3)$$

Below we show explicitly (see eq. (2.12)) that varying the parameters ϕ_1 and ϕ_2 is equivalent to translating the WF along the y and x directions respectively. These parameters are therefore interpreted as solenoid fluxes passing through the two periodic orbits (see Figure 1.9).

In order for (2.2) to be consistent with (2.3) one gets the Dirac's condition

$$L_1 L_2 = 2\pi l_H^2 N_\phi \quad (2.4)$$

where N_ϕ is any integer². Physically N_ϕ is the number of flux quanta perpendicular to the torus' surface. This is also (as proven for the LLL in what follows) the number of independent states per Landau level, same result previously obtained for the other geometries. Note that as we are dealing with a magnetic field perpendicular to the surface of a physical torus, the magnetic field lines leaving the torus' surface must come from some source. One such (theoretically) possible source is the Dirac's magnetic monopoles. The condition (2.4) just expresses the Dirac's monopole quantization condition. We believe these monopoles are responsible to the symmetry breaking already present in the problem³. After all, the Dirac's monopoles should be arranged in some configuration inside the torus. Onofri [32] has studied this symmetry breaking to some extent and uses the words "monopoles charges have, so to speak, horns". In any case this is a totally theoretical but nevertheless quite interesting discussion.

Let us return to the original problem of finding the eigenfunctions of (1.3) with the boundary conditions (2.2) and (2.3) for the LLL. Haldane and Rezayi have used the general form of a LLL (Landau gauged) eigenfunction

$$\varphi(x, y) = e^{-y^2/2l_H^2} f(z) \quad (2.5)$$

²To get this condition try to relate $\varphi(x + L_1, y + L_2)$ to $\varphi(x, y)$. One can use (2.2) and then (2.3) or visa versa. The same result is obtained only if (2.4) is valid.

³It might seem as if the problem should have a continuous symmetry, as the magnetic field is uniform and the electrons are living on a torus surface. Still the symmetry is not continuous. The Hamiltonian, depending explicitly on the vector potential, does not commute with all translation operators and a solution with strictly uniform density cannot be built using the full set of LLL eigenfunctions to be given in (2.12).

where $f(z)$ is any analytic function of $x + iy$. Using the periodicity (2.2), (2.3) and condition (2.4) we get

$$f(z + L_1) = e^{i\phi_1} f(z) \quad (2.6)$$

$$f(z + iL_2) = e^{i\phi_2} e^{-i\pi N_\phi (\frac{2z}{L_1} + \tau)} f(z) \quad (2.7)$$

with $\tau \equiv iL_2/L_1$.

These conditions, together with the function's analyticity, determine the number of zeroes $f(z)$ has inside the unit cell to be N_ϕ (refer to Appendix A for more details). The most general form obeying the periodicity is obtained using the so called elliptic odd theta function [33] $\theta_1(z|\tau)$,

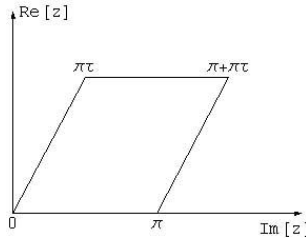
$$\theta_1(z|\tau) \equiv (-i) \sum_{n=-\infty}^{\infty} (-1)^n e^{i\pi\tau(n+1/2)^2} e^{i(2n+1)z} \quad (2.8)$$

where τ and z are complex variables with $\text{Im}[\tau] > 0$. This theta function has the following characteristics

- Periodicity

$$\begin{aligned} \theta_1(z + \pi|\tau) &= -\theta_1(z|\tau) \\ \theta_1(z + \pi\tau|\tau) &= -e^{-i\pi\tau} e^{-2iz} \theta_1(z|\tau) \end{aligned}$$

- It is analytic therefore the periodicity implies the existence of one zero inside the cell



- $\lim_{z \rightarrow 0} \theta_1(z|\tau) \propto z$, therefore $\theta_1(0|\tau) = 0$.

These features inspire the general form of $f(z)$

$$f(z) = e^{ikz} \prod_{j=1}^{N_\phi} \theta_1\left(\frac{\pi}{L_1}(z - \zeta_j) \mid \tau\right). \quad (2.9)$$

The parameter k and the N_ϕ zeroes locations $\{\zeta_j\}$ are determined by the periodicity and satisfy

$$e^{ikL_1} = (-1)^{N_\phi} e^{i\phi_1} \quad (2.10)$$

$$\exp\left[2\pi i \sum_{j=1}^{N_\phi} \zeta_j/L_1\right] = (-1)^{N_\phi} e^{i\phi_2 - ikL_1\tau} \quad (2.11)$$

An explicit set of N_ϕ orthogonal WFs can be found by requiring the WFs to be eigenstates of an operator translating things in the x direction in $\frac{L_1}{N_\phi}$ and denoted by $t(\frac{L_1}{N_\phi}\hat{x})$ (this operator naturally commutes with the Hamiltonian). So the zeroes are chosen to be equally spaced along a string in the direction of the x axis. The obtained orthonormal set is⁴

$$\begin{aligned} \varphi_j(x, y) = A_j e^{-y^2/2l^2} e^{i(\pi N_\phi + \phi_1 - 2\pi j)z/L_1} \theta_1\left(\frac{\pi N_\phi}{L_1}(z - a) - j\pi\tau \mid N_\phi\tau\right) \\ j = 0, 1, \dots, N_\phi - 1 \end{aligned} \quad (2.12)$$

where

$$a \equiv \frac{L_1}{2\pi N_\phi} [\pi + \phi_2 - \tau(\pi N_\phi + \phi_1)] \quad (2.13)$$

and

$$A_j = (L_1\sqrt{\pi})^{-1/2} e^{i\tau(\pi N_\phi + \phi_1 - 2\pi j)^2/4\pi N_\phi} \quad .$$

The index j is referred to as quasi-momentum quantum number. The WFs in this set have a gaussian-like distribution in the y direction. The

⁴The straightforward expression is (2.9) with $\zeta_{j+1} = \zeta_j + L_1/N_\phi$ and $\zeta_1 = a$ (given in (2.13)). Nevertheless, this has the same periodicity and the same zeroes locations as (2.12). Two functions having the same periodicity which vanish at the same points, are equal up to a constant (see Appendix A). We use (2.12) which is more user friendly.

gaussian center of φ_j is located at $(j - \phi_1/2\pi)L_2/N_\phi$, so adjacent guiding centers are distanced L_2/N_ϕ from one another.

It is worthwhile to summarize the results obtained above using magnetic translation operators [34]. We have already mentioned the fact that the regular translation operators in general do not commute with the Hamiltonian (1.3). But one can define a set of Hamiltonian-commuting magnetic translation operators by

$$t(\mathbf{L}) \equiv \exp \left[\frac{i}{\hbar} \mathbf{L} \cdot (\mathbf{P} - \frac{e}{c} \mathbf{A}) - i(\mathbf{L} \times \mathbf{r})_z \right] \quad (2.14)$$

where \mathbf{L} is the translation vector. Besides the translation, the operators include multiplication by a phase, related to the gauge choice. In Landau's gauge one explicitly gets

$$t(L_1 \hat{x}) = e^{L_1 \frac{\partial}{\partial x}} \quad (2.15)$$

$$t(L_2 \hat{y}) = e^{L_2 \frac{\partial}{\partial y}} e^{\frac{iL_2 x}{l^2}}. \quad (2.16)$$

The periodicity conditions (equations (2.2) and (2.3)) are equivalent to requiring the WFs to be not just Hamiltonian eigenfunctions, but simultaneously eigenstates of these two operators. In order for this to be valid, the operators must commute among themselves. This leads to the Dirac's condition. Lastly, the set given at (2.12) satisfies

$$t\left(\frac{L_1}{N_\phi} \hat{x}\right) \varphi_j(x, y) = e^{i(\phi_1 - 2\pi j)/N_\phi} \varphi_j(x, y) \quad (2.17)$$

$$t\left(\frac{L_2}{N_\phi} \hat{y}\right) \varphi_j(x, y) = \varphi_{j-1}(x, y) \quad (2.18)$$

so indeed the WFs in the set are eigenstates of $t\left(\frac{L_1}{N_\phi} \hat{x}\right)$ and can be spanned using the operator $t\left(\frac{L_2}{N_\phi} \hat{y}\right)$. Figure 2.1 summarizes this description and gives the distribution of the obtained WFs.

Laughlin's Wavefunction

The $\nu = 1$ LWF is known. For this case all the LLL available states are occupied, and LWF is a SD built out of all these single particle states :

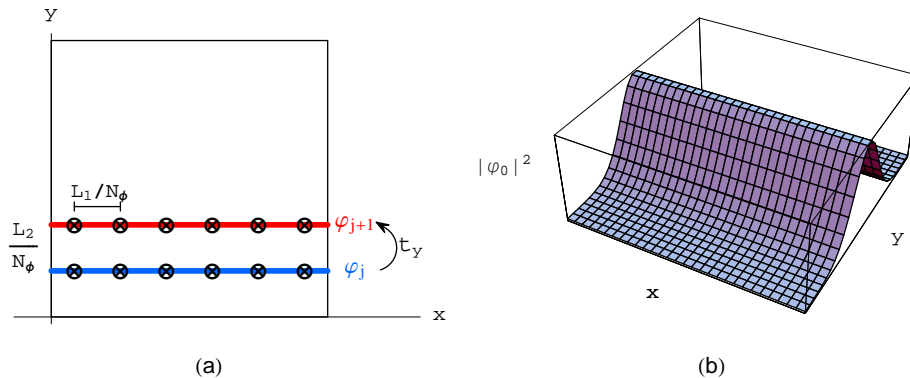


Figure 2.1: (a) The torus unit cell and a presentation of the N_ϕ zero locations (\otimes) of the presented single particle wave eigenfunctions. Different eigenfunctions are presented by parallel lines. (b) The single particle distribution function of $|\varphi_0(x, y)|^2$. Note the y gaussian-like and the x uniform-like dependencies.

$|0, 1, \dots, N-1\rangle$ (see eqs. (1.13) and (1.14)). This SD can be shown to have the general form⁵

$$e^{-\sum_j y_j^2/2l^2} F(z_{cm}) \prod_{i<j} f(z_i - z_j)$$

with $f(z) = \theta_1(\pi z/L_1|\tau)$ and $z_{cm} \equiv \sum_{j=1}^N z_j$ (the particular form for $F(z_{cm})$ is to be found for a general \mathbf{m} in what follows). Generalizing this to any \mathbf{m} leads to

$$\Psi(x_1, y_1, \dots, x_N, y_N) \propto e^{-\sum_j y_j^2/2l^2} F(z_{cm}) \prod_{i<j} \theta_1^{\mathbf{m}}(\pi(z_i - z_j)/L_1|\tau) . \quad (2.19)$$

For odd \mathbf{m} , Ψ is anti-symmetric as required. Based on the fact that a good LWF minimizes the hardcore interaction (and on our knowledge from the disk and the cylinder WFs), this particular WF is expected to vanish whenever $z_i = z_j$ ($i \neq j$). Indeed this is satisfied for the WF given in (2.19).

For brevity we shall write $\Psi(z_1, \dots, z_N)$ even it actually depends on $\{x_j\}$ and $\{y_j\}$ explicitly.

⁵As we noted already (see Appendix A) two analytic WFs having the same doubly periodicity and zeroes locations are equal, up to a constant. One can show that this form is equivalent, in this sense, to the mentioned SD.

The periodicity of Ψ is given by

$$\begin{aligned}\Psi(z_1, \dots, z_j + L_1, \dots, z_N) &= e^{i\phi_1} \Psi(z_1, \dots, z_j, \dots, z_N) \\ \Psi(z_1, \dots, z_j + iL_2, \dots, z_N) &= e^{i\phi_2} e^{-iL_2 x_j / l_H^2} \Psi(z_1, \dots, z_j, \dots, z_N)\end{aligned}\quad (2.20)$$

and leads to the periodicity of $F(z)$

$$\begin{aligned}F(z + L_1) &= (-1)^{N_\phi - \mathfrak{m}} e^{i\phi_1} F(z) \\ F(z + iL_2) &= (-1)^{N_\phi - \mathfrak{m}} e^{-i\pi \mathfrak{m} (2z/L_1 + \tau)} e^{i\phi_2} F(z)\end{aligned}\quad (2.21)$$

These equations are very similar to the single particle expressions (2.6) and (2.7). This suggests the existence of \mathfrak{m} independent solutions ⁶

$$\begin{aligned}F_s(z) &= e^{i(\pi N_\phi + \phi_1 - 2\pi s)z/L_1} \theta_1\left(\frac{\pi \mathfrak{m}}{L_1}(z - b) - s\pi\tau | \mathfrak{m}\tau\right) \\ &\quad s = 0, 1, \dots, (\mathfrak{m} - 1) \\ b &\equiv \frac{L_1}{2\pi \mathfrak{m}} [\pi N_\phi + \phi_2 - \pi(\mathfrak{m} - 1) - \tau(\pi N_\phi + \phi_1)] .\end{aligned}\quad (2.22)$$

We have already chose the \mathfrak{m} zeroes to lie on a string stretched along the x direction. Finally we give the \mathfrak{m} orthogonal degenerate LWFs for the torus

$$\Psi_s = \beta B_s e^{-\sum_j y_j^2/2l^2} F_s(z_{cm}) \prod_{i < j} \theta_1^{\mathfrak{m}}\left(\frac{\pi}{L_1}(z_i - z_j) | \tau\right) , \quad (2.23)$$

where

$$B_s \equiv e^{i\tau(\pi N_\phi + \phi_1 - 2\pi s)^2/4\pi \mathfrak{m}} \quad (2.24)$$

is defined for convenience so that β (a normalizing constant) is independent of s . As discussed in [35] the \mathfrak{m} fold degeneracy is related to the fact that the center of mass coordinate can be varied without changing the particle's relative motion⁷. This is explicitly expressed in (2.23) by noting that the s -dependence is related only to $F_s(z_{cm})$. WFs having different s correspond to different zeroes locations of $F_s(z_{cm})$. Regarding the density one

⁶ \mathfrak{m} is now the number of zeroes $F(z)$ has in the unit cell.

⁷Without impurities the Hamiltonian can be separated into two parts - one describing the particle's center of mass and the other the particle's relative motion.

finds that functions having adjacent s are practically the same, only shifted in L_2/m one with respect to the other. This property is manifested with the use of the following many-body (magnetic translation) operators. The WFs orthogonality is also clarified. We define the unitary operators

$$T_1 \equiv \prod_{j=1}^N t_j\left(\frac{L_1}{N_\phi} \hat{x}\right) \quad (2.25)$$

$$T_2 \equiv \prod_{j=1}^N t_j\left(\frac{L_2}{N_\phi} \hat{y}\right) , \quad (2.26)$$

where $t_j(\mathbf{L})$ is given in (2.14), the index j refers to the j th particle. The LWFs are eigenstates of T_1 while T_2 spans the m fold set. Explicitly

$$T_1 \Psi_s = (-1)^{N+1} e^{i(\phi_1 - 2\pi s)/m} \Psi_s \quad (2.27)$$

$$T_2 \Psi_s = \Psi_{s-1} . \quad (2.28)$$

In the next section we use (2.27) and show that each Ψ_s has a specified known TAM.

Note also that besides being a simultaneous eigenfunction of H and T_1 , Ψ_s is an eigenfunction of T_2^m

$$T_2^m \Psi_s = \Psi_{s-m} = e^{i\phi_2} (-1)^{N_\phi - m} \Psi_s . \quad (2.29)$$

Figure 2.2 gives the LWF density distribution for two particles and $m = 3$. In general it has (very negligible) N_ϕ peaks along the x direction and N peaks along the y direction⁸.

Localized Holes Wavefunctions

Finally we would like to present the LWF plus N_h localized holes WF. Starting with the usual periodicity (eq. (2.20)), only now

$$N_\phi = mN + N_h , \quad (2.30)$$

⁸These N peaks exist also when one deals with a cylinder. In both cases the peaks visibility is influenced by the proportions of the "tube". For a thick tube (large L_1 or R for the torus or cylinder respectively), these peaks are minor.

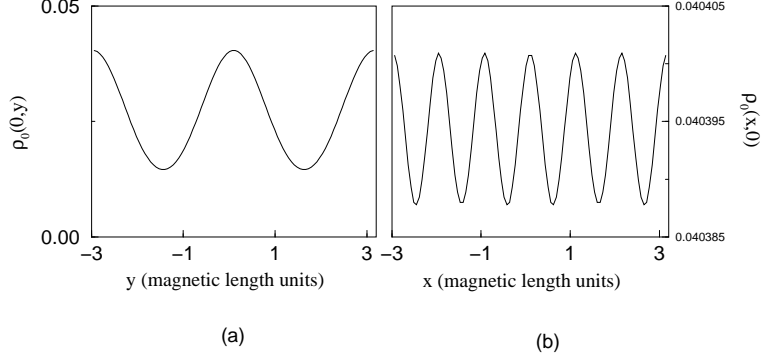


Figure 2.2: Particles distribution function for $N = 2, m = 3, L_1 = L_2$ plotted along the : (a) y direction (x kept constant : $x=0$), (b) x axis ($y=0$).

as the WF should present N_h "dried" localized areas, and $1/m$ filling anywhere else. Based on the form of the N_h localized holes WF for the disk geometry (1.17), and also on the trivial case of $m = 1$ ⁹ one can guess

$$\Psi_{\{z_{0j}\}} \propto \tilde{F}(z_{cm}) \prod_{j=1}^{N_h} \prod_{i=1}^N \theta_1\left(\frac{\pi}{L_1}(z_i - z_{0j})|\tau\right) \prod_{i<j} \theta_1^m\left(\frac{\pi}{L_1}(z_i - z_j)|\tau\right) .$$

As expected, this WF vanishes whenever $z_i = z_{0j}$ ($i = 1, \dots, N, j = 1, \dots, N_h$). This given form also ensures the minimization of hard-core interaction energy, because whenever two particles come very close the WF vanishes like $(z_i - z_j)^m$.

As usual, the periodicity of $\Psi_{\{z_{0j}\}}$ implies the condition over $\tilde{F}(z_{cm})$ which is satisfied by choosing

$$\tilde{F}(z_{cm}) = F\left(z_{cm} + \frac{1}{m} \sum_{j=1}^{N_h} z_{0j}\right) .$$

The set of m WFs describing N_h localized holes on a torus might therefore be

⁹For $m = 1$ the WF for any number of holes is (up to the different normalizing factor) formally the same as a WF of $N + N_h$ non-interacting particles.

$$\Psi_{s;\{z_{0j}\}}(z_1, \dots, z_N) = \tilde{B} e^{-\sum_{j=1}^N y_j^2/2l_H^2} F_s(z_{cm} + \frac{1}{\mathfrak{m}} \sum_{j=1}^{N_h} z_{0j}) \times \prod_{k=1}^{N_h} \prod_{j=1}^N \theta_1\left(\frac{\pi}{L_1}(z_j - z_{0k})|\tau\right) \prod_{i<j} \theta_1^{\mathfrak{m}}\left(\frac{\pi}{L_1}(z_i - z_j)|\tau\right) \quad (2.31)$$

where \tilde{B} is a normalizing factor (depending on the locations of the localized holes) and $F_s(z)$ is given in (2.22). Note that the TAM is no longer a good quantum number, and this chosen set is one of independent but not orthogonal WFs¹⁰.

2.2 Slater Determinant Decomposition Of Laughlin's Wave Functions

The SD decomposition of any WF makes calculations simpler¹¹. In our work it has some extra role as it provides clues for the valley-WFs definition given in the next section. These WFs are crucial to our tunnelling treatment.

This section treats the following:

- TAM calculation of the torus' LWF (no holes). This is mainly done as an exercise and is less relevant to the valley-WFs definition given in the next section. Nevertheless the calculation simplicity compensates...
- Study the SD expansion of a LWF with one localized hole. The expansion involves introducing single particle WFs living on an *extended* unit cell, a cell which is $\mathfrak{m}L_1 \times \mathfrak{m}L_2$ in size, and whose definition is strongly connected to the charge fractionality. These functions are the heart of valley-WFs definition.

¹⁰As we re-mention along the thesis, this is not unique to the torus localized hole WFs, and is true also for the disk and the cylinder common choices.

¹¹Calculations involving single particle potential are expressible using the $V_{kl} = \int \varphi_k^* V \varphi_l$ whose calculation is usually much simpler than calculating things straightforwardly. For two particle potential, knowing $V_{klmn} = \int \int \varphi_k(\mathbf{r}_1) \varphi_l^*(\mathbf{r}_1) V(\mathbf{r}_1 - \mathbf{r}_2) \varphi_m(\mathbf{r}_2) \varphi_n^*(\mathbf{r}_2)$ together with the SD expansion is enough.

- A description of a method enables to find the expansion coefficients explicitly. Finding these coefficients is crucial for some of the following presented calculations (they are even used in calculating the density distributions we give in this chapter) but is unimportant for understanding the core of matter (so it can be skipped by the uninterested reader).

The Total Angular Momentum Of Laughlin's Function

Given a specified LWF (in what follows we shall concentrate on a LWF with one localized hole or without any), we would like to determine what SDs participate in the WFs expansion. For the case of LWF on a disk the answer is pretty trivial. LWF (no holes) is a polynomial of a known degree $M_0 = \mathfrak{m}N(N - 1)/2$, and that is also the TAM, therefore the expansion includes only SDs having exactly this TAM. For example, for two particles and $\mathfrak{m} = 3$, $\Psi_L = C_L(z_1 - z_2)^3 e^{-(|z_1|^2 + |z_2|^2)/4}$ (l_H is taken to unity in what follows). Defining

$$[j_1, \dots, j_N] \equiv e^{-\sum_{j=1}^N |z_j|^2/4} \begin{vmatrix} z_1^{j_1} & z_1^{j_2} & \dots & z_1^{j_N} \\ \vdots & \vdots & & \vdots \\ z_N^{j_1} & z_N^{j_2} & \dots & z_N^{j_N} \end{vmatrix} \quad (2.32)$$

(for a cylinder just replace z by $e^{-iz/R}$ and $e^{-|z|^2/4}$ by $e^{-y^2/2}$) one can rewrite LWF as

$$\Psi_L = C_L(-[0, 3] + 3[1, 2]) \quad (2.33)$$

so indeed the SDs are only those with TAM equals 3. This triviality is due to the fact that the single particle WFs are just powers of z (multiplied by the exponential factor which can be factored out the determinant).

Deciding which are the SDs participating in the expansion of LWF with one localized hole (and actually any number of holes) is also easy. As this WF is (up to a constant) just the multiple of $\prod_{j=1}^N (z_j - z_0)$ with Ψ_L , its TAM varies between M_0 and $M_0 + N$ (in general $M_0 \leq M_{N_h} \leq M_0 + NN_h$, where M_{N_h} is the TAM for a state with N_h localized holes). For example

creation of one hole in the state given at (2.33) is done by multiplying it by $(z_1 - z_0)(z_2 - z_0)$. The result is

$$\Psi_{(z_0)} \propto z_0^2(-[0, 3] + 3[1, 2]) - z_0(2[1, 3] - [0, 4]) - ([1, 4] - 3[2, 3]) \quad (2.34)$$

in which the TAM varies between 3 and 5.

Finding the LWF SD decomposition for the case of a torus seems more complicated as the single particle WFs have a more complicated form than the simple disk (or cylinder) WFs. Still it can be easily found. We write LWF as

$$\Psi_s = \sum_{j_1, \dots, j_N} c_{s; j_1, \dots, j_N} |j_1, \dots, j_N \rangle . \quad (2.35)$$

where $c_{s; j_1, \dots, j_N}$ are constants. We are interested in finding the allowed quantum numbers in $|\mathbf{j}\rangle$ for a given s . In the previous section we have defined the translation operators T_1 and T_2 (equations (2.25) and (2.26)). Applying T_1 to (2.35) gives

$$(-1)^{N+1} e^{2\pi i s/m} = e^{2\pi i (\sum_{n=1}^N j_n/N)/m} , \quad (2.36)$$

where we have also used (2.17) and (2.27). This condition determines the TAM of the SD participating in the above expansion.

Let us give an example with two particles, $m = 3$ and $s = 2$. Using (2.36) we get that in this example the WF necessarily has the expansion

$$\Psi_2 = c_{3,4} |3, 4 \rangle + c_{0,1} |0, 1 \rangle + c_{2,5} |2, 5 \rangle . \quad (2.37)$$

The possible SDs for $s = 0$ and 1 can be found directly using (2.36) or alternatively one can apply T_2 on (2.37) and get

$$\begin{aligned} \Psi_1 &= c_{2,3} |2, 3 \rangle + c_{0,5} |0, 5 \rangle + c_{1,4} |1, 4 \rangle \\ \Psi_0 &= c_{1,2} |1, 2 \rangle + c_{4,5} |4, 5 \rangle + c_{0,3} |0, 3 \rangle . \end{aligned} \quad (2.38)$$

We have used (2.18) and (2.28), basically suggesting that up to a phase T_2 lowers the s quantum number as well as each of the single particle quantum numbers in $|\mathbf{j}\rangle$. Of course by using T_2 one can explicitly obtain the

coefficients in (2.38) once they are initially known in (2.37)¹². Moreover, by applying T_2 again (or directly apply T_2^m on Ψ_2) one can get some extra knowledge about the coefficients, as on one hand Ψ_s is an eigenstate of T_2^m but on the other the SDs "shuffle" (try it). For the above example the benefit is knowing $c_{3,4} = -e^{i\phi_2} c_{0,1}$. As we review below a method to find (numerically) all the expansion coefficients, this practically serves mainly as a recheck.

The Expansion of The Localized Hole State

What can be said about the localized hole WF ? In general the TAM varies over all (N_ϕ) possibilities. But note that for the disk one knows not only the TAM of the SDs participating in the WF's expansion, but also the z_0 dependence. In general a LWF with one localized hole is of the form

$$\Psi_{(z_0)} \propto \sum_{j=0}^N c_j \varphi_j(z_0) \psi_j(z_1, \dots, z_N) \quad (2.39)$$

where c_j are constants, φ_j are the single particle WFs and ψ_j is a many-body WF with a definite TAM equals $(M_0 + N - j)$.

For $m = 1$, as an example, the WF is given by

$$\Psi_{(z_0)} = \left(\sum_{j=0}^N |\varphi_j(z_0)|^2 \right)^{-1/2} \sum_{j=0}^N (-1)^j \varphi_j(z_0) |0, 1, \dots, j-1, j+1, \dots, N \rangle . \quad (2.40)$$

For the torus things are again less trivial. Still we will be able to have an expression similar to (2.39). The (un-normalized) LWF with one localized hole is given hereby (check equation (2.31))

$$\Psi_{s;(z_0)} = B_s e^{-y_0^2/2ml^2} e^{-\sum_j y_j^2/2l^2} F_s(\tilde{z}) \prod_{i<j} \theta_1^m\left(\frac{\pi}{L_1}(z_i - z_j)|\tau\right) \prod_{j=1}^N \theta_1\left(\frac{\pi}{L_1}(z_j - z_0)|\tau\right) \quad (2.41)$$

with the same B_s defined in (2.24). The first exponential factor is added for convenience, motivated by the wish to have a form of $N + 1$ particle WF

¹²This makes sense - as we have noted already, different s present the center of mass degeneracy, so knowing one WF's decomposition must easily give the whole set's decomposition. In getting the decomposition explicitly one should use $\varphi_{j+N_\phi} = t(L_2 \hat{y}) \varphi_j = e^{i\phi_2} \varphi_j$.

when m localized holes are injected to the same z_0 . There is no problem in doing that because by the end of the day the WF should be normalized (and for a given z_0 this exponential is just a constant). We start by writing this in a pretty general way

$$\Psi_{s;(z_0)} = \sum_{j_1, \dots, j_N} c_{s;j_1, \dots, j_N} g_{s;j_1, \dots, j_N}(z_0) |j_1, \dots, j_N\rangle \quad (2.42)$$

where $g_{s;j_1, \dots, j_N}$ are functions to be determined in what follows.

Next we define hole magnetic translation operators

$$t_0(L_1 \hat{x}) \equiv e^{L_1 \frac{\partial}{\partial x}} \quad (2.43)$$

$$t_0(L_2 \hat{y}) \equiv e^{L_2 \frac{\partial}{\partial y}} e^{iL_2 x_0 / ml^2} , \quad (2.44)$$

and also

$$T_3 \equiv t_0\left(\frac{L_1}{N_\phi} \hat{x}\right) T_1 \quad (2.45)$$

$$T_4 \equiv t_0\left(\frac{L_2}{N_\phi} \hat{y}\right) T_2 . \quad (2.46)$$

These mathematical operators are defined in order to get the following identities (2.47)- (2.50), which are in the spirit of (2.27) and (2.28) for the case of no holes. The definition also hints to the charge fractionality as the phase in (2.44) is $e^{iL_2 x_0 / ml^2} = e^{i\tilde{e}\Lambda/\hbar c}$ with charge $\tilde{e} \equiv e/m$. It is straightforward to get

$$t_0(L_1 \hat{x}) \Psi_{s;(z_0)} = -e^{i(\pi + \phi_1 - 2\pi s)/m} \Psi_{s;(z_0)} \quad (2.47)$$

$$t_0(L_2 \hat{y}) \Psi_{s;(z_0)} = (-1)^N \Psi_{s-1;(z_0)} , \quad (2.48)$$

and

$$T_3 \Psi_{s;(z_0)} = -e^{i(\pi N_\phi + \phi_1 - 2\pi s)/m} \Psi_{s;(z_0)} \quad (2.49)$$

$$T_4 \Psi_{s;(z_0)} = \Psi_{s-1;(z_0)} . \quad (2.50)$$

Using these identities together with

$$\Psi_{s-m;(z_0)} = (-1)^{N_\phi - m} e^{i\phi_2} \Psi_{s;(z_0)} \quad (2.51)$$

leads to the explicit expression for the possible g 's. This is done in the Appendix D. The result is

$$g_{s;n}(z) = A_{s;n} e^{-y_0^2/2\mathfrak{m}l_H^2} e^{i(\pi N_\phi + \phi_1 - 2\pi[s+\mathfrak{m}n])z/\mathfrak{m}L_1} \theta_1\left(\frac{\pi N_\phi}{L_1}(z - \tilde{a}) - [s + \mathfrak{m}n]\pi\tau/\mathfrak{m}N_\phi\tau\right) \\ n = 0, 1, \dots, N_\phi - 1 \quad (2.52)$$

where

$$A_{s;n} \equiv (\mathfrak{m}L_1\sqrt{\mathfrak{m}\pi})^{-\frac{1}{2}} e^{i\tau(\pi N_\phi + \phi_1 - 2\pi[s+\mathfrak{m}n])^2/4\pi\mathfrak{m}N_\phi}$$

and

$$\tilde{a} \equiv \frac{L_1}{2\pi N_\phi} \left(\phi_2 - \frac{1}{2}\pi N_\phi(N_\phi - 3) - \tau(\pi N_\phi + \phi_1) \right).$$

For a fixed s there exist N_ϕ possible g -functions, much less than the $\binom{N_\phi}{N}$ possibilities suggested in the general expansion (2.42). So we can now write a refined expression for $\Psi_{s;(z_0)}$

$$\Psi_{s;(z_0)} = \sum_{n=0}^{N_\phi-1} c_{s;n} g_{s;n}(z_0) \psi_{s;n}(z_1, \dots, z_N). \quad (2.53)$$

The WFs $\psi_{s;n}$ have a definite TAM $(\sum_{k=1}^N j_k)$ obeying

$$e^{2\pi i s N/N_\phi} (-1)^N e^{-2\pi i n/N_\phi} = e^{2\pi i \sum_{k=1}^N j_k/N_\phi}. \quad (2.54)$$

This is shown by applying T_3 to the expression (2.53) (see also Appendix D).

In comparing the torus WFs expansion (2.53) to the expansion (2.39) of the common geometries, one immediately observe the main difference. The single particle WFs φ appearing in the (say) disk geometry are replaced by the set of g -functions (2.52). These $\mathfrak{m}N_\phi$ functions are single particle WFs on an *extended* cell, a cell of size $\mathfrak{m}L_1 \times \mathfrak{m}L_2$, they form an orthonormal set on this cell

$$\int_{\mathfrak{m}L_1 \times \mathfrak{m}L_2} g_{s;n}^*(z) g_{s';n'}(z) dz = \delta_{ss'} \delta_{nn'} \quad (2.55)$$

and obey the following identities

$$t_0\left(\frac{L_1}{N_\phi}\hat{x}\right)g_{s;n} = -e^{i(\pi N_\phi + \phi_1 - 2\pi[s+nm])/mN_\phi}g_{s;n} \quad (2.56)$$

$$t_0\left(\frac{L_2}{N_\phi}\hat{y}\right)g_{s;n} = g_{s-1;n} \quad (2.57)$$

$$g_{s-m;n} = g_{s;n-1} \quad (2.58)$$

$$t_0(L_2\hat{y})g_{s;n} = g_{s-1;n-N} \quad (2.59)$$

$$g_{s;n-N_\phi} = e^{-i\pi(N_\phi-1)(N_\phi-2)/2}g_{s;n} . \quad (2.60)$$

Let us give an example illustrating the WF's decomposition. We choose $N = 2$, $m = 3$ and, of course, one localized hole, so that $N_\phi = 7$. Using the expansion (2.53) and condition (2.54) one can immediately write

$$\begin{aligned} \Psi_{0;z_0} = & g_{0;0}(z_0) [c_{3,4}|3, 4 \rangle + c_{1,6}|1, 6 \rangle + c_{2,5}|2, 5 \rangle]_0 + \\ & g_{0;1}(z_0) [c_{0,6}|0, 6 \rangle + c_{2,4}|2, 4 \rangle + c_{1,5}|1, 5 \rangle]_3 + \\ & g_{0;2}(z_0) [c_{2,3}|2, 3 \rangle + c_{0,5}|0, 5 \rangle + c_{1,4}|1, 4 \rangle]_6 + \\ & g_{0;3}(z_0) [c_{5,6}|5, 6 \rangle + c_{1,3}|1, 3 \rangle + c_{0,4}|0, 4 \rangle]_2 + \\ & g_{0;4}(z_0) [c_{1,2}|1, 2 \rangle + c_{4,6}|4, 6 \rangle + c_{0,3}|0, 3 \rangle]_5 + \\ & g_{0;5}(z_0) [c_{4,5}|4, 5 \rangle + c_{0,2}|0, 2 \rangle + c_{3,6}|3, 6 \rangle]_1 + \\ & g_{0;6}(z_0) [c_{0,1}|0, 1 \rangle + c_{3,5}|3, 5 \rangle + c_{2,6}|2, 6 \rangle]_4 . \end{aligned} \quad (2.61)$$

The square bracket's subscript should be ignored for now (and is explained in the next section).

As we already declared, the g-functions serve a main role in the valley-WFs definition. As these were already introduced one can now skip to the next section. Alternatively one can do something else such as following the route we hereby give: explicitly getting the coefficients appearing in the expansion (2.42) by diagonalizing the hard-core interaction matrix.

Getting The Expansion Coefficients

We would like to get the explicit value of the LWF expansion coefficients. We first explain how they are found if LWF with no holes is treated. The system related to LWF is described by the many body Hamiltonian which consists of kinetic and interaction terms, with the hard-core interaction given by (1.15).

We write this Hamiltonian in the Hilbert space restricted to the LLL. The kinetic term can therefore be ignored¹³, and the Hamiltonian is described most generally by the $\binom{N_\phi}{N} \times \binom{N_\phi}{N}$ interaction matrix. In diagonalizing this matrix the Laughlin state should occur as an eigenvector with eigenvalue *zero*.

The terms we need to calculate are

$$\langle \mathbf{j} | V_{int} | \mathbf{j}' \rangle \equiv \langle j_1, \dots, j_N | \sum_{i < j} V(\mathbf{r}_i - \mathbf{r}_j) | j'_1, \dots, j'_N \rangle \quad . \quad (2.62)$$

Using the explicit definition of $|\mathbf{j}\rangle$ one gets that there are two cases where $\langle \mathbf{j} | V_{int} | \mathbf{j}' \rangle$ does not vanish

- A diagonal term : $|\mathbf{j}\rangle = |\mathbf{j}'\rangle$. Then
$$\langle \mathbf{j} | V_{int} | \mathbf{j}' \rangle = \sum_{\alpha, \beta, \alpha', \beta'=1}^N (-1)^{\alpha+\beta+\alpha'+\beta'} (V_{j_{\alpha'}, j_{\alpha}, j_{\beta'}, j_{\beta}} - V_{j_{\beta'}, j_{\alpha}, j_{\alpha'}, j_{\beta}}).$$
- Exactly two quantum numbers in $|\mathbf{j}\rangle$ are different than the ones in $|\mathbf{j}'\rangle$. Denoting the different quantum numbers by $j_{\alpha}, j_{\beta}, j'_{\alpha'}, j'_{\beta'}$ one gets $\langle \mathbf{j} | V_{int} | \mathbf{j}' \rangle = (-1)^{\alpha+\beta+\alpha'+\beta'} (V_{j'_{\alpha'}, j_{\alpha}, j'_{\beta'}, j_{\beta}} - V_{j_{\beta'}, j_{\alpha}, j'_{\alpha'}, j_{\beta}}).$

We have used the following definition [37]

$$V_{klmn} \equiv \int \int d^2r_1 d^2r_2 \varphi_k(\mathbf{r}_1) \varphi_l^*(\mathbf{r}_1) V(\mathbf{r}_1 - \mathbf{r}_2) \varphi_m(\mathbf{r}_2) \varphi_n^*(\mathbf{r}_2) \quad . \quad (2.63)$$

For the hard core interaction doing the integration in parts leads to

$$V_{klmn} = \int d^2r \varphi_k(\mathbf{r}) \varphi_l^*(\mathbf{r}) \nabla^2 (\varphi_m(\mathbf{r}) \varphi_n^*(\mathbf{r})) \quad . \quad (2.64)$$

This can be solved explicitly for any previously mentioned boundary conditions. For the disk one gets that $V_{klmn} = 0$ unless $m + k = n + l$. This is no more than the conservation of angular momentum. The interaction term conserves the TAM, so states with different TAM do not couple. This is helpful in calculations as the Hamiltonian matrix becomes a block diagonal

¹³All the states have the same kinetic energy $N\hbar\omega_c/2$.

one, each block corresponds to a different TAM. Denoting $\Delta = k - l = n - m$, the non zero terms are given by

$$V_{k-\Delta,k,j+\Delta,j} = \frac{1}{2^{j+k+2}\pi l_H^4} \frac{1}{\sqrt{(k-\Delta)! k! (j+\Delta)! j!}} \times \quad (2.65)$$

$$[4j(j+\Delta)(j+k-1)! - 2(1+2j+\Delta)(j+k)! + (j+k+1)!] .$$

For the cylinder a similar calculation gives

$$V_{k-\Delta,k,j+\Delta,j} = (2\pi)^{-5/2} (R l_H)^{-6} e^{-\frac{l_H^2}{2R^2}(\Delta^2+(j-k+\Delta)^2)} \times \quad (2.66)$$

$$[l_H^2(j-k+\Delta)^2 - R^2(1+\Delta^2)] .$$

The conservation of TAM for the torus is of course valid as well. The only principle difference is due to the fact that angular momentum (and therefore its sum) is defined modulo N_ϕ , therefore the conservation condition is

$$m + k = (n + l) \bmod(N_\phi) . \quad (2.67)$$

The straightforward calculation, done with the help of (2.8) gives the complicated series ($l_H = 1$)

$$V_{klmn} = -\frac{4\pi}{L_1^3} \sum_{q,p,d=-\infty}^{\infty} \{(N_\phi d - (k-l))^2 I_1[N_\phi(p+q+2) - (l+n)] +$$

$$\frac{\pi}{L_1} e^{(D_{k+l,2p+d}^2 + D_{m+n,2q-d-\Delta'}^2)\pi^2/L_1^2} I_2[D_{k+l,2p+d}, D_{m+n,2q-d-\Delta'}]\} \times$$

$$e^{i\pi\tau((n+d+1)N_\phi-k)^2 + ([n+1]N_\phi-l)^2 + ([m-d-j+1]N_\phi-p)^2 + ([m+1]N_\phi-q)^2}/N_\phi \quad (2.68)$$

where

$$D_{r,s} \equiv 2N_\phi - r + sN_\phi ,$$

$$I_1[v] \equiv \int_0^{L_2} e^{-4\pi v y/L_1} e^{-2y^2} dy ,$$

$$I_2[v, w] \equiv \int_0^{2N_\phi} (y+v)(y+w)e^{-((y+v)^2+(y+w)^2)\pi^2/L_1^2} dy$$

and

$$\Delta' \equiv \frac{1}{N_\phi}(n+l-k-m)$$

is necessarily an integer due to the conservation condition (2.67).

This infinite series converge pretty fast so it can be calculated numerically. Knowing V_{klmn} one can now find the interaction matrix in the LLL subspace, and by its diagonalization, get the torus LWF. We remind again that one does not have to diagonalize the $\binom{N_\phi}{N} \times \binom{N_\phi}{N}$ matrix as the Hamiltonian is block diagonal, and finding one of LWFs with a known TAM (see equation (2.36)) can be worked out in the subspace of WFs having only this TAM.

Getting the Slater decomposition of LWF with N_h localized holes can be done in a similar way by introducing the background impurity potential (1.19). As now the TAM is not restricted, one has to diagonalize the whole LLL space. At the next section we shall give a slightly modified version way of getting the coefficients, which is done by diagonalizing a LLL subspace having a specified TAM.

2.3 Valley States

We are looking for an appropriate set of WFs for the description of the possible electron or quasi particle tunnelling. The idea present in this work is to build Laughlin-like WFs with the "ability" to minimize the energy of a possible potential barrier¹⁴. These WFs have filling $1/m$ all over except for a

¹⁴We do not explicitly define the potential. The potential one should have in mind is a (positive) mountain that particles want to avoid. The description we give will be valid in the limit of a potential which is weak compared to the magnetic field energy (so that it does not mix different Landau levels). In addition the potential should not be much wider than l_H . This is because the valley-WFs present in what follows are l_H in width. Wider potentials can be treated similarly, by making the valleys wider. This is explained to some extent in Chapter four.

drier valley. The dry valley enables minimizing the barrier's energy. If the valley "sits" on the mountain, the barrier's energy is minimal. Building the valley-WFs explicitly is motivated by the very simple case of $m = 1$. If N_ϕ is chosen to be $N + 1$, the possible many body WFs are obtained by choosing N single particle states out of the $N + 1$ available ones. The resulting WFs are

$$\psi_n = |0, 1, \dots, n-1, n+1, \dots, N \rangle \equiv |0, 1, \dots, \underbrace{}_n, \dots, N \rangle . \quad (2.69)$$

The distribution of these WFs is indeed valley-like, with a valley sitting on the location of the n th missing single particle WF. But how can this be generalized to other values of m ?

First we choose

$$N_\phi = mN + 1 , \quad (2.70)$$

so that it will be possible to have the desired valley distribution. Then following the expansion of the $m = 1$ LWF to SDs (2.40) and the single particle WFs orthogonality we immediately get (at least up to unimportant sign)

$$\psi_n = \int dz_0 \varphi_n^*(z_0) \Psi_{(z_0)} \quad (2.71)$$

(for $m = 1$).

This was actually mentioned already in the first presentation of the localized hole WF (see eq. (1.18)). Equation (2.71) can basically be "continued" to any m . It will work perfectly for the disk or the cylinder, creating $N + 1$ possible different valley-WFs¹⁵. But for the torus it fails! This integral, defined naturally on the unit cell, is not unique as it depends on the location of the unit cell. This can be shown using the periodicity of $\varphi_n(z_0)$ and $\Psi_{(z_0)}$, equations (2.2) and (2.47) respectively. It turns out that the integrand in (2.71) collects a phase when $z \rightarrow z + L_1$. So the integral is not periodic in L_1 . Mathematically this is strongly connected to the fact that the expansion of $\Psi_{(z_0)}$ to SDs involved the extended unit cell single particle WFs (2.52), rather

¹⁵We explain the (disk) counting: $\Psi_{(z_0)}$ is a polynomial of degree N . Its expansion contains z_0 to all powers n with $n \leq N$ only. Therefore for $n > N$, $\psi_n = 0$ while $n \leq N$ ensures $\psi_n \neq 0$.

than those of the regular unit cell (recall equation (2.53)). The natural way of defining the valley-WFs for the torus is therefore

$$\psi_{s;n} \equiv \int_{\mathfrak{m}L_1 \times \mathfrak{m}L_2} g_{s;n}^*(z_0) \Psi_{s;(z_0)} dz_0 . \quad (2.72)$$

As $s = 0, 1, \dots, \mathfrak{m} - 1$ and $n = 0, 1, \dots, N_\phi - 1$ the maximal number of WFs created by this procedure is $\mathfrak{m}N_\phi$. Still the number of independent (and actually orthogonal) WFs is really N_ϕ . This is shown using the translation operations. By applying T_1 over (2.72) one can show that

$$T_1 \psi_{s;n} = -e^{2\pi i n / N_\phi} e^{iN(\pi N_\phi + \phi_1 - 2\pi s) / N_\phi} \psi_{s;n} . \quad (2.73)$$

This immediately confirms that the set defined for a fixed s is orthogonal. So for a given s we have N_ϕ orthogonal WFs. Showing that sets with different s are equivalent is a bit more tricky: we first state that the valley-WFs defined hereby are the ones appearing in the expansion of $\Psi_{s;(z_0)}$ (equation (2.53)). This is true because the extended unit cell WFs are orthogonal (equation (2.55)). By applying $t_0(L_2 \hat{y})$ to this expansion one gets

$$\begin{aligned} t_0(L_2 \hat{y}) \Psi_{s;(z_0)} &= t_0(L_2 \hat{y}) \sum_n c_{s;n} g_{s;n}(z_0) \psi_{s;n} \\ \text{using (2.59)} &= \sum_n c_{s;n} g_{s-1;n-N}(z_0) \psi_{s;n} \\ \text{by (2.48)} &= (-1)^N \Psi_{s-1;(z_0)} \\ \text{expanding it} &= (-1)^N \sum_n c_{s-1;n} g_{s-1;n}(z_0) \psi_{s-1;n} \\ n \rightarrow n - N &= (-1)^N \sum_n c'_{s-1;n-N} g_{s-1;n-N}(z_0) \psi_{s-1;n-N} . \end{aligned}$$

The prime in the last equality is there because in general $g_{s;n-N}$ is only proportional to $g_{s;n}$ (equation (2.60)). Nevertheless it does not really matter for our business as comparing the last equality to the second one, and using the g 's orthogonality immediately suggests that

$$\psi_{s;n} \propto \psi_{s-1;n-N} \quad (2.74)$$

and indeed (2.72) defines exactly N_ϕ orthogonal WFs. In order to emphasize this, one can define

$$p \equiv s + mn \pmod{N_\phi} \quad (2.75)$$

and identify ψ_p with $\psi_{s;n}$. The WF ψ_p has a valley centered at the maximum of the single particle WF φ_p .

Using this identification together with T_2 operations (2.50) and (2.57) leads to

$$T_2\psi_p = T_2\psi_{s;n} = \psi_{s-1,n} = \psi_{p-1} . \quad (2.76)$$

So states with adjacent valleys ($\Delta p = 1$) have TAM difference of N , as could be expected (since adjacent WF are obtained by increasing each single particle quantum number by one).

We emphasize again that for the disk (or the cylinder) the localized hole WFs were expanded using the single particle WFs while for the torus it was necessary to use the extended unit cell WFs. This led to a set of $N + 1$ valley-WFs if the disk is treated (also for the case of $m = 3$), but to N_ϕ WFs for the torus. The reason for the difference is exactly why the torus was treated in the first place. In case a disk is treated it is found that a valley necessarily "cuts" the sample into two regions, each containing an integer number of electrons. Therefore there exists only $N + 1$ possible valleys. For the torus there is no such problem. The restriction is removed and the set contains N_ϕ valley-functions.

Let us come back to a previously mentioned example- the expansion (2.61). Each square brackets is a defined ψ_p . The subscript appearing next to the right bracket is just the quantum number p . We note that due to (2.76) the expansion of $\Psi_{s;(z_0)}$ is basically known once one ψ_p is known. Still this involves finding many coefficients. Once these are found, $\Psi_{s;(z_0)}$ expansion can be found by a set of algebraic equations obtained by the requirement that $\Psi_{s;(z_0)} = 0$ whenever $z_i = z_j$ ($i \neq j$) or $z_j = z_0$. That is the promised modification for finding the decomposition of $\Psi_{s;(z_0)}$.

Getting the coefficients in the expansion of ψ_p and actually giving an alternative definition to the valley-WFs, can be done by the scheme given in the previous section. First choose $N_\phi = mN + 1$. Then select only SDs having a desired specified TAM. Finally diagonalize the interaction matrix. The result is one eigenstate with zero interaction energy, which is no other than ψ_p having the specified TAM. The obtained distributions for $N = 2$ to 5

are plotted in Figure 2.3. One clearly observes the desired valley "come alive".

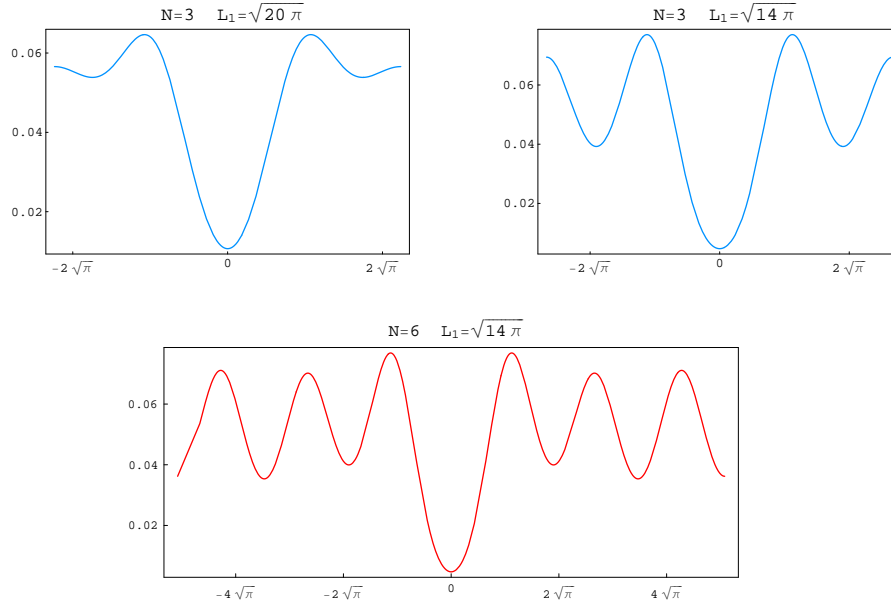


Figure 2.3: Valley WF distribution: The density distribution function of ψ_p practically does not depend on x . These graphs present the distribution as a function of y . The valley is at the origin ($p = 0$ and therefore, following eq. (2.54), the TAM, defined modulo N_ϕ , is 0 or $N_\phi/2$ depending on whether N is even or odd respectively). The distribution is given for three particles on a torus with two different proportions (different L_1 , top figures), and also for two given L_1 ($L_1 = \sqrt{14}\pi$) with $N = 3$ and 6. Note that for the latter case the two distributions are identical in the valley's neighborhood.

Let us end this section by summarizing the main characters of ψ_p :

- They have a valley-like distribution.
- Their interaction (hard core) energy is zero.
- They are eigenstates of the translation operator T_1 having different eigenvalues.
- The TAM difference of WFs with adjacent valleys is N .

2.4 Tunnelling Through A Barrier : An Electron Versus A Quasi Particle

We have described the possible electron or fractional charge tunnelling schematically in the closing section of the first chapter. In this section we rephrase things more rigourously, studying the problem to first order by using the valley-WFs we have defined in the previous section. We will eventually show, by calculating how the tunnelling depends on the size of the system, that the electron's tunnelling occurs through the barrier potential as opposed to the fractionally charged quasi particle tunnelling only via the quantum Hall liquid. This section contains two major parts : we first explain how we "measure" the tunnelling (equation (2.78) is the calculated quantity). Then we estimate its system's size dependency for the case of $m = 1, 3$ corresponding to integer and fractional charge tunnelling respectively.

What We Calculate In Studying The Tunnelling

We start with the Hamiltonian $H = H_0 + V_{int} + V_{barrier}$ and the number of flux quanta perpendicular to the sample's area is $N_\phi = mN + 1$. The wave functions $\{\psi_p\}$ given in the previous section are degenerate groundstates of the Hamiltonian $H' = H_0 + V_{int}$. Note that H' (and therefore ψ_p) depends on the parametric fluxes ϕ_1 and ϕ_2 . For our purpose the relevant flux is ϕ_1 . Changing it adiabatically corresponds to a valley slowly sliding along the y axis. The degeneracy of $\{\psi_p\}$ regarding H' is removed by the barrier potential. The closest a valley is to the barrier, the smaller the energy is.

The system is set to start in the minimal energy state, having its valley sitting on the mountain. This state is denoted by ψ . Changing ϕ_1 adiabatically will increase the energy of ψ , while decreasing the energy of states whose valley gets closer to the barrier. Let us concentrate on the two states whose valleys are the closest to the barrier (amongst all other available states). The relevant states are ψ and an adjacent state we shall denote by $\tilde{\psi}$. At a certain value of ϕ_1 (for a symmetrical barrier it would be $\phi_0/2$), the two states become degenerate. Increasing ϕ_1 further makes $\tilde{\psi}$ energetically favorable and the system might prefer to make a transition to this state. Such a transition fits an e/m charge change from one side of the barrier to the other. The possibility for a fractional charge or an electron to jump over the mountain, can

therefore be studied to first order by calculating the transition probability

$$\mathcal{T} = \langle \psi | V_{\text{barrier}} | \tilde{\psi} \rangle \quad . \quad (2.77)$$

(this is calculated in for a case where ψ and $\tilde{\psi}$ are symmetrical (degenerate) regarding the barrier potential).

Let us explain why this is the calculated quantity. The Hamiltonian is $H = H' + V_{\text{barrier}}$. Written in the subspace of ψ and $\tilde{\psi}$ it is

$$\mathcal{H} = \begin{pmatrix} E_b & \mathcal{T}^* \\ \mathcal{T} & \tilde{E}_b \end{pmatrix}$$

where $E_b = \langle \psi | V_{\text{barrier}} | \psi \rangle$ and $\tilde{E}_b = \langle \tilde{\psi} | V_{\text{barrier}} | \tilde{\psi} \rangle$. Diagonalizing \mathcal{H} leads to two possible eigenstates with energy difference of $\sqrt{(E_b - \tilde{E}_b)^2 + 4|\mathcal{T}|^2}$. These are actually energy levels, because E_b and \tilde{E}_b both depend on the flux ϕ_1 (Figure 1.10). At first the state with minimal energy is ψ and E_b is much smaller than \tilde{E}_b . Changing the flux eventually leads to $\tilde{\psi}$ acting as lowest energy state. Then, \tilde{E}_b is the smaller energy. At some point in between, E_b and \tilde{E}_b are of the same order. Here the energy difference between the energy levels is $2|\mathcal{T}|$. If this quantity is zero the levels cross and the tunnelling investigation is out of the question. If \mathcal{T} is finite it measures the gap existing between the two energy levels. For a large gap, the tunnelling probability is large, as the possibility of a Zener tunnelling [38] is small. So \mathcal{T} indeed gives the probability for tunnelling.

The apparent jump can fit a charge moving through the quantum Hall liquid as well as a real jump through the barrier. How can we distinguish the two? In the former case the tunnelling probability is expected to be strongly dependent on the sample's length (L_2), much more appreciably than in the case of a particle jumping through the barrier. So we are basically interested to know how \mathcal{T} scales with the size of the system L_2 .

As the valley-WFs are eigenstates (having different eigenvalues) of T_1 , the translation operator in the x direction, a potential depending on y alone (and in the general case a potential which commutes with T_1), will not couple the two states, and \mathcal{T} vanishes¹⁶. So in order to investigate (2.77) we need to break the potential into two parts :

¹⁶The proof is pretty simple:

T_1 is unitary. Therefore $\langle \psi | V_{\text{barrier}} | \tilde{\psi} \rangle = \langle \psi | T_1^\dagger T_1 V_{\text{barrier}} | \tilde{\psi} \rangle$. If V_{barrier} commutes with T_1 we have $\langle \psi | V_{\text{barrier}} | \tilde{\psi} \rangle = \langle \psi | T_1^\dagger V_{\text{barrier}} T_1 | \tilde{\psi} \rangle = e^{i(\lambda' - \lambda)} \langle \psi | V_{\text{barrier}} | \tilde{\psi} \rangle$ (where $\lambda' \neq \lambda \pmod{2\pi}$). Therefore $\langle \psi | V_{\text{barrier}} | \tilde{\psi} \rangle = 0$.

- V_{mount} : A part depending on y alone, having a general mountain shape¹⁷. This part is responsible to choosing ψ and $\tilde{\psi}$ as the relevant minimal energy states describing the system.
- V_{imp} : A part which does not commute with T_1 , therefore depends on x (and possibly on y). This part makes \mathcal{T} finite. It can be an impurity potential.

In order to estimate the tunnelling probability, we need to understand

$$\mathcal{T} = \langle \psi | V_{imp} | \tilde{\psi} \rangle \quad . \quad (2.78)$$

Estimating The Tunnelling

First we calculate (2.78) for the case of $m = 1$. This case involves $\psi = |1, 2, \dots, N \rangle$ and $\tilde{\psi} = |0, 1, \dots, N - 1 \rangle$ therefore

$$\mathcal{T} = \int_{L_1 \times L_2} \varphi_N^*(x, y) V_{imp}(x, y) \varphi_0(x, y) \equiv \langle N | V_{imp} | 0 \rangle \quad . \quad (2.79)$$

The single particle part $\langle N | V_{imp} | 0 \rangle$ can be calculated once a specified form for the potential V_{imp} is given using the following general formula (proven in Appendix B)

$$\begin{aligned} \langle j | V(y) e^{2\pi i k x / L_1} | j' \rangle &= & (2.80) \\ & \frac{1}{\sqrt{\pi} l_H} e^{-iq\phi_2} e^{-\left(\frac{kL_2}{2N_\phi l_H}\right)^2} \int_{-\infty}^{\infty} e^{-(w+w_0)^2 / l_H^2} V(w) dw \end{aligned}$$

where

$$q \equiv \frac{j' - j - k}{N_\phi} \quad (2.81)$$

is necessarily an integer, and

¹⁷and as noted earlier, the mountain's width in our scheme should be smaller than l_H .

$$w_0 \equiv \frac{\pi l_H^2}{L_1} (2N_\phi + \phi_1/\pi - j - j' + qN_\phi) .$$

As one deals with a torus $V(y)$ should be periodic in L_2 : $V(y + L_2) = V(y)$.

We are interested in taking two simple examples for V_{imp} :

$$\begin{aligned} V_{imp}(x) &= \delta_{L_1}(x) \\ V_{imp}(x, y) &= \delta_{L_1}(x) \delta_{L_2}(y - Y) \end{aligned}$$

where $\delta_L(x)$ is a Dirac delta function with period L

$$\delta_L(x) = \sum_{n=-\infty}^{\infty} \delta(x - nL) = \frac{1}{L} \sum_{n=-\infty}^{\infty} e^{2\pi i n x / L} , \quad (2.82)$$

and Y is preferably picked in between the studied valleys. Using (2.80) leads to¹⁸

$$\langle j | e^{2\pi i k x / L_1} | j' \rangle = e^{-iq\phi_2} e^{-\left(\frac{kL_2}{2N_\phi l_H}\right)^2} . \quad (2.83)$$

Hence (using (2.82))

$$\langle j | \delta_{L_1}(x) | j' \rangle = \frac{1}{L_1} \sum_{q=-\infty}^{\infty} e^{-iq\phi_2} e^{-\left(\frac{[j' - j - qN_\phi]L_2}{2N_\phi l_H}\right)^2} . \quad (2.84)$$

One can also get

$$\begin{aligned} \langle j | \delta_{L_1}(x) \delta_{L_2}(y - Y) | j' \rangle &= \quad (2.85) \\ \frac{1}{L_1 \sqrt{\pi} l_H} \sum_{q, n=-\infty}^{\infty} e^{-iq\phi_2} e^{-\left(\frac{[j' - j - qN_\phi]L_2}{2N_\phi l_H}\right)^2} e^{-(Y + \frac{L_2}{2N_\phi} [\phi_1/\pi - (j+j') + (2n+q)N_\phi])^2 / l_H^2} . \end{aligned}$$

¹⁸It is pretty simple to understand (2.83). In calculating $\langle j | e^{2\pi i k x / L_1} | j' \rangle$ for the cylinder, the WFs are y dependent gaussians. The exponential part just couples the two WFs, leading to the condition $j' - j = k$. For the torus the periodicity generalizes the condition to (2.81). As regarding the y dependence we are left with the overlap between two gaussians whose center is distanced $|j' - j|L_2/N_\phi$. This leads to the exponential decaying factor in (2.83).

Taking the leading term in (2.84) or (2.85) leads to an exponential behavior of the form

$$\mathcal{T}_{\mathbf{m}=1}^{el} \propto e^{-(L_2/2N_\phi)^2}. \quad (2.86)$$

The dependence for a general \mathbf{m} can be obtained in a similar way. Any two adjacent states have TAM difference of N . Neglecting the influence of the SD expansion coefficients¹⁹ one gets (the second equality is obtained using (2.84) or (2.85))

$$\mathcal{T}_{\mathbf{m}=3,5,\dots}^{\text{FC}} \propto \langle j|V_{imp}|j+N\rangle \propto e^{-(L_2/2\mathbf{m})^2}. \quad (2.87)$$

This result can be understood pictorially in the following way. The element $\langle \psi|V_{imp}|\tilde{\psi}\rangle$ just sums to an overlap between two gaussians²⁰. As the difference in TAM between the two valley-states is N , the distance between gaussian's peaks is $N\frac{L_2}{N_\phi}$. But for the torus things are periodic therefore for $\mathbf{m} = 1$ a distance of $N\frac{L_2}{N_\phi}$ is actually shorter. It is just $\frac{L_2}{N_\phi}$ (see Figure 2.4). For $\mathbf{m} \neq 1$, the shortest distance remains $NL_2/N_\phi \approx L_2/\mathbf{m}$.

This picture suggests that electron-tunnelling in the *fractional* regime, corresponding to a WF shift of $\mathbf{m}L_2/N_\phi$, will resemble the $\mathbf{m} = 1$ electron. Indeed

$$\mathcal{T}_{\mathbf{m}=3,5,\dots}^{el} \propto \langle j|V_{imp}|j+\mathbf{m}N\rangle \propto e^{-(L_2/2N_\phi)^2}, \quad (2.88)$$

same dependence as in (2.86).

Summarizing the above we conclude that

$$\mathcal{T} \propto \begin{cases} e^{-(L_2/N_\phi)^2/4l_H^2} & \text{for an electron} \\ e^{-(L_2/\mathbf{m})^2/4l_H^2} & \text{for a quasi particle.} \end{cases} \quad (2.89)$$

Increasing the torus length L_2 without changing L_1 immediately suggests that $L_2 \propto N_\phi$ (as $2\pi N_\phi l_H^2 = L_1 L_2$). This is mathematically done by increasing the number of particles. So L_2 and N_ϕ are proportional. This means that while the quasi-particle exhibits a real exponential (gaussian-like) decay, the electron's tunnelling avoids this strong decaying faith.

¹⁹This is verified numerically in what follows.

²⁰Recall that $\int e^{-y^2/2} e^{-(y-\Delta)^2/2} \propto e^{-\Delta^2/4}$.

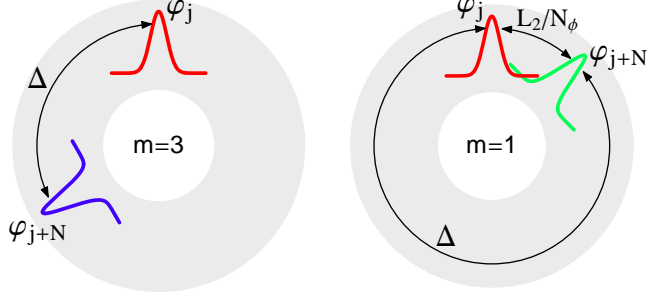


Figure 2.4: The tunnelling probability is proportional to the single particle overlap $\int \varphi_j^* V_{imp} \varphi_{j+N}$. Here we schematically explain why this decrease exponentially for a quasi-particle and not for an electron. In either case the overlap is $e^{-\Delta^2/4}$ (Δ is the distance between the functions' center) and the distance between overlapping functions is $N \frac{L_2}{N_\phi}$. But as the torus is periodic, such a distance for $m = 1$ (electron) is actually $\frac{L_2}{N_\phi}$.

One can be bothered with the fact that in the case of $m = 3$ we have only used the estimate

$$\mathcal{T} = \langle \psi | V_{imp} | \tilde{\psi} \rangle \approx \langle j | V_{imp} | j' \rangle$$

with $\Delta j = j' - j = N$ (or mN if an electron in this regime is treated). The real calculation involves many possible wave functions. In order to check the how the approximation affects the result we have chosen to calculate \mathcal{T} numerically for $V_{imp} = \delta_{L_1}(x)$. This potential is convenient as the expression (2.84) depends only on Δj (and not on explicitly on the j 's), therefore \mathcal{T} is of the form

$$\mathcal{T} = s(N) \langle j | V_{imp} | j' \rangle .$$

$s(N)$ is was calculated numerically for $N = 2, \dots, 6$ (Figure 2.5). The result for $\Delta j = N$ (fractional charge) is an exponential decay dependence $\mathcal{T} \sim e^{-\alpha L^2}$, with $\alpha \approx 1/14$. Neglecting $s(N)$, we got $\mathcal{T} \sim e^{-L^2/4m^2}$, so the coefficients are responsible for a stronger decaying parameter. Based on Auerbach's calculation (or on the calculation we give in the next chapter)

one can naively expect to have $\alpha = 1/12$ (see e.g. eq. (3.5)). The obtained value is close but different. This could be related to the different geometries (torus versus cylinder). For the electron in this regime ($\Delta j = mN$) we get that $s(N)$ hardly depends on N , so (2.88) indeed captures the right behavior.

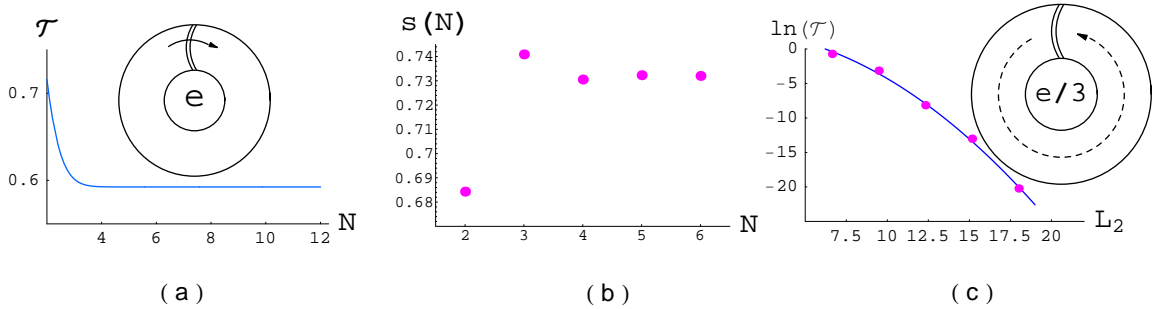


Figure 2.5: Electron versus fractional charge tunnelling (delta function impurity perturbing potential). (a) The tunnelling probability of an electron at $m = 1$ filling. Tunnelling in this regime equals $\mathcal{T}_{m=1}^{el} = \langle j | V_{imp} | j + N \rangle$, weakly depending on N , therefore on the size of the system. The conclusion is that the electron is able to tunnel through the mountain, as shown schematically. (b) For the fractional regime $\mathcal{T}_{m=3}^{el} = s^{el}(N) \langle j | V_{imp} | j + mN \rangle$. Here we give $s^{el}(N)$ for $N \leq 6$. Again the N -dependence is weak, meaning that the electron's tunnelling in the fractional regime also occurs through the mountain. (c) The fractional charge lacks this tunnelling ability. Here we plot $\ln(\mathcal{T})$ as a function of L_2 (dots). The solid line is a fit to $\mathcal{T} \propto e^{-\alpha L^2}$, giving the value of $\alpha \approx \frac{1}{14}$. This strong gaussian dependence tell us that the fractional charge tunnels only through the quantum Hall sea.

Based on the results we have described we therefore conclude that the electron indeed tunnels through the barrier, while the fractional charge does not. This is summarized in the sketches of Figure 2.5.

2.5 Summary

- The problem of electrons on a torus with uniform perpendicular magnetic field, was reviewed. This includes presenting Ψ_s , the Laughlin wave function on a torus. This function is m -fold degenerate, $s = 0, 1, \dots, m-1$. We have found that the total "angular momentum" (TAM) of Ψ_s is given by $(-1)^{N+1} e^{2\pi i s/m} = e^{2\pi i (\text{TAM})/N\phi}$.

- The Laughlin wave function with N_h localized holes, $\Psi_{s;\{z_{0j}\}}$, was obtained and investigated. For $N_h = 1$ we have found that it has the following expansion $\Psi_{s;(z_0)} = \sum_{n=0}^{N_\phi-1} c_{s;n} g_{s;n}(z_0) \psi_{s;n}$, with $g_{s;n}$ being extended-unit-cell single particle wave functions (eq. (2.52)) and $\psi_{s;n}$ having a specified TAM given by $(-1)^N e^{2\pi i(sN-n)/N_\phi} = e^{2\pi i(\text{TAM})/N_\phi}$. It was shown that the sets of $\psi_{s;n}$ with different s are equivalent. One can therefore use the shorter notation ψ_p with $p = (s + mn) \bmod N_\phi$, $p = 0, 1, \dots, N_\phi - 1$.
- We have studied the properties of ψ_p . Among these is the its valley-like distribution with valley at the guiding center of φ_p (the single particle WF). It was shown that numerically diagonalizing a Hamiltonian consisting a hard-core interaction term, results in exactly one state with zero interaction energy and specified TAM, which is no other than ψ_p .
- The valley-wave-functions ψ_p were used as a basis for studying the electron vs. fractional charge tunnelling. We have shown that the tunnelling depends weakly on the size of the system if an electron is treated (in both the integer and the fractional regimes) but is exponentially (gaussian-like) small for a fractional charge. Therefore we conclude that the electron "digs its way" through the barrier mountain, while the fractional charge can only "swim" thorough the Hall sea.

Chapter 3

Tunnelling Through The Quantum Hall Liquid

The previous chapter dealt with the problem of tunnelling through a barrier. We have found that the electron indeed tunnels through the potential barrier, while the fractional charge does not. In this chapter we shall study the tunnelling through the quantum Hall liquid, apparently the only tunnelling process the fractional charge experiences and a possible one for an electron. As was reviewed in the first chapter Auerbach has studied this in a cylindrical geometry. From many aspects the cylinder geometry resembles the torus one. Tunnelling through the quantum Hall liquid is essentially the same for the two geometries, the cylinder being much simpler to handle. In Auerbach's problem one impurity was present in the middle of the sample. Here we look at the influence of more impurities. We are interested to know how the tunnelling scales with the system's size. We examine a few scenarios of increasing the sample's area. The result is generic. When a uniform density of impurities is present, the gaussian decrease Auerbach has reported on changes into an exponential one. This resembles a previous result in the IQH regime reported by Shklovskii and by Li & Thouless. Here it is numerically generalized to fractional filling, with fractional charge tunnelling still decaying *slower* than the electron one.

3.1 The Cylinder Tunnelling Problem

Auerbach's Approach

Auerbach has studied the problem of tunnelling through the quantum Hall liquid by a first order calculation done in a cylindrical geometry. The unperturbed Hamiltonian is $H_0 + V_{int}$ (eq. (1.9)). One possible eigenstate of this Hamiltonian is LWF

$$\Psi = e^{-\sum y_j^2/l_H^2} \prod_{j<k} (e^{-iz_j/R} - e^{-iz_k/R})^m. \quad (3.1)$$

This state has a nonzero density in length of the order of $L = N_\phi l_H^2/R$ (recall Dirac's condition).

For an infinitely long cylinder the problem is infinitely degenerate. For example, moving the center of mass does not effect the energy of the above ground state¹. This degeneracy is lifted if a confining potential is present, choosing one (or few) possible states as groundstates. Figure 3.1 present a scheme of such a possible potential, choosing two groundstates for the system: the above Laughlin's state Ψ and a shifted state marked by $\tilde{\Psi}$. The state $\tilde{\Psi}$ has the same density landscape as that of Ψ , only shifted in $L/N_\phi = l_H^2/R$. It is obtained by increasing the flux quantum passing through the cylinder in ϕ_0 , therefore increasing each quantum number by one. If

$$\Psi = \sum_{\{j_k\}} A_{j_1, \dots, j_N} |j_1, \dots, j_N\rangle \quad (3.2)$$

then

$$\begin{aligned} \tilde{\Psi} &\propto \sum_{\{j_k\}} A_{j_1, \dots, j_N} |j_1 + 1, \dots, j_N + 1\rangle = \\ &= \sum_{\{j_k\}} A_{j_1, \dots, j_N} \prod_{k=1}^N \left(\frac{c_{j_k+1}}{c_{j_k}} e^{-iz_k/R} \right) |j_1, \dots, j_N\rangle \approx \\ &\approx \prod_{j=1}^N e^{-iz_j/R} \Psi \end{aligned} \quad (3.3)$$

¹In general any multiple of Ψ with a polynomial $\mathbf{f}(e^{-iz_1/R}, \dots, e^{-iz_N/R})$, which is even in all variables, is a good groundstate for $H_0 + V_{int}$

with $c_j \equiv (2\pi R l_H \sqrt{\pi})^{-1/2} e^{-(j l_H/R)^2}$ being the single particle normalization factors (see eq. (1.20)).

The approximation done here is the same as the one done in building the Laughlin's localized WF. The thrown normalizing factors should have little effect on the WF [1].

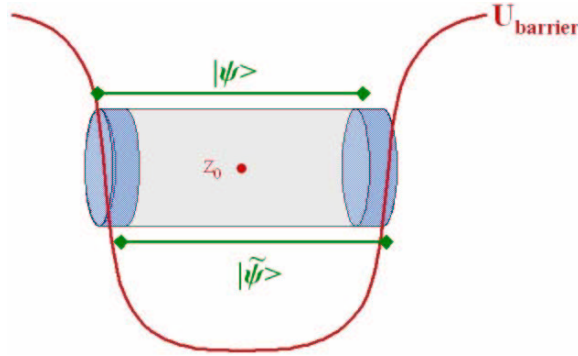


Figure 3.1: A schematic description of the tunnelling problem. The infinite cylinder becomes finite-like, by introducing a background potential. The tunnelling is studied by the possibility of starting with the "left" Laughlin state $|\Psi\rangle$, and ending with the "right" state $|\tilde{\Psi}\rangle$. The shift is accompanied by a charge of e/m moving from left to right, with the help of the impurity potential.

Note the similarity between Auerbach procedure to the one we have presented in the previous chapter, the confining potential plays the role of the torus barrier potential, both selecting two adjacent states, having TAM momentum difference of N , as the possible groundstates of the system. The main difference is, of course, that for the cylinder the tunnelling is necessarily through the quantum Hall liquid.

Meanwhile we have presented the Hamiltonian $H_0 + V_{int} + V_{conf}$, and the two minimum energy states (sitting as usual in the LLL), Ψ and $\tilde{\Psi}$. The last term we shall add to that Hamiltonian is a perturbing impurity potential denoted by V_{imp} . In Auerbach's paper it was taken as either $\delta(x)$ or $\delta(x)\delta(y - Y)$, Y being the cylinder's center. This potential couples Ψ and $\tilde{\Psi}$, and the tunnelling probability, similarly to the torus case, is given to first order by

$$\mathcal{T} = \langle \Psi | V_{imp} | \tilde{\Psi} \rangle . \quad (3.4)$$

Auerbach has shown, for $m = 1, 3$ that

$$\mathcal{T} \propto e^{-L^2/4ml_H^2} . \quad (3.5)$$

This result indicates that the quantum Hall liquid tunnelling rate for a quasi particle is faster than that of an electron, both decrease like a gaussian with the size of the system.

Below we present an alternative calculation, which gives the same result, and generalizes it to the case of more impurities.

Our Approach

The full Hamiltonian is still taken as

$$H = H_0 + V_{int} + V_{conf} + V_{imp} \quad (3.6)$$

In Auerbach's approach the chosen wave functions minimize $H_0 + V_{int} + V_{conf}$ while V_{imp} is treated as a perturbation. Alternatively, one can work with wave functions based on the full Hamiltonian. In what follows we concentrate on the impurity potential

$$V_{imp} = \delta(x - x_0)\delta(y - y_0) . \quad (3.7)$$

The LWF with one hole localized at (x_0, y_0) obviously vanishes at that point, its energy regarding V_{imp} is therefore zero. This fact joins the characteristics making LWF favorable, present also in the localized hole WF. We shall therefore work with Ψ_{z_0} , LWF with one localized hole at $z_0 = x_0 + iy_0$, and a shifted state $\tilde{\Psi}_{z_0}$ which is related to Ψ_{z_0} similarly to (3.3). The tunnelling probability is given by the overlap between these two states

$$\mathcal{T} = \langle \Psi_{z_0} | \tilde{\Psi}_{z_0} \rangle . \quad (3.8)$$

That the overlap measures the tunnelling probability seems pretty natural. After all, the two states differ, from the point of view of function's density, by a fractional charge displacement from one cylinder's side to the other. Nevertheless, one can show it more rigorously. First assume that the Hilbert space can be reduced to Ψ_{z_0} and $\tilde{\Psi}_{z_0}$, two non-orthogonal WFs. Finding possible eigenvalues when working with a non-orthogonal basis is done by diagonalizing $\hat{H}\hat{O}^{-1}$, where $\hat{H}_{ij} \equiv \langle \Psi_i | H | \Psi_j \rangle$ and $\hat{O}_{ij} \equiv \langle \Psi_i | \Psi_j \rangle$ (in general i and j run over all possible basis functions). Here is the proof: a desired eigenstate χ

satisfies $H\chi = E\chi$. Expanding $\chi = \sum_j A_j \Psi_j$, and using the definitions of \hat{H} and \hat{O} leads to $\sum_j A_j (\hat{H}_{ij} - E\hat{O}_{ij}) = 0$ which is satisfied if and only if $|\hat{H} - E\hat{O}| = |\hat{H}\hat{O}^{-1} - E\hat{1}| |\hat{O}| = 0$. So indeed $\hat{H}\hat{O}^{-1}$ should be diagonalized. Coming back to our problem yields

$$\hat{H} = \begin{pmatrix} E_b & 0 \\ 0 & \tilde{E}_b \end{pmatrix}$$

$$\hat{O} = \begin{pmatrix} 1 & \mathcal{T}^* \\ \mathcal{T} & 1 \end{pmatrix}$$

where $E_b \equiv \langle \Psi | V_{conf} | \Psi \rangle = \langle \tilde{\Psi} | V_{conf} | \tilde{\Psi} \rangle$ (the confining potential is chosen to be independent of x , and symmetrical regarding Ψ and $\tilde{\Psi}$). Diagonalizing $\hat{H}\hat{O}^{-1}$ leads to two eigenstates with energy difference of $2|\mathcal{T}|E_b/(1 - |\mathcal{T}|^2)$. For $|\mathcal{T}| \ll 1$, this is just $2E_b\mathcal{T}$.

This approach can be easily extended to any number of impurities (and as we shall see it goes on beyond first order calculation). One just has to look at the overlap

$$\mathcal{T} = \langle \Psi_{\{z_{0j}\}} | \tilde{\Psi}_{\{z_{0j}\}} \rangle \quad (3.9)$$

where j runs over all impurities, the impurity potential now having N_h impurities

$$V_{imp} = \sum_{j=1}^{N_h} \delta(x - x_{0j}) \delta(y - y_{0j}) \quad . \quad (3.10)$$

By this approach we study how the addition of impurities influences the gaussian decrease Auerbach has reported on. Can the impurities soften this strong decrease ? In Shklovskii-Li-Thouless the Green's function tail was changed from a gaussian to an exponent by the influence of a random white noise potential. We will show that the same happens here. Can one find a physical arrangement with even softer decrease ? A power law decrease could have been nice...

Studying more impurities was motivated by the understanding that the overlap contains more non-vanishing terms if the number of impurities is increased. This is seen by comparing the TAM of the two overlapping WFs. We noted already that

$$M_0 \leq \text{TAM of } \Psi_{\{z_{0j}\}} \leq M_0 + NN_h$$

$$M_0 + N \leq \text{TAM of } \tilde{\Psi}_{\{z_{0j}\}} \leq M_0 + NN_h + N$$

where $M_0 = mN(N-1)/2$. So the larger the number of impurities is, the larger is the overlap (at least in TAM space) of $\Psi_{\{z_{0j}\}}$ and $\tilde{\Psi}_{\{z_{0j}\}}$. This is shown for $m = 3$ in Figure 3.2.

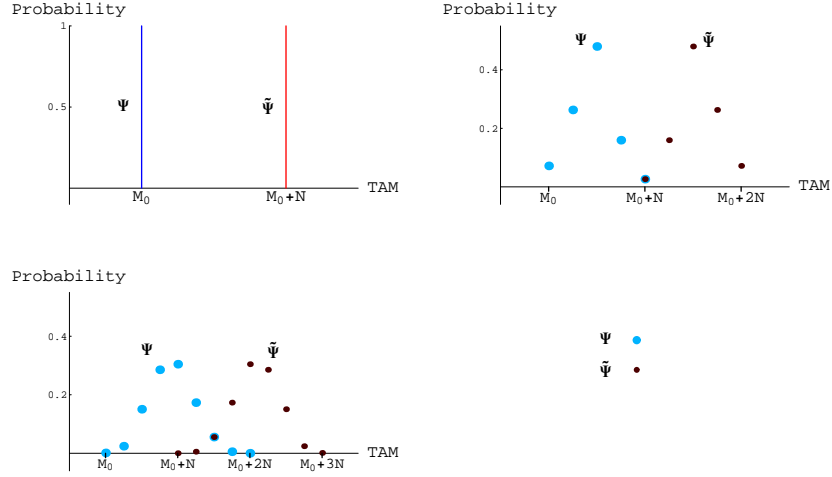


Figure 3.2: TAM distribution for Ψ and $\tilde{\Psi}$, for 0 (top left), 1 (top right), and 2 holes. The TAM distribution gets wider as the number of holes is increased, leading to more non-vanishing terms in the overlap's expression.

Quick Summary

We have argued above that in a system with N_h (positive) impurities, the tunnelling probability of an electron or a quasi-particle is given by

$$\langle \Psi_{\{z_{0j}\}} | \tilde{\Psi}_{\{z_{0j}\}} \rangle, \quad (3.11)$$

where

$$\Psi_{\{z_{0j}\}} = C_{\{z_{0j}\}} \prod_{k < j} (e^{-iz_k/R} - e^{-iz_j/R})^m \prod_{k=1}^N \prod_{j=1}^{N_h} (e^{-iz_k/R} - e^{-iz_{0j}/R}) \quad (3.12)$$

and

$$\tilde{\Psi}_{\{z_{0j}\}} = \frac{\tilde{C}_{\{z_{0j}\}}}{C_{\{z_{0j}\}}} \prod_{j=1}^N e^{-iz_j/R} \Psi_{\{z_{0j}\}} . \quad (3.13)$$

$C_{\{z_{0j}\}}$ and $\tilde{C}_{\{z_{0j}\}}$ are normalizing constants.

The Studied Arrangements Of Impurities

In the sections that follow we study the tunnelling of e/m charged particles by calculating the overlap between Ψ and $\tilde{\Psi}$ at $1/m$ filling factor. The main interest is the dependence of the overlap on the size of the cylinder. Two main cases are considered. At first the number of impurities is held fixed. Then we study the case of a fixed density of impurities.

In a general real problem one expects the impurities to be distributed randomly all over the sample. We start with a more modest problem. We choose a definite typical configuration with impurities equally spaced regarding the y direction². As for the x direction, we first study configurations with all the impurities sharing the same coordinate, so they all lie on a string stretched along the y axis. Then we vary the x -location randomly and reexamine things. The main different studied arrangements are presented in Figure 3.3.

Note that while the cylinder's radius R , being a periodic coordinate, is well defined, one has to clarify the definition of cylinder's length L . After all, the boundaries in the y direction are not sharp, as the eigenstates we work with are taken from the problem of an infinitely long cylinder. In what follows we take the length as

$$L = N_\phi l_H^2 / R , \quad (3.14)$$

following the Dirac's condition.

Another possible natural definition is the distance between the two most distanced guiding centers, $L' = [m(N-1)+1+N_h]l_H^2/R = [N_\phi - m + 1]l_H^2/R$. The two definitions are equivalent for $m = 1$ and become equivalent for any

²For a general N_h this still leaves two degrees of freedom, e.g. the first and last zeroes location. In our study the locations are usually chosen to be symmetrical regarding Ψ and $\tilde{\Psi}$. This leaves only one degree of freedom, the first zero location, taken to be $\frac{1}{2}L/N_h$. In any case, the particular chosen configuration do not change the general behavior.

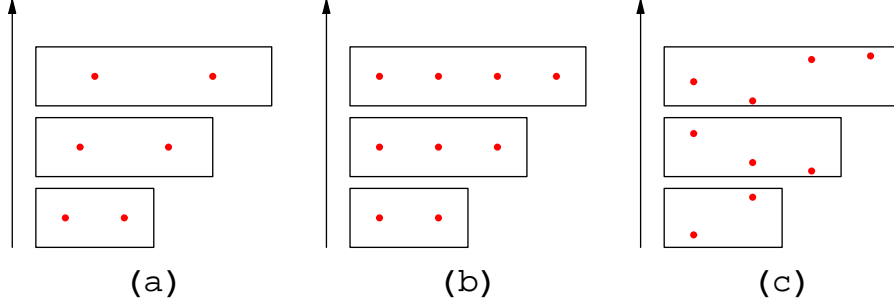


Figure 3.3: The studied impurity arrangements. In all realizations the localized holes are equally spread in the y direction. (a) The number of impurities is held fixed while increasing the cylinder's length. The holes share the same x coordinate. (b) The impurities density is the fixed quantity. Holes still share the same x coordinate. (c) same as (b), besides the x coordinates chosen in random, and averaged.

m in the thermodynamic limit. We mention L' mainly because the cylinder's central symmetry point is $y = L'/2$.

3.2 Fixed Number Of Impurities

The main message of this section is that the tunnelling for a system with fixed number of impurities, N_h , scales (in the limit of a large cylinder) like a gaussian for both an electron and a fractional charge, the latter decaying-factor being m times smaller than that of the electron

$$\langle \Psi_{\{z_0\}} | \tilde{\Psi}_{\{z_0\}} \rangle \sim e^{-L^2/4N_h m} . \quad (3.15)$$

This is no more than generalizing Auerbach's result (3.5) for any number of impurities. Note that as expected, the tunnelling decays slower when more impurities are present. Still the decay has the same gaussian structure.

Generally the overlap depends on a few parameters: the number of particles N , the cylinder's length L and radius R and, of course, on the tunnelling object, either an electron or a fractional charge (carrying in what follows a charge of $e/3$) which is determined by $m = 1, 3$ respectively.

These are not independent parameters as

$$N_\phi = \mathbf{m}N + N_h = LR/l_H^2 .$$

Increasing L while keeping N_h fixed can be done (for a given \mathbf{m}) either by increasing N , keeping the cylinder's radius fixed, or by keeping N constant, while decreasing the cylinder's radius R (we skip the possibility of combining the two). The L dependence we have numerically verified was the same for the two possibilities. We will therefore concentrate on the calculational easier way- varying L by squeezing R .

The remainder of the section includes some technical calculational details, together with a qualitative understanding of (3.15).

One Localized Impurity

We start by writing the normalized Ψ_{z_0} and $\tilde{\Psi}_{z_0}$ for the case of $\mathbf{m} = 1$

$$\begin{aligned} |\Psi_{z_0}\rangle &= A_{0,N}(z_0) \sum_{n=0}^N (-1)^n \varphi_n(z_0) |0, 1, \dots, \underbrace{n}, \dots, N\rangle \\ |\tilde{\Psi}_{z_0}\rangle &= A_{1,N+1}(z_0) \sum_{n'=1}^{N+1} (-1)^{n'} \varphi_{n'}(z_0) |1, \dots, \underbrace{n'}, \dots, (N+1)\rangle \end{aligned} \quad (3.16)$$

with

$$A_{q,p}(z_0)^{-2} \equiv \sum_{n=q}^p |\varphi_n(z_0)|^2 .$$

When taking the overlap between these two WFs only one term does not vanish, the $n = 0$ term in Ψ_{z_0} multiplied by the $n' = N + 1$ term in $\tilde{\Psi}_{z_0}$. The overlap therefore satisfies

$$\begin{aligned} |\langle \Psi_{z_0} | \tilde{\Psi}_{z_0} \rangle| &= A_{0,N}(z_0) A_{1,N+1}(z_0) |\varphi_0^*(z_0) \varphi_{N+1}(z_0)| = \\ &= \tilde{A}_{0,N}(y_0) \tilde{A}_{1,N+1}(y_0) e^{(N+1)y_0/R} e^{-(N+1)^2/2R^2} \end{aligned} \quad (3.17)$$

where

$$\tilde{A}_{p,q}(y) = \left(\sum_{n=p}^q e^{2ny/R} e^{-n^2/R^2} \right)^{-1/2} .$$

Naturally the overlap's absolute value does not depend on the hole's location along the x axis. The y dependence is gaussian-like centered at $y_0 = L/2$. As expected the overlap, and therefore the tunnelling, is maximized by choosing the impurity exactly at the middle of the cylinder. Writing the maximal overlap explicitly gives

$$\langle \Psi_{z_0} | \tilde{\Psi}_{z_0} \rangle^{-1} = \tilde{A}_{0,N}(L/2) \tilde{A}_{1,N+1}(L/2) . \quad (3.18)$$

This can be estimated by taking the maximal term in each of the two sums, the one with $n \sim (N+1)/2$. The result is the gaussian decrease behavior Auerbach has reported on

$$\langle \Psi_{z_0} | \tilde{\Psi}_{z_0} \rangle \xrightarrow{L \rightarrow \infty} e^{-L^2/4l_H^2} . \quad (3.19)$$

A better estimate is obtained by converting each sum into an integral. For $N \gg 1$ the results is

$$\langle \Psi_{z_0} | \tilde{\Psi}_{z_0} \rangle \xrightarrow{N \gg 1} \frac{L}{(N+1)\sqrt{\pi}l_H} \text{erf}(L/2) e^{-L^2/4l_H^2} . \quad (3.20)$$

In the large L limit $\text{erf}(L/2) \approx 1$ therefore

$$\langle \Psi_{z_0} | \tilde{\Psi}_{z_0} \rangle \xrightarrow{L \rightarrow \infty} \frac{L}{(N+1)\sqrt{\pi}l_H} e^{-L^2/4l_H^2} , \quad (3.21)$$

so besides the gaussian decay, a power low dependence of the pre-factor is found.

The procedure of tunnelling described here can be thought of as a transfer of a gaussian shaped hole (an "extended" hole) from one side of the cylinder to the other, with the assistance of the impurity. Mathematically (neglecting the normalizing factors, justified for a very long cylinder) the overlap reduces

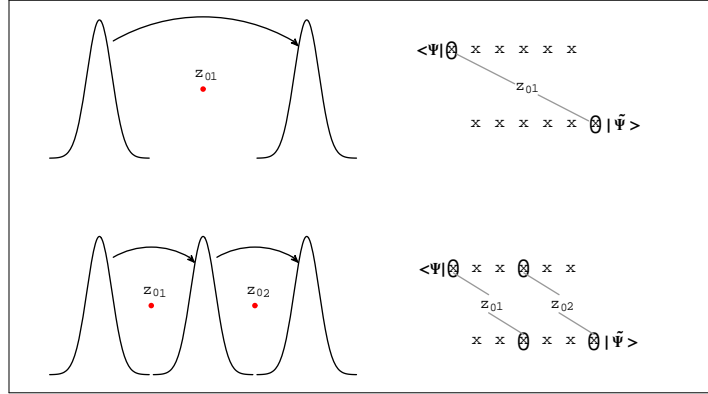


Figure 3.4: A schematic description of the overlap between Ψ and $\tilde{\Psi}$ for one (top) and two (bottom) localized holes. The overlap is a measure of tunnelling probability. We first explain the top graph (one impurity). In the *left* we describe the tunnelling as a gaussian jumping from one cylinder's edge to the other. This is mathematically justified by noting that in the limit of a long cylinder the overlap expression involves the product of two gaussians whose variable lies at the location of the impurity (see eq. (3.17)). The *right* figure describes the overlap's approximate calculation schematically. The "x" are available single particle states of Ψ (top line of "x") and the shifted ones of $\tilde{\Psi}$ (bottom line). The circle is a state not occupied by a particle (an "extended hole" state). Again, the impurity is an agent connecting the two farthest hole states. This pictures is easily extended to the case of more (e.g. two) impurities: the tunnelling is carried out in steps of the order of L/N_h (see eq. (3.24)).

to the multiple of two gaussians $\varphi_0(z_0) \times \varphi_{N+1}(z_0)$ with z_0 as the impurity location³. For an impurity exactly in the middle $y_0 = L/2$, this product gives $e^{-(\Delta L)^2/4}$, where ΔL is the distance between the two gaussians' centers. This immediately explains the gaussian L dependence decay and is depicted schematically in Figure 3.4.

One might also be interested in the limit of a very narrow cylinder. Estimating the overlap in this limit of $L \rightarrow 0$ (keeping the number of particles fixed) starting from eq. (3.20) leads to

$$\langle \Psi_{z_0} | \tilde{\Psi}_{z_0} \rangle \xrightarrow{L \rightarrow 0} \frac{1}{N+1} \left[1 - \frac{1}{6(N+1)} L^2 \right]. \quad (3.22)$$

³See first equality in eq. (3.17).

In what follows we give an expression for a general N_h (eq. (3.28)).

Studying the overlap system size dependence was done numerically for the case of m different than 1. If the overlap is calculated for a hole localized at $y_0 = L/2$ the result (in the large L limit) is a gaussian decrease, decaying slower than the $m = 1$ case

$$\langle \Psi_{z_0} | \tilde{\Psi}_{z_0} \rangle \sim e^{-L^2/4m} .$$

This result is verified in Figure 3.5 for both $m = 1$ and 3.

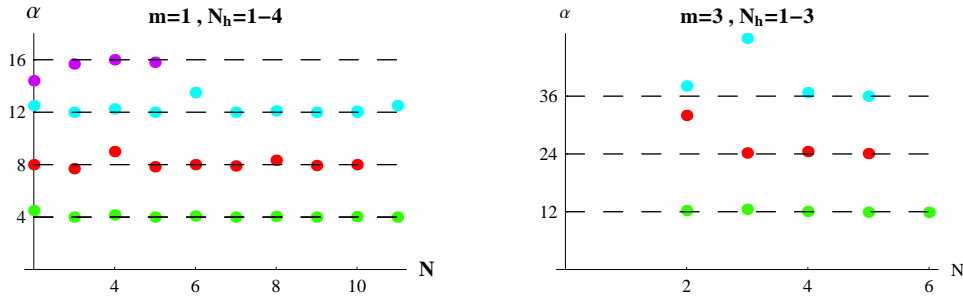


Figure 3.5: The studied overlap behaves, for a large system, as a gaussian: $\exp[-\alpha L^2]$. Here we plot the numerically calculated α for various number of impurities ($N_h = 1, \dots, 4$, for $m = 1, 3$). It is clear that in as N increases α become closer to $1/mN_h$. [We thank A. Auerbach for sharing with us the expansion coefficients of LWF].

Two Localized impurities

The $m = 1$ wave functions with two localized impurities are

$$|\Psi\rangle = A_{0,N+1} \sum_{\substack{n_1 < n_2 \\ n_1, n_2 = 0, \dots, N+1}} (-1)^{n_1+n_2} SD[n_1, n_2] |0, 1, \dots, N+1\rangle$$

$$|\tilde{\Psi}\rangle = A_{1,N+2} \sum_{\substack{n'_1 < n'_2 \\ n'_1, n'_2 = 1, \dots, N+2}} (-1)^{n'_1+n'_2} SD[n'_1, n'_2] |1, \dots, N+2\rangle$$

with

$$(A_{q,p})^{-2} \equiv \sum_{\substack{n_1 < n_2 \\ n_1, n_2 = q, \dots, p}} |SD[n_1, n_2]|^2$$

and

$$SD[n_1, n_2] \equiv \begin{vmatrix} \varphi_{n_1}(z_{01}) & \varphi_{n_2}(z_{01}) \\ \varphi_{n_1}(z_{02}) & \varphi_{n_2}(z_{02}) \end{vmatrix}.$$

The overlap is zero unless $n_1 = 0$, $n'_2 = N+2$ and $n_2 = n'_1 = 1, 2, \dots, (N+1)$, so

$$\langle \Psi | \tilde{\Psi} \rangle = A_{0,N+1} A_{1,N+2} \sum_{n_1=1}^{N+1} SD[0, n_1]^* SD[n_1, N+N_h]. \quad (3.23)$$

This calculation is schematized in Figure 3.4. A typical term in the sum (3.23) has the form

$$\varphi_0(z_{0,j_1})^* \varphi_n(z_{0,j_2})^* \varphi_n(z_{0,j_3}) \varphi_{N+2}(z_{0,j_4})$$

with $j_1, \dots, j_4 = 1, 2$. Denoting the impurity closest to the left edge of the cylinder ($y = 0$) by z_{01} , it seems that the maximal (absolute) value of such a term is obtained for $j_1 = 1$ and $j_4 = 2$ (this way the gaussian variable is the closest it can be to the gaussian's guiding centers of φ_0 and φ_{N+2}). The absolute value of this dominant term is

$$|\varphi_0(z_{0,1}) \varphi_n(z_{0,1})| |\varphi_n(z_{0,2}) \varphi_{N+2}(z_{0,2})| \quad (3.24)$$

which is maximized for $n \sim (N+2)/2$, $y_1 = L/4$ and $y_2 = 3L/4$.

Note that we have totally neglected the x dependence which might twist things appreciably. We come back to this dependence in the next section.

By studying the problem numerically it was verified that the approximations done above are valid in the limit of a long cylinder. Figure 3.6 presents a graph with the locations of the y_{01} and y_{02} (the two impurities share the

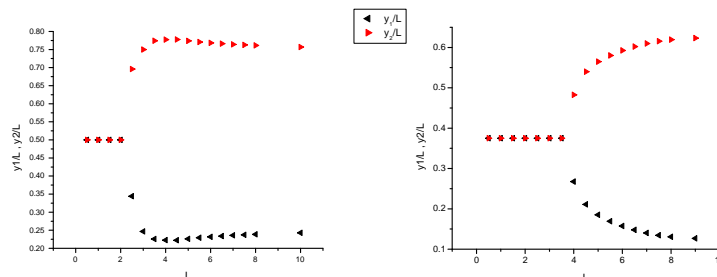


Figure 3.6: Location of impurities maximizing the overlap for various cylinder's lengths ($N = 2$, $N_h = 2$, $m = 1$ (left), 3 (right)): for an incredibly thin cylinder if both impurities are localized at the middle of the cylinder then the overlap is maximized. But as the system become more physically reasonable ($L > l_H$) the apparent bifurcation show-up and for $L \gg l_H$ the maximal overlap is obtained for impurities sitting at distances $\pm L/4$ from the cylinder's center. (note that for $m = 3$ the symmetry point is shifted towards the origin as explained in the paragraph following eq. 3.14)

same x coordinate) that maximize the overlap, as a function of cylinder's length. Indeed a long cylinder prefers the impurities at $L/4$ and $3L/4$.

Setting the impurities at these preferable points, we get that (for a long cylinder) the tunnelling scales like a gaussian

$$\langle \Psi_{z_{01}, z_{02}} | \tilde{\Psi}_{z_{01}, z_{02}} \rangle \sim e^{-L^2/8m} . \quad (3.25)$$

Based on the estimated calculation above (eq. (3.24)), this can be easily explained for $m = 1$. The dominant term contributing mostly to the overlap consists of two gaussian overlaps, each scales like $e^{-\Delta^2/4}$, with $\Delta = L/N_h$ (being the distance between the guiding centers of each pair). So the overall overlap is in this case

$$\left[e^{-(\frac{L}{2})^2/4} \right]^2 \quad (3.26)$$

leading to (3.25).

General Results

Previously we have showed and explained why the maximal overlap for a long cylinder and $N_h = 1, 2$, is obtained by choosing the impurities as given in Figure 3.4. For such a choice we argued that the overlap decreases with the cylinder's length as

$$\langle \Psi | \tilde{\Psi} \rangle \propto e^{-L^2/4mN_h} . \quad (3.27)$$

This result remains true for general N_h , as we have verified for $N_h \leq 4$.

The $m = 1$ argument given for one or two holes (see e.g. eq. (3.26)) is valid also for a general number of impurities. A product of N_h pairs of gaussians, each contributing a decay factor of $e^{-(\frac{L}{N_h})^2/4}$, leads to (3.27).

Unlike the case of $N_h = 1, 2$, the calculated overlap for a general N_h is not the maximal valued. Even for a case with impurities equally spaced and symmetrical regarding the cylinder's center, some other configurations⁴ exist that maximize that overlap. Therefore the given configuration should be thought of as typical one rather than maximal.

We have also showed numerically that for small L

$$\mathcal{T} = \frac{N_h}{N + N_h} \left[1 - \frac{N(N + 2N_h)}{(N + N_h)^2} \frac{N_h}{2(4N_h^2 - 1)} L^2 + o(L^4) \right] . \quad (3.28)$$

This is believed to be exact for any N and N_h , and is consistent with the one impurity result (3.22) in the limit of large N .

⁴Among these are, for example, the artificial configuration with some impurities far beyond the cylinder's edge, a realization that "squeezes" the two many body WFs and therefore maximizes the overlap.

3.3 Constant Density Of Impurities

The tunnelling was described as a process of charge transfer from one size of the cylinder to the other, done with the help of the impurities. Previously when the length of the cylinder was increased, the average hopping distance⁵ increased as well (Figure 3.3(a)). In this section we shall study a more realistic problem in which the average distance between the impurities, together with the impurities density, remains fixed. It was noted already that the overlap is a function of few parameters: N , N_h , L and R , satisfying $LR = \mathfrak{m}N + N_h$. We start, as before, with the case of impurities all sharing the same x coordinate. The distance between impurities along the y direction (the longitudinal impurities density)

$$\lambda = L/N_h \quad (3.29)$$

is held constant together with

$$\gamma = N/N_h \quad (3.30)$$

which guaranties a specified impurities' surface density⁶

$$\begin{aligned} \sigma_h &= 2\pi RL/N_h \\ &= 2\pi N_\phi l_H^2/N_h \\ &= 2\pi l_H^2(\mathfrak{m}\gamma + 1) . \end{aligned}$$

An educated guess for the overlap at this described configuration can be made using the result from the previous section. Taking the gaussian like dependence $e^{-L^2/4\mathfrak{m}N_h}$ together with (3.29) immediately leads to

$$e^{-\lambda L/4\mathfrak{m}}, \quad (3.31)$$

⁵The tunnelling can visualized as if the charge jumps from one edge to the nearest impurity, then to next impurity, and so on until it reaches the other edge (see Figure 3.4). The average hopping distance is the averaged distance between the impurities.

⁶Note that in the previous section, we usually looked at a situation of fixed N and N_h . So previously the impurities surface density was also chosen as fixed. The main difference between the two choices is, as was already noted, the hopping distance.

replacing the gaussian L dependency with an exponent decay. In turns out this is actually the obtained result, in the limit of $\lambda \gg l_H$. This is verified in Figure 3.8.

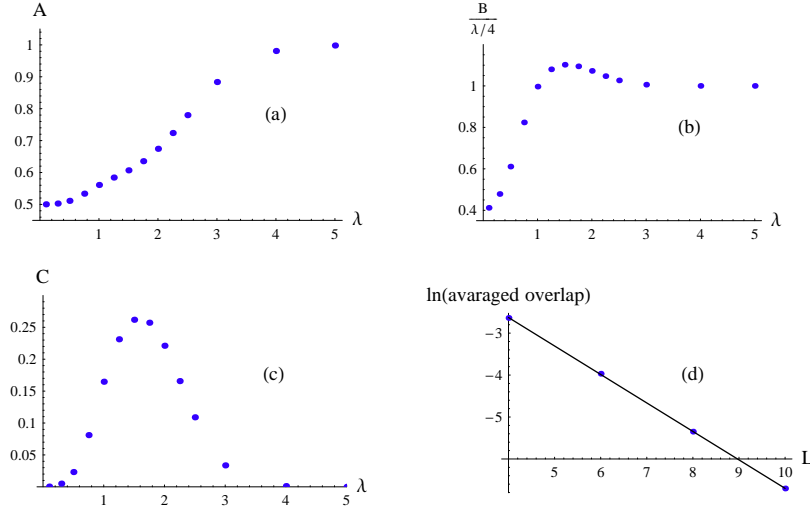


Figure 3.7: Exponentially decaying tunnelling in the IQH regime. (a)-(c): We show results obtained choosing $\gamma = N/N_h = 1$ and equally spaced impurities. The overlap is calculated as a function of L for various values of $\lambda = L/N_h$. For each such value we fit the L -dependence to a function of the form: $Ae^{-BL}L^C$. Here we plot the calculated A, B and C as a function of λ . One clearly see that in the limit of large λ the overlap $\rightarrow e^{-\lambda L/4l_H^2}$. The chosen function should not be taken too seriously. It just serves as a guide and includes the desired exponential. Still the limit of small λ is shown to be related to the limit of small L discussed in the previous chapter: $A \rightarrow 1/(\gamma + 1)$ (here $1/2$), as can be read from eq. (3.28). (d) In randomizing $\{x_{0j}\}$ and averaging the exponential dependency remains.

This gaussian-to-exponential result is familiar, for integer filling factor, from the work of Shklovskii [27] and then Li and Thouless [26]. The latter has reported the gaussian Green function's tail $G \sim e^{-r^2/4}$ for a system of independent electrons in a magnetic field, turning into an exponential tail $G \sim e^{-\alpha r}$ in the presence of a white noised random potential (α measures the noise strength). Here the result is extended to $m = 3$.

For the case of $m = 1$ we have also checked how randomizing things in

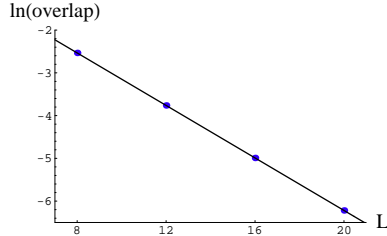


Figure 3.8: Gaussian-to-exponential in the FQH regime. We choose the holes equally spaced on a line (the following values are taken: $\lambda = L/N_h = 4$, $\gamma = N/N_h = 1$, this gives $L = 4N$ while $R = 1$ is held fixed). The exponential behavior is clear, with decaying factor of approximately $1/3.26$ (the expected value according to (3.31) is $\lambda/4m$, or $1/3$ in the chosen values.)

the x direction influences this exponential dependence. In a system where the impurities are distributed randomly in the x direction the overlap still decreases exponentially. The decaying factor is obviously stronger, but the general decrease is the same. We expect this to be true for a general m .

Lastly we would like to find out whether there exist a configuration where the decrease of the overlap with the system's size is even slower than an exponent. A possible candidate is a configuration in which both L and R are increased simultaneously, keeping their ratio $\kappa = L/R$ fixed. As seen in the inset of Figure 3.9 when the impurities are localized along a string stretched in the y direction, not only the overlap does not decrease exponentially, but rather it remains roughly constant (and even increases a bit). But this should not be a total surprise. With increasing L the longitudinal impurity density λ is reduced: $\lambda = L/N_h = (m\gamma + 1)\kappa l_H^2/L$, and therefore $e^{-L^2/4mN_h} \rightarrow e^{(m\gamma+1)\kappa/4}$ which is L independent. But as the x impurity positions are being randomized, the exponential comes back to life. This is shown in Figure ?? The exponential tail is therefore generic.

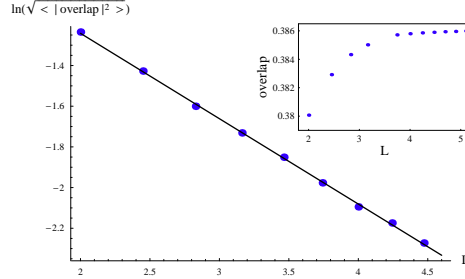


Figure 3.9: The exponential L dependence remains also when the cylinder size is being increased keeping the ratio $\kappa = L/R$ fixed. Here we take $\kappa = 1$. *Inset:* When the impurities are distributed along a string (same x location), the overlap hardly depends on L (and actually increases!). *Outset:* But as randomness comes into play the exponential dependence returns. This was studied for different values of κ and γ . We note that as κ becomes large the exponential decaying parameter become independent of κ .

3.4 Summary

In this chapter we have explained why the overlap $\langle \Psi_{\{z_0 k\}} | \tilde{\Psi}_{\{z_0 k\}} \rangle$ is a good theoretical measurement for the tunnelling of electron or quasi-particle from one cylinder's edge to the other, a tunnelling which is possible due to a given set of localized impurities spreading over the sample. We then described a few impurity arrangements and studied the way the overlap depends on the system's length. The main result is that the gaussian decrease observed when the number of impurities was fixed is turning into an exponent decrease, found in cases with fixed average hopping length. The different arrangements together with the resultant dependency are summarized in the next table.

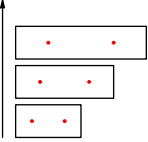
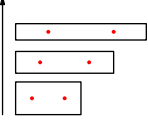
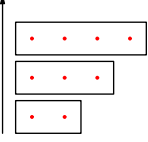
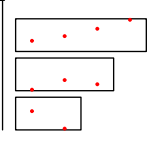
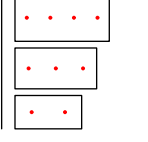
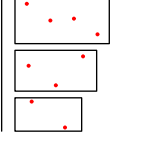
Configuration	Dependency	Fixed Properties
	gaussian $e^{-L^2/4N_h m}$	N_h, R
	gaussian $e^{-L^2/4N_h m}$	N, N_h therefore σ_h
	exponent $e^{-\lambda L/4m}$	λ, γ and therefore R and σ_h
	exponent	λ, γ
	independent of L	γ, κ therefore σ_h
	exponent	γ, κ

Table 3.1: A table summarizing chapter three. Reminders: σ_h =surface hole density, $\lambda = L/N_h$, $\gamma = N/N_h$ and $\kappa = L/R$.

Chapter 4

Conclusions and Plans

The main question we address in this thesis is "Can a fractional charged quasi particle tunnel through a mountain?". The apparent answer is the conventional answer which is no. This was demonstrated in detail in chapter two. It supports the Kane&Fisher arguments and justifies throwing away the possibility of fractional charge tunnelling in the case of a strong scatterer, even when a periodic geometry is considered. Still there is a possibility that a fractional charge from one side of the barrier will show-up on the other side of the mountain, an event that can be interpreted as a tunnelling event. This tunnelling occurs only through the electron sea, and was studied in chapter three. The general result in this limit is that the fractional charge tunnelling is more dominant than the electron one, both tunnelling events are exponentially small. In what follows we give a bit more detailed summary of these results. We then end with some possible future plans, including the possibility of studying the crossover between the weak and strong Kane&Fisher limits.

4.1 Tunnelling Through A Mountain

In chapter two we have defined a set of valley ("extended hole") wave functions, Laughlin-like in spirit and valley-like in shape. We have studied the possible tunnelling events by calculating the matrix element $\langle \psi | V_{imp} | \tilde{\psi} \rangle$, where V_{imp} was some perturbing (delta-function impurity) potential and the wave functions are two adjacent ones, with dried electrons valley which is

closest to the barrier, chosen from the set of defined valley wave functions. The calculation gives an exponential (gaussian-like) decrease for a fractional charge and a negligible dependence for electrons in either the integer or the fractional regimes

$$\langle \psi | V_{imp} | \tilde{\psi} \rangle \sim \begin{cases} e^{-\alpha L^2}, & \text{fractional charge} \\ \text{constant}, & \text{electron.} \end{cases} \quad (4.1)$$

The main argument was based on the fact that (4.1) is related to the overlap between two (single particle) gaussians sitting over the two sides of the mountain, with distance of L_2/N_ϕ when an electron is treated as opposed to a distance of the order of L_2 , for the case of fractional charges. The "electron distance" (and therefore its tunnelling) is independent in the size of the system (as $L_2 \propto N_\phi$) which is not the case for the quasi-particle. We give a summary of this result in Figure 4.1 describing what we expect when a tunnelling experiment in the spirit we have presented along the thesis¹ will be performed in the fractional quantum Hall regime.

The system starts at the valley-state, adjusted to the mountain. In the figure we also present the other states' energy. As the magnetic field flux ϕ_1 is increased, the energy levels develop as shown. As we explained already a couple of times along these notes, without disorder the levels cross at some point (this was exemplified in the first chapter, Figure 1.10). The perturbing potential removes the crossing, creating a gap of the size of (4.1). We emphasize that the periodicity in the energy levels is ϕ_0 , the unit flux. Yet when the system is large, the first opening gap (which fits a fractional charge tunnelling) is much smaller than the one opening for the electron, so a large system periodicity must only be $m\phi_0$. A large toroidal system therefore prefers electron's tunnelling.

4.2 Tunnelling Through The Sea

This result was explicitly shown by Auerbach and is investigated here for *several* delta function impurities (rather than just one). By studying the overlap between two adjacent Laughlin wave functions having N_h holes localized at the impurity location, marked by Ψ and $\tilde{\Psi}$, we show that

¹Assuming the difficulties in finding the Dirac's monopoles will be overcome...

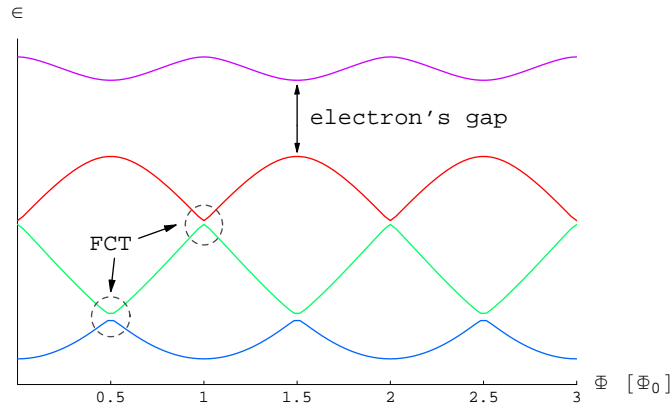


Figure 4.1: A schematic description of the barrier's energy levels as a function of ϕ_1 , the magnetic flux passing inside the torus. The gap associated with the fractional charge decreases exponentially as the system enlarges. This means that the probability to follow the bottom line (describing a fractional charge tunnelling (FCT)) decreases as the system increases. As opposed, the electron's gap remains appreciable also in the large L limit, in principle not allowing a Zener tunnelling to the top level. (The figure presents a calculation done using the effective Hamiltonian model described in Appendix E.)

$$\langle \Psi | \tilde{\Psi} \rangle \sim \begin{cases} e^{-L^2/12N_h l_H^2}, & 1/3 \text{ fractional charge} \\ e^{-L^2/4N_h l_H^2}, & \text{electron.} \end{cases} \quad (4.2)$$

The N_h impurities give a helping hand for the tunnelling, decreasing the decaying factor by N_h . For the case of fixed surface density of impurities, spread all over the sample, the reported gaussian decrease is modified to a pure exponential one. This is related to Shklovskii and Li&Thouless results, and was numerically generalized here to the case of fractional filling factor. It was found that the gaussian to exponential behavior is generic if the impurities are being chosen in random all over the sample, and that in any case the fractional charge decaying factor is m times smaller, hence its dominance in this regime.

4.3 Plans

The Crossover Between Weak And Strong Scattering

We have reported that for a tunnelling through a barrier the electron is impressively dominant over the fractional charge, but when the tunnelling occurs through the quantum Hall liquid, the fractional charge leads. This is in agreement with the Kane&Fisher presented results (Figure 4.2). Note also that by continuously increasing the width of the barrier's mountain (starting with thin barrier), one gets that an electron dominant tunnelling becomes fractional charge one, hence the possibility of studying the crossover by this mechanism is raised.

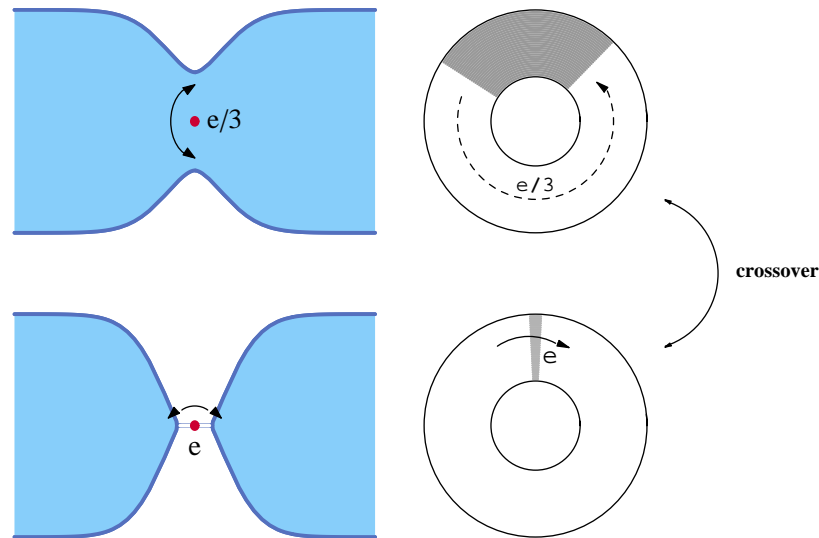


Figure 4.2: A graphic comparison between the Kane&Fisher and the torus approaches. The limit of weak scatterer (Left), or tunnelling through the quantum Hall sea, is dominated by the fractional charge, while the limit of strong scatterer (tunnelling through a mountain) is the electron's regime (Right). By changing the width of the torus studied potential (presented here by the gray area), one can investigate the crossover between the two limits.

The crossover study as displayed here involves a potential becoming wider

and wider. One therefore might be interested in defining a set of valley WFs whose valley contains more than just one extended hole. For N_{ext} extended holes this might be taken naturally as

$$\psi_{s;n_1,\dots,n_{N_{ext}}} = \int dz_{01} \cdots dz_{0N_{ext}} \Psi_{z_{01},\dots,z_{0N_{ext}}} g_{n_1}^*(z_{01}) \cdots g_{n_{N_{ext}}}^*(z_{0N_{ext}}), \quad (4.3)$$

where Ψ_{\dots} is the LWF with N_{ext} localized holes given at (2.31) and the g 's are the same functions defined for one extended hole² (eq. (2.52)).

This form, for the case of more than two extended holes, is more of an educated guess rather than a real a detailed study. One should first study the orthogonality, the valley widths and depth and other characteristics of (4.3) before confidently using it as the set describing tunnelling through a wider or stronger barrier. Still the case of two extended holes supports (4.3). For this case one also finds that equation (2.54) describing the connection between the TAM and the g -numbers is still valid, so it really seems as if this is indeed the right definition.

One other possible extension of our work, which might have implications on the crossover study, is its generalization to valley WFs at filling factors which are not of the studied form $1/m$, but rather of the general form, eq. (1.2).

Tunnelling in these fillings was studied both theoretically and experimentally. This includes investigating the crossover between the weak and strong limits. For example, Griffiths et.al. have reported a different crossover behavior for a fractional charge at $1/3$ filling versus one at $2/5$ filling [39]. It is interesting to find out what our approach has to say, if at all, about this observation.

Effective Hamiltonian Approach

One possible approach for studying the crossover, as well as other problems such as tunnelling through barriers with various shapes, is a model of effective Hamiltonian we briefly describe in Appendix E. The main ingredient is taking into account the fact that adjacent states have a TAM difference of

²This can be extended even further by creating also localized holes, if one is too risky to deal with such a resulting WF. One should just take Ψ in the integrand to be a WF with additional localized holes in the desired locations.

N, so possible coupling of states (existing in the tunnelling problem) has, for a given V_{imp} , a weight of $\langle j|V_{imp}|j + N \rangle$, the single particle element. This coupling is added to the (diagonal) energy of the barrier, which have a landscape easily determined by the shape of the potential and the valley. The model completely ignored the many body coefficients in the expansion of thee valley WFs. It is assumed (as was verified in chapter two) that although these influence the decay parameter, they have no effect at all on the general behavior. The effective Hamiltonian approach has the advantage of being much simpler to handle, still having the same spirit of the treatment we presented along the thesis.

Arovas, Shrieffer And Wilczek On A Torus

Last but not least is the study of fractional statistics on a torus. As an example one can think of extending the work of Arovas et.al. [40] to torus geometry. It should be interesting even to repeat the charge determination by the attitude presented in their work. They basically start with a LWF with one localized hole and by adiabatically moving the hole around a closed loop the WF gains a Berry phase [41] which is related to the charge "seen" by the moving charge. The result is, of course, a charge of e/m when the $1/m$ Laughlin state was taken. But for the torus it is hard to guess what is the total charge the quasi-hole sees, as the geometry is doubly periodic. This might have relevance also to the Dirac's monopoles distribution we already noted.

4.4 Closing Notes

We would like to close with a caricature showing some features we have touched along the lines.

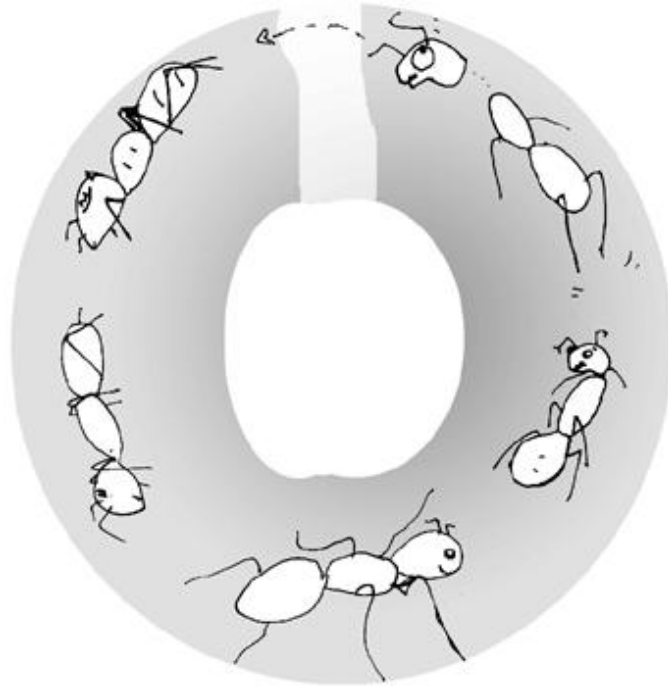


Figure 4.3: Pretzel Logic: A caricature of a fractional charge trying to tunnel through a mountain. The picture can serve as an illustration for a such possible tunnelling (Of course, one should not take this picture too seriously. We are not dealing with an sawn electron... rather the quasi particle can be thought of as an electron entangled with a number of magnetic flux lines.). Whenever I was asked to describe the work by non-physicists, I usually use this description: a series of line arranged ants (=the electrons) living on the surface of a pretzel, and being pushed (=flux change) towards a salty pretzel's area (the lighter area), ants want to avoid (=the barrier). So the question we were asking is whether a third of an ant can jump through the disturbance, or whether the jump is only that of a whole ant. Putting it this way, the answer is indeed trivial... The roundabout tunnelling we have studied on chapter three can also be visualized, by thinking of the impurities as little rods distributed along the pretzel, helping the ants to tunnel backwards (the advantage of the fractional charge is also understood in this picture as it involves three times smaller shifting).

Appendix A

Periodicity, Vanishing and Equalization

We hereby show two (known) results we use along the text. The statements to be proven in short are

1. A quasi-periodic analytic function with periodicity given by

$$\begin{aligned} f(z + L_1) &= \alpha f(z) \\ f(z + iL_2) &= \beta e^{-2\pi i N z / L_1} f(z) \end{aligned} \quad (\text{A.1})$$

(with constant α and β) have N zeroes inside the unit cell $L_1 \times L_2$.

2. Two analytic functions having the same doubly periodicity (therefore by the previous statement have the same number of zeroes inside a unit cell), and whose zeroes locations are similar, are the same (up to a constant).

The first statement is easily proven by using the expression

$$2\pi i \times (\text{the zeroes number inside a closed loop } \Gamma) = \oint_{\Gamma} \frac{f'(z)}{f(z)} dz \quad (\text{A.2})$$

which is true for any analytic function $f(z)$ ([33], p.119)).

Taking the loop Γ to be the square $L_1 \times L_2$ one gets

$$\text{Number of Zeroes} = \frac{1}{2\pi i} \left(\int_0^{L_1} + \int_{L_1}^{L_1+iL_2} + \int_{L_1+iL_2}^{iL_2} + \int_{iL_2}^0 \right) \frac{f'(z)}{f(z)} dz .$$

In the second and third terms we define $z \rightarrow z - L_1$ and $z \rightarrow z - iL_2$ respectively, obtaining

$$\text{Number of Zeroes} = \frac{1}{2\pi i} \left(\int_0^{L_1} \left[\frac{f'(z)}{f(z)} - \frac{f'(z+iL_2)}{f(z+iL_2)} \right] dz + \int_0^{iL_2} \left[\frac{f'(z)}{f(z)} - \frac{f'(z+L_1)}{f(z+L_1)} \right] dy \right) .$$

By (A.1) we get

$$\begin{aligned} f'(z + L_1) &= \alpha f'(z) \\ f'(z + iL_2) &= -\frac{2\pi i N}{L_1} f(z + iL_2) + \beta e^{-2\pi i N z / L_1} f'(z) \end{aligned}$$

hence

$$\text{Number of Zeroes} = \frac{1}{2\pi i} \int_0^{L_1} \frac{2\pi i N}{L_1} dz = N . \quad (\text{A.3})$$

This completes the first proof.

To prove the second statement we start by taking two analytic functions, f_1 and f_2 , both satisfying (A.1). We define $r(z) = \frac{f_1(z)}{f_2(z)}$. It is clear that by (A.1) the *analytic* function $r(z)$ satisfies

$$r(z + L_1) = r(z + iL_2) = r(z) .$$

It is therefore bounded for all values of z . By Liouville's theorem from the theory of complex variables ([33], p.105) we get $r(z) = \text{constant}$, hence $f_1 \propto f_2$ as claimed.

Appendix B

A Useful Identity For The Single Particle Torus Wave Function

In this section we are going to prove equation (2.80), a useful identity involving torus single particle WFs

$$\begin{aligned} \langle j|V(y)e^{2\pi ikx/L_1}|j' \rangle &= & (B.1) \\ \frac{1}{\sqrt{\pi}l_H} e^{-iq\phi_2} e^{-\left(\frac{kL_2}{2N_\phi l_H}\right)^2} \int_{-\infty}^{\infty} e^{-(w+w_0)^2/l_H^2} V(w) dw \end{aligned}$$

with integer q (otherwise the integral vanishes) given by

$$q = \frac{j' - j - k}{N_\phi} \quad (B.2)$$

and

$$w_0 \equiv \frac{\pi l_H^2}{L_1} (2N_\phi + \phi_1/\pi - j - j' + qN_\phi) .$$

Some simple applications of this identity are given in chapter two, in the context of electron versus fractional charge tunnelling. Another trivial

application is the proving the orthonormality of the torus single particle WFs, obtained by using this identity with $k = 0$ and $V(y) = 1$.

The proof starts with writing the single particle expression (2.12) using the explicit sum defining the theta function (2.8)

$$\varphi_j = \sum_{n=-\infty}^{\infty} f_{j,n} g_{j,n}(x) h_{j,n}(y)$$

where

$$\begin{aligned} f_{j,n} &\equiv A_j(-i)(-1)^n e^{i\pi\tau(n+1/2)^2} e^{-i(2n+1)[\pi N_\phi a/L_1 + j\pi\tau]} \\ g_{j,n}(x) &\equiv e^{i(\pi N_\phi + \phi_1 - 2\pi j)x/L_1} e^{i(2n+1)\pi N_\phi x/L_1} \\ h_{j,n}(y) &\equiv e^{-y^2/2L_H^2} e^{-(\pi N_\phi + \phi_1 - 1\pi j)y/L_1} e^{-(2n+1)\pi N_\phi y/L_1} . \end{aligned} \quad (\text{B.3})$$

Using these definitions

$$\begin{aligned} \langle j|V(y)e^{2\pi ikx/L_1}|j' \rangle &= \sum_{n,n'=-\infty}^{\infty} f_{j,n}^* f_{j',n'} \times \\ &\int_{y=0}^{L_2} dy h_{j,n}(y)V(y)h_{j,n}(y) \times \\ &\int_{x=0}^{L_2} dx g_{j,n}^*(x)e^{2\pi ikx/L_1} g_{j',n'}(x) . \end{aligned}$$

The integral over x vanishes unless

$$j - j' + N_\phi(n - n') + k = 0 .$$

In other words,

$$\frac{1}{N_\phi}(j - j' + k) = \text{integer} \equiv q . \quad (\text{B.4})$$

By this definition $n' = n + q$ therefore

$$\langle j|V(y)e^{2\pi ikx/L_1}|j'\rangle = L_1 \sum_{n=-\infty}^{\infty} f_{j,n}^* f_{j',n+q} \int_0^{L_2} dy h_{j,n}(y) h_{j',n+q}(y) V(y) .$$

Arranging things using (B.3) leads to

$$\langle j|V(y)e^{2\pi ikx/L_1}|j'\rangle = L_1 \sum_{n=-\infty}^{\infty} f_{j,n}^* f_{j',n+q} \int_0^{L_2} dy e^{-y^2/l_H^2} e^{2\varrho y/l_H} V(y) ,$$

where we have defined

$$\begin{aligned} \varrho &\equiv y + \tilde{\varrho} + nL_2 \\ \tilde{\varrho} &\equiv \frac{\pi l_H^2}{L_1} (2N_\phi + \phi_1/\pi - j - j' + qN_\phi) \end{aligned}$$

and used the Dirac's condition $L_1 L_2 = 2\pi N_\phi l_H^2$.

A change of variables $w = y + nL_2$ switches the n dependence from the integrand to the integral boundaries

$$\langle j|V(y)e^{2\pi ikx/L_1}|j'\rangle = L_1 \sum_{n=-\infty}^{\infty} f_{j,n}^* f_{j',n+q} e^{\varrho^2} \int_{nL_2}^{(n+1)L_2} dw e^{-(w+\varrho l_H)^2/l_H^2} V(w)$$

(note that $V(y + L_2) = V(y)$).

The nice thing is that (again using Dirac's condition)

$$f_{j,n}^* f_{j',n+q} e^{\varrho^2} = \frac{1}{\pi L_1 l_H} e^{-iq\phi_2} e^{-\left(\frac{kL_2}{2N_\phi l_H}\right)^2}$$

which is n -independent. The summation and integration can therefore be replaced with one integration covering the space $\{-\infty, \infty\}$

$$\langle j|V(y)e^{2\pi ikx/L_1}|j'\rangle = \frac{1}{\pi l_H} e^{-iq\phi_2} e^{-\left(\frac{kL_2}{2N_\phi l_H}\right)^2} \int_{-\infty}^{\infty} dw e^{-(w+\varrho l_H)^2/l_H^2} V(w) .$$

This completes the proof.

Appendix C

A Summary Of Torus Wave Functions and Translation Operations

Single Particle WF

$$\varphi_j(x, y) = A_j e^{-y^2/2l^2} e^{i(\pi N_\phi + \phi_1 - 2\pi j)z/L_1} \theta_1\left(\frac{\pi N_\phi}{L_1}(z - a) - j\pi\tau | N_\phi\tau\right) \\ j = 0, 1, \dots, N_\phi - 1 \quad (\text{C.1})$$

where

$$a \equiv \frac{L_1}{2\pi N_\phi} [\pi + \phi_2 - \tau(\pi N_\phi + \phi_1)]$$

and

$$A_j = (L_1\sqrt{\pi})^{-1/2} e^{i\tau(\pi N_\phi + \phi_1 - 2\pi j)^2/4\pi N_\phi} .$$

Single Particle Translation Operations

$$t(L_1/N_\phi \hat{x}) \varphi_j = e^{i(\phi_1 - 2\pi j)/N_\phi} \varphi_j \quad (\text{C.2})$$

$$t(L_2/N_\phi \hat{y}) \varphi_j = \varphi_{j-1} \quad (\text{C.3})$$

Laughlin's Wave Function

$$\Psi_s = \beta B_s e^{-\sum_j y_j^2/2l^2} F_s(\sum_{j=1}^N z_j) \prod_{i<j} \theta_1^m(\frac{\pi}{L_1}(z_i - z_j)|\tau)$$

$$s = 0, 1, \dots, (m-1)$$
(C.4)

where

$$F_s(z) = e^{i(\pi N_\phi + \phi_1 - 2\pi s)z/L_1} \theta_1(\frac{\pi m}{L_1}(z - b) - s\pi\tau|m\tau)$$

$$b \equiv \frac{L_1}{2\pi m} [\pi N_\phi + \phi_2 - \pi(m-1) - \tau(\pi N_\phi + \phi_1)]$$
(C.5)

and

$$B_s \equiv e^{i\tau(\pi N_\phi + \phi_1 - 2\pi s)^2/4\pi m}$$
(C.6)

Laughlin's Wave Function Translation Operations

$$T_1 \Psi_s = (-1)^{N+1} e^{i(\phi_1 - 2\pi s)/m} \Psi_s$$

$$T_2 \Psi_s = \Psi_{s-1}$$

$$\Psi_{s-m} = e^{i\phi_2} (-1)^{N_\phi - m} \Psi_s .$$
(C.7)

One Localized Hole Wave Function

$$\Psi_{s;(z_0)} = B_s e^{-y_0^2/2ml^2} e^{-\sum_j y_j^2/2l^2} F_s(\frac{z_0}{m} + \sum_{j=1}^N z_j) \times$$

$$\prod_{i<j} \theta_1^m(\frac{\pi}{L_1}(z_i - z_j)|\tau) \prod_{j=1}^N \theta_1(\frac{\pi}{L_1}(z_j - z_0)|\tau)$$
(C.8)

Localized Hole Translation Operations

$$t_0(L_1 \hat{x}) \Psi_{s;(z_0)} = -e^{i(\pi + \phi_1 - 2\pi s)/m} \Psi_{s;(z_0)}$$
(C.9)

$$t_0(L_2 \hat{y}) \Psi_{s;(z_0)} = (-1)^N \Psi_{s-1;(z_0)}$$
(C.10)

$$\Psi_{s-m;(z_0)} = (-1)^{N_\phi - m} e^{i\phi_2} \Psi_{s;(z_0)}$$
(C.11)

$$T_3 \Psi_{s;(z_0)} = -e^{i(\pi N s + \phi_1 - 2\pi s)/m} \Psi_{s;(z_0)}$$
(C.12)

$$T_4 \Psi_{s;(z_0)} = \Psi_{s-1;(z_0)}$$
(C.13)

Extended Unit Cell Wave Function

$$g_{s;n}(z) = A_{s;n} e^{-y_0^2/2\mathfrak{m}l_H^2} e^{i(\pi N_\phi + \phi_1 - 2\pi[s+mn])z/\mathfrak{m}L_1} \theta_1\left(\frac{\pi N_\phi}{L_1}(z - \tilde{a}) - [s+mn]\pi\tau/\mathfrak{m}N_\phi\tau\right) \\ n = 0, 1, \dots, N_\phi - 1 \quad (\text{C.14})$$

where

$$A_{s;n} \equiv (\mathfrak{m}L_1\sqrt{\mathfrak{m}\pi})^{-\frac{1}{2}} e^{i\tau(\pi N_\phi + \phi_1 - 2\pi[s+mn])^2/4\pi\mathfrak{m}N_\phi}$$

and

$$\tilde{a} \equiv \frac{L_1}{2\pi N_\phi} (\phi_2 - \frac{1}{2}\pi N_\phi(N_\phi - 3) - \tau(\pi N_\phi + \phi_1)) .$$

Extended Cell Translation Operations

$$\begin{aligned} t_0(L_1/N_\phi\hat{x}) g_{s;n} &= -e^{i(\pi N_\phi + \phi_1 - 2\pi[s+nm])/\mathfrak{m}N_\phi} g_{s;n} \\ t_0(L_2/N_\phi\hat{y}) g_{s;n} &= g_{s-1;n} \\ g_{s-m;n} &= g_{s;n-1} \\ t_0(L_2\hat{y}) g_{s;n} &= g_{s-1;n-N} \\ g_{s;n-N_\phi} &= e^{-i\pi(N_\phi-1)(N_\phi-2)/2} g_{s;n} . \end{aligned} \quad (\text{C.15})$$

Valley Wave Functions

$$\psi_p \equiv \int_{\mathfrak{m}L_1 \times \mathfrak{m}L_2} g_{s;n}^*(z_0) \Psi_{s;(z_0)} dz_0 \\ p = 0, 1, \dots, (N_\phi - 1) . \quad (\text{C.16})$$

where

$$p \equiv s + mn \pmod{N_\phi} \quad (\text{C.17})$$

Extended Cell Translation Operations

$$\begin{aligned} T_1\psi_p &= -e^{2\pi in/N_\phi} e^{iN(\pi N_\phi + \phi_1 - 2\pi s)/N_\phi} \psi_p \\ T_2\psi_p &= \psi_{p-1} . \end{aligned} \quad (\text{C.18})$$

Appendix D

Localized Hole Wave Function's Coefficients

Here we find the g -functions appearing in the expansion form of LWF with one localized hole

$$\Psi_{s;(z_0)} = \sum_{n=0}^{N_\phi-1} c_{s;n} g_{s;n}(z_0) \psi_{s;n}(z_1, \dots, z_N) . \quad (\text{D.1})$$

We start with the general expansion¹

$$\Psi_{s;(z_0)} = \sum_{j_1, \dots, j_N} c_{s;j_1, \dots, j_N} g_{s;j_1, \dots, j_N}(z_0) |j_1, \dots, j_N\rangle . \quad (\text{D.2})$$

We will show that the g -functions belong to a set of $\mathfrak{m}N_\phi$ functions, with the form of a single particle WFs on an extended unit cell $\mathfrak{m}L_1 \times \mathfrak{m}L_2$.

We start by applying $t_0(L_2\hat{y})$ over the expansion (D.2). Doing it \mathfrak{m} times (using (C.10) and (C.11)) leads to

$$t_0(\mathfrak{m}L_2\hat{y})g_{s;j_1, \dots, j_N} = e^{i\phi_2} g_{s;j_1, \dots, j_N} . \quad (\text{D.3})$$

Applying $t_0(L_1\hat{x})$ over the expansion gives (eq. (C.9))

$$t_0(L_1\hat{x})g_{s;j_1, \dots, j_N} = -e^{i(\pi+\phi_1-2\pi s)} g_{s;j_1, \dots, j_N} ,$$

¹The g -functions in this expansion are actually functions of z_0 and y_0 . The explicit dependence in y_0 is a gaussian $e^{-y_0^2/2\mathfrak{m}L_H^2}$, and enters as a result of multiplying $\Psi_{s;(z_0)}$ with it (see eq. (2.41))

and therefore

$$t_0(\mathbf{m}L_1\hat{x})g_{s;j_1,\dots,j_N} = -e^{i\phi_1}g_{s;j_1,\dots,j_N} . \quad (\text{D.4})$$

By (D.3) and (D.4) we get that the g -functions are indeed of single particle WFs on an extended unit cell $\mathbf{m}L_1 \times \mathbf{m}L_2$. Still they have $\mathbf{m}N_\phi$ zero locations yet to be determined. These are found by applying T_3 to the expansion. Doing that using (C.12) and

$$T_1|j_1, \dots, j_N \rangle = e^{iN\phi_1/N_\phi} e^{-2\pi i \sum_{k=1}^N j_k/N_\phi} |j_1, \dots, j_N \rangle$$

(obtained by (C.2) and T_1 definition), leads to

$$t_0\left(\frac{L_1}{N_\phi}\hat{x}\right)g_{s;j_1,\dots,j_N} = (-1)^{N+1} e^{2\pi i \sum_{k=1}^N j_k/N_\phi} e^{i\pi/\mathbf{m}} e^{-2\pi i s/\mathbf{m}} e^{-i\phi_1/\mathbf{m}N_\phi} g_{s;j_1,\dots,j_N} \quad (\text{D.5})$$

so the zeroes are equally spaced on a string along the x -direction, with distance of L_1/N_ϕ in between adjacent zeroes. This determines $g_{s;j_1,\dots,j_N}$ completely. These functions are chosen from the set $\{g_{s;n}\}$ given at (C.14).

One last thing is to show the relation between n and $\{j_1, \dots, j_N\}$. This is done by applying $t_0\left(\frac{L_1}{N_\phi}\hat{x}\right)$ over $g_{s;n}$

$$t_0\left(\frac{L_1}{N_\phi}\hat{x}\right)g_{s;n} = -e^{-2\pi i n/N_\phi} e^{i\pi/\mathbf{m}} e^{-2\pi i s/\mathbf{m}N_\phi} e^{-i\phi_1/\mathbf{m}N_\phi} g_{s;n} .$$

Comparing this to (D.5) leads to

$$e^{2\pi i s N/N_\phi} (-1)^N e^{-2\pi i n/N_\phi} = e^{2\pi i \sum_{k=1}^N j_k/N_\phi} , \quad (\text{D.6})$$

which finalize the functions determination.

Appendix E

Effective Hamiltonian Approach

In the effective Hamiltonian model one tries to capture the essence of the torus tunnelling description:

- There exists the barrier's (first order) energy, just the overlap of the WF with the barrier. The closest the valley is to the barrier, the minimal this energy is.
- In order to discuss tunnelling possibility different states should be coupled. This is the job of the disturbing potential. Note that when two states ψ and $\tilde{\psi}$ having a TAM difference of \mathcal{N} are coupled, the coupling strength $\langle \psi | V | \tilde{\psi} \rangle$ is proportional to $\langle \varphi_j | V | \varphi_{j+\mathcal{N}} \rangle$ which in turn is proportional to $e^{-(\mathcal{N} L_2 / 2N_{\phi} l_H)^2}$. Recall that \mathcal{N} of adjacent states is N .

We start with the first term. The valley can be thought of as if it is a full LLL with a missing state in the p th (single particle) state. Its density is "almost uniform", with the exception of the valley. So we denote the p th valley state by $d_p |\Psi_g\rangle$, where $|\Psi_g\rangle$ is a state with no valley (uniform distribution) and d_p is a destruction operator of the p th state. The Hamiltonian expression for the barrier's energy is therefore

$$H_0 = \sum_p \epsilon_p d_p d_p^\dagger, \quad (\text{E.1})$$

and the Hilbert space consists the states $d|\Psi_g\rangle$. This has the form of a kinetic term. If one deals with a simple mountain shape barrier (say a gaussian), ϵ_p has a general landscape given in Figure E.0.i. The energy depends on ϕ_1 because of the valley location flux dependence. In the figure we give the energy for two value of ϕ_1 , the starting one ($\phi_1 = 0$) with one state having the minimal energy, and the flux with two degenerate states ($\phi_1 = \phi_0/2$).

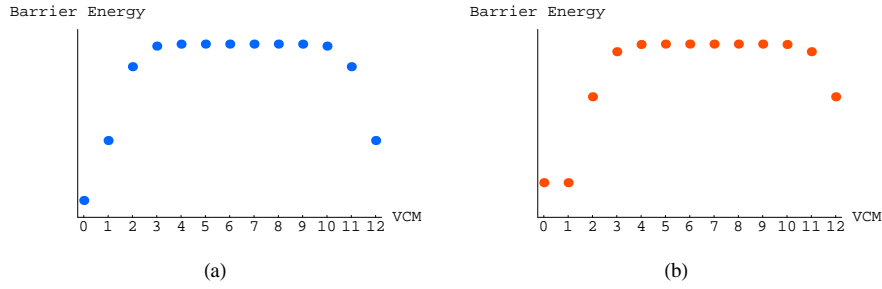


Figure E.0.i: A schematic description of the barrier's energy presented in the (valley's) center of mass (VCM) representation. Adjacent p numbers corresponds to adjacent valleys. (a) $\phi_1 = 0$. (b) $\phi_1 = \phi_0/2$.

Besides this "kinetic" term, we also have a term coupling the states. As we have explained above, the relevant issue here is the WF's TAM. Considering this "interaction" term, it therefore make sense to write it in the "TAM representation": just order the states differently according to

$$n = pN(\text{mod}N_\phi) . \quad (\text{E.2})$$

The state number n , is the TAM of the n th state. The interaction term has a general form

$$H' = \sum_{n,m} V_{nm} d_n^+ d_{n+m} + h.c. \quad (\text{E.3})$$

with $V_{nm} \propto e^{-(\mathcal{N}L_2/2N_\phi l_H)^2}$.

The kinetic term has a different landscape after the new "ordering" : $p \rightarrow n$, going from a center of mass representation to the TAM one. Figure E.0.ii is the same as Figure E.0.i plotted in the TAM representation.

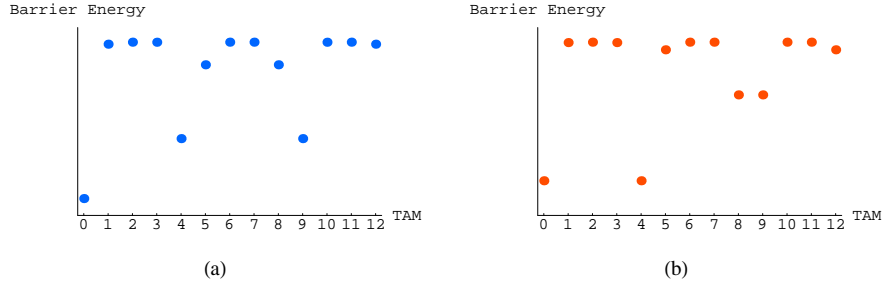


Figure E.0.ii: A schematic description of the barrier's energy presented in the TAM representation. Adjacent n numbers correspond to states with adjacent TAM. (a) $\phi_1 = 0$. (b) $\phi_1 = \phi_0/2$. Compare this to Figure E.0.i

The overall Hamiltonian one should study is $H = H_0 + H'$.

This model allows studying the energy ϕ_1 dependence taking into account all the N_ϕ valley states (and not just the two barrier-closest). It is much simpler to handle mathematically, because one does not use the explicit form of the WFs, which is complicated. It can be used as a good candidate for further study of the tunnelling (wider barrier, different shapes such as a double barrier, etc.).

Appendix F

Notations and Abbreviations

(1)2D	(One) Two Dimensional
FQHE	Fractional Quantum Hall Effect
IQHE	Integer Quantum Hall Effect
KF	Kane & Fisher
LLL	Lowest Landau Level
LWF	Laughlin's Wave Function
QH	Quantum Hall
QHE	Quantum Hall Effect
SD	Slater Determinant
TAM	Total $\left\{ \begin{array}{ll} \text{Angular} & \text{(disk)} \\ \text{x direction} & \text{(cylinder)} \\ \text{quasi} & \text{(torus)} \end{array} \right\}$ Momentum
WF	Wave Function

ν	filling factor
τ	iL_2/L_1
φ	single particle wave function
ϕ	magnetic flux through the sample's surface
ϕ_1, ϕ_2	magnetic flux through torus' "holes", see Figure 1.9
ϕ_0	flux quanta = hc/e
Ψ	many body wave function
\mathbf{A}	vector potential
B	magnetic field
$g(z)$	extended $(L_1 \times L + 2)$ unit cell wave function
H_0	Hamiltonian consisting only the magnetic field kinetic part
l_H	magnetic length = $\hbar c/eB$
L	cylinder's length
L_1, L_2	torus' x and y dimensions respectively
m	1/filling factor, along the thesis it takes odd integer values.
N	number of particles
N_h	number of (localized) holes
N_ϕ	number of flux quanta perpendicular to the surface, = ϕ/ϕ_0
R	cylinder's radius
\mathcal{T}	tunnelling probability
V_{back}	background potential
$V_{barrier}$	barrier potential
V_{conf}	confining potential
V_{imp}	impurity potential (might contain several localized impurities).
V_{int}	interaction energy
V_{mount}	mountain (barrier) potential
x, y, z	cartesian coordinates
z	complex variable $z = x + iy$
z_{cm}	center of mass coordinate = $\sum_{j=1}^N z_j$
z_{0j}	j th localized hole location.

Bibliography

- [1] R.E.Prange & S.Girvin, *The Quantum Hall Effect*, Springer-Verlag 1990.
- [2] S.M. Girvin, *The Quantum Hall Effect: Novel Excitations and Broken Symmetries*, Les Houches 1998 (cond-mat/9907002).
- [3] A. H. MacDonald, cond-mat/9410047.
- [4] (includes C.L. Kane and M. P. A. Fisher review) S. Das Sarma and A. Pinczuk, *Perspectives in Quantum Hall Effects*, 1996.
- [5] G. Murthy and R. Shankar, cond-mat/0205326.
- [6] (short and popular) S. Rao, cond-mat/9902292.
- [7] N.W. Ashcroft & N.D. Mermin, *Solid State Physics*, Holt, Rinehart and Winston, 1976.
- [8] K.v.Klitzing et al., Phys. Rev. Lett.**45**,494 (1980)
- [9] D.C. Tsui, H.L. Störmer and A.C. Gossard, Phys. Rev. Lett., **48**, 1559 (1982).
- [10] R. E. Prange, Phys. Rev. B.**23**, 4802 (1981).
- [11] R. E. Prange and R. Joynt, Phys. Rev. B.25, 2943 (1982).
- [12] R. E. Prange and R. Joynt, Phys. Rev. B.29, 3303 (1984)
- [13] R.B. Laughlin, Phys. Rev. B., **27**, 3383 (1983).
- [14] R.B. Laughlin, Phys. Rev. Lett., **50**, 1395 (1983).

- [15] J.K. Jain, Phys. Rev. Lett.**63**, 199 (1989), Phys. Rev. B.**41**, 7653 (1990), Science **266**, 1199 (1994). F.D.M. Haldane, Phys. Rev. Lett.**51**, 605 (1983). B.I. Halperin, Helv. Phys. Acta **556**, 75 (1983), Phys. Rev. Lett.**52**, 1583 (1984).
- [16] F.D.M. Haldane, Phys. Rev. Lett., **51**, 605 (1983).
- [17] S.A. Trugman and S. Kivelson, Phys. Rev. B., **31**, 5280 (1985).
- [18] S.M. Girvin, Phys. Rev. B., **29** 6012 (1984).
- [19] D.J. Thouless, Surf. Sci. **142**, 147 (1984).
- [20] F.D.M. Haldane, E.H. Rezayi, Phys. Rev. B., **31**, 2529 (1985).
- [21] C.L. Kane and M.P.A. Fisher, Phys. Rev. Lett., **68**, 1220 (1992) ; C.L. Kane and M.P.A. Fisher, Phys. Rev. B., **46**, 7268 (1992); C.L. Kane and M.P.A. Fisher, Phys. Rev. B., **46**, 15233 (1992); K. Moon, H. Yi, C.L. Kane, M. Girvin and M.P.A. Fisher, Phys. Rev. Lett., **71**, 4381 (1993); (the most relevant one:) C.L. Kane and M.P.A. Fisher, Phys. Rev. Lett., **72**, 724 (1994); C.L. Kane and M.P.A. Fisher, Phys. Rev. B., **51**, 13449 (1995).
- [22] (short and popular) C.L. Kane and M.P.A. Fisher, Nature, **389**, 119 (1997).
- [23] M.P.A. Fisher and L.I. Glazman, cond-mat/9610037.
- [24] R. de-Picciotto, M. Reznikov, M. Heiblum, V. Umansky, G. Bunin, D. Mahalu, Nature, **389**, 162 (1997).
- [25] L. Saminadayar, D.C. Glatli, Y. Jin, B. Etienne, Phys. Rev. Lett., **79**, 2526 (1997).
- [26] Q. Li and D.J. Thouless, Phys. Rev. B., **40**, 9738 (1989).
- [27] B. I. Shklovskii, Pis'ma Zh. Eksp. Teor. Fiz. 36, 43 (1982) [JETP Lett. 36, 51 (1982)].
- [28] A. Auerbach, Phys. Rev. Lett., **80**, 817 (1998); A. Auerbach, cond-mat/9707331.

- [29] B.I. Halperin, Phys. Rev. B., **25**, 2185 (1982).
- [30] R.B. Laughlin, Phys. Rev. B., **23**, 5632 (1981).
- [31] X.G.Wen, Phys. Rev. Lett.**64**, 2206 (1990); Phys. Rev. B., **43**,11025 (1991).
- [32] E. Onofri, Int. Jou. of Theo. Phys. , **40**, 537 (2001).
- [33] E.T. Whittaker, G.N. Watson, *A Course of modern Analysis* (Cambridge, 4th add.), p.462.
- [34] J. Callaway, *Quantum Theory of the Solid State, Part B* (Academic Press, 1974), p. 480.
- [35] R. Tao and F.D.M. Haldane, Phys. Rev. B., **33**, 3844 (1986).
- [36] R. Tao and D.J. Thouless, Phys. Rev. B.**28**, 1142 (1983); K. Takano and A. Isihara, Phys. Rev. B., **34**, 1399 (1986); G.V. Dunne, cond-mat/9306022.
- [37] G. D. Mahan, *Many-Particle Physics* (Plenum, New York, 1990).
- [38] J.M. Ziman, *Principles Of The Thoery Of Solids* (Cambridge, 1965), p.163.
- [39] T.G. Griffith, E. Comforti, M. Heiblum, Ady Stern, and V. Umansky, Phys. Rev. Lett., **85**, 3918 (2000).
- [40] D. Arovas, J.R. Schrieffer, and F. Wilczek, Phys. Rev. Lett., **53**, 722 (1984).
- [41] M.V. Berry, Proc. Roy. Soc. Lond. , A **392**, 45 (1984).